University of Alberta

The Role of Eosinophils in Neonatal Murine Thymus; Expression of Indoleamine 2, 3-dioxygenase

by

Olga Vladimir Cravetchi

A thesis submitted to the Faculty of Graduate Studies and Research
in partial fulfillment of the requirements for the degree of

Master of Science

in

Experimental Medicine

Department of Medicine

©Olga Vladimir Cravetchi
Fall 2009
Edmonton, Alberta

Examining Committee

Redwan Moqbel, Medicine

Hanne L. Ostergaard, Medical Microbiology and Immunology

Lakshmi Puttagunta, Laboratory Medicine and Pathology

Troy A. Baldwin, Medical Microbiolgy and Immunology

Dedication

I am dedicating this work to my parents Valentina and Vladimir and to my dear friend Alexander Floaria, who died of cancer at age 25.

Olga V. Cravetchi.

Abstract

Rationale: Eosinophils are "end cell" leucocytes, associated with allergy, asthma and helminthiasis. At sites of inflammation, eosinophils may modulate immune response through expression of the extra-hepatic tryptophan-catabolising enzyme, Indoleamine 2, 3-dioxygenase (IDO). Kynurenines, products of tryptophan cleavage, induce apoptosis of T-cells, including thymocytes. Eosinophils naturally home to the thymi in mammals. Thymus is a primary lymphoid organ, where T-cells develop and undergo selection. My hypothesis is that eosinophils homing to the thymi participate in T-cell development through their expression of IDO. **Methods:** Immunohistochemistry revealed eosinophils in thymic tissue. Immunocytochemistry and flow cytometry were used to locate IDO protein expression in the thymus particularly in thymic eosinophils. RT-PCR and real-time PCR determined the presence of IDO mRNA in the thymus. **Results:** thymic eosinophils express IDO and infiltrate compartments associated with negative selection. The highest IDO transcription correlated with the influx of eosinophils and prevalence of immature thymocytes.

Preface

This thesis is written in a thesis format according to the guidelines of the University of Alberta's "Thesis Format Specifications."

Acknowledgements

The amazing memories I have accumulated during my time and experience at the University of Alberta I attribute to my Professors and colleagues. They made my time at the Faculty of Medicine truly fulfilling, not only professionally but also to in relation to my entire life's experience while studying there. I picked up knowledge in the laboratory, the lecture hall and even during the extracurricular activities within the group. The University of Alberta provided me with great opportunity to grow and learn. I will always treasure and cherish these fond memories.

I would like to extend my special thanks to my supervisor Dr. Redwan Moqbel and also Dr. Dean Befus, who kindly stepped in to supervise my work during Dr Moqbel's sabbatical and sick leaves. They both guided me towards my goal and greatly affected my day-to-day learning process. I would not be where I am today professionally and personally without the consistent support, encouragement and interest I received. For this, I am truly thankful.

Also, I would like to acknowledge members of my supervisory committee: Dr. Lakshmi Puttagunta (Department of Laboratory Medicine and Pathology) and Dr. Hanne L. Ostergaard, (Department of Medical Microbiology and Immunology) for their understanding, instant attention, knowledgeable guidance and extraordinary help with my attempt to fulfill my project. As well, I wish to

thank Dr. Troy A. Baldwin (Department of Medical Microbiology and Immunology) who agreed to serve as an external examiner in my thesis defense.

I would like to thank all members of Pulmonary Research Group for their regular support and cooperation. In particular I wish to thank Drs.: Francis Davoine, Cory Ebeling, SO (Wole) Odemuyiwa, Saswati Das, Jason Coughlin, Florentina Duta, TaeChul Moon, Ramses Ilarraza, Sorin Musat-Marcu, and Ms Courtney Davidson, Yanling Feng from the PRG lab. Also Tom Terner who assisted me with photography of pathological material, and Members of Dr Bernard Thebaud's Laboratory, Thank you all for your deeply appreciated help.

Also, I would like to extend my deepest thank to my dear family: my husband Igor and beloved children Xenia and Maximillian, who has been my greatest help and inspiration during my studies. I am the happiest person because of their love and support.

Table of Contents

Chapter 1

Introduction

Chapter 2

Materials and Methods

Chapter 3

Results

Chapter 4

Discussion

List of figures

Commonly used abbreviations

APC	Antigen Presenting Cell
APC	Allophycocyanine
BM	bone marrow
bp	base pairs
CCR3	C-chemokine receptor 3
CLP	Common lymphoid progenitor
CD	Cluster of differentiation
DAB	diaminobenzidine
DC	dendritic cell
cDNA	copy deoxyribonucleic acid
FACS	Fluorescence Activated Cell Scanning
FBS	Fetal Bovine Serum
GIT	gastro-intestinal tract
ICAM	inter cellular adhesion molecule
IDO	Indoleamine 2, 3-dioxygenase
IFN-γ	Interferon-gamma
Ig	Immunoglobulins
IL	Interleukin
KYN	Kynurenine
MBP	Major basic protein
MHC	Major histocompatibility complex
mRNA	messenger ribonucleic acid
NRS	Normal Rabbit Serum

PBS	Phosphate Buffered Saline
PCR	Polymerase chain reaction
R-PE	R-Phycoerythrin
RT-PCR	Reverse transcription polymerase chain reaction
Siglecs	Sialic acids-binding immunoglobulin-like lectins
TBST	Tris-buffered saline + 0.5% Tween-20
TAE	Tris-acetate
TCR	T-cell Receptor
VCAM-1	Vascular cellular adhesion molecule

Chapter 1

Introduction

Eosinophil Biology

The overarching premise of this thesis is that eosinophils may be potent immunomodulating cells in primary lymphoid tissue, such as the thymus, and may therefore contribute to the T-cell development and selection throughout their expression of immune active molecules.

Eosinophils are major inflammatory cells associated with a number of conditions including helminth infections, atopy and asthma. They are leucocytes that contain a segmented nucleus and prominent granules in their cytoplasm. In healthy individuals eosinophils are low in abundance, constituting between 1% and 3% of the total circulating leukocyte population (1). Paul Ehrlich first identified eosinophils in 1879 when he ascertained that their granules bind intensively with eosin, a negatively charged dye (2). These cells contain proteins with the highest isoelectric point (>11; i.e., extremely basic in nature). The cationic properties of eosinophils, which contributed to their discovery, were shown to be critical for the function of these leukocytes (3). Some of the basic proteins stored within eosinophilic granules are toxic to microorganisms (including helminths larvae) as well as host tissue. Eosinophils are adequately

equipped to cause damage to and ultimately eliminate parasitic worm material within infected tissue. For a long time they were considered end-stage effector cells in helminthiasis and allergic inflammation. Studies over the past three decades have expanded knowledge about the pathophysiological role and immunobiology of the eosinophil. It is now generally accepted that eosinophils are important elements in pathogenesis of a number of rare but severe conditions, including Churg-Strauss syndrome, eosinophilic endocarditis and various hypereosinophilic syndromes (4). Eosinophils are also found in draining lymph nodes of allergic subjects, numerous human tumors (tumor-associated tissue eosinophilia (TATE)) such as oral squamous cell carcinoma, and non-small cell lung carcinoma (5). These observations suggest that the presence of eosinophils may play a significant role in inflammatory and immune modulation. The better understanding of the complexity of eosinophils' function could be drawn from detailed examination of their structure.

Human eosinophils are approximately 8 μm in diameter, containing segmented nuclei (2-3 lobes) and well developed ubiquitous organelles (2). The most important structural feature of eosinophils that makes them distinct from other leucocytes is their granules, which intensively attract acidic dyes such as eosin. Eosinophils have four populations of granules: primary, secondary ("specific"), small granules and lipid bodies that are all present in mature cells and enclose distinct components (6). The primary granules appear only at the myelocyte stage and are enriched in distinct bipyramidal Charcot–Leyden crystal (CLC) protein. Later they differentiate either into specific secondary granules or

form homogeneous cytoplasmic bodies containing lysophosphatase (7). During the process of maturation, secondary granules acquire and store the majority of highly specific proteins (8). The most abundant among them are: major basic protein (MBP), eosinophil peroxidase (EPO), eosinophil cationic protein (ECP), and eosinophil-derived neurotoxin (EDN). Secondary granules have dense crystalloid cores, formed of MBP, and matrix, containing three other cationic proteins (9). All eosinophilic proteins possess some differences in their structure and function. They do not express enzymatic activity aside from EPO, but it is assumed that they all are organized to generate toxicity as a defense against parasitic worm invaders. In addition to the general information about eosinophil-specific proteins, I also present some important details about these proteins.

Major basic protein has two homologues namely, MBP-1 and MBP-2 that are enriched in arginine and tryptophan. These two amino acids contribute to the high cationic charge and toxicity of these proteins (10). MBPs *in vivo* act as natural heparinase-inhibiting proteins (11) and are able to kill helminthic targets, stimulate neuro-muscular synapses (12), and are lethal to malignant and host cells. Moreover, MBP was demonstrated to be involved in direct activation of mast cells during allergic inflammation (13). Eosinophil cationic protein (ECP) and eosinophil-derived neurotoxin (EDN) are ribonucleases and can also exert cytotoxic activity against parasitic helminth. In addition, EDN wields neurotoxicity, remodeling factors activation, and the inhibition of T-cell proliferation (14). The complexity of EDN functionality adds more immune regulating properties to the eosinophil leukocyte. During an immune response

EDN alters APCs to promote Th2 lymphocyte predominance and the corresponding cytokine profile (15). Eosinophil peroxidase (EPO) functions as cationic toxin in the absence of peroxide and as a peroxidase when hydrogen peroxide is present. EPO converts halide ions (especially bromide) and hydrogen peroxide into hypohalous acid, which is bactericidal, but also damages host tissue (16). Appropriately-stimulated eosinophils synthesize, encompass and release active oxygen species, such as superoxide (O_2^-), hydrogen peroxide (H_2O_2) and nicotinamide adenine dinucleotide phosphate (NADPH) oxidase.

NADPH oxidase activity was reported to be three to ten times greater in eosinophils compared to neutrophils (17). In addition to relatively prominent primary and secondary granules, eosinophils possess smaller cytoplasmic inclusions with different constituents.

Other cytoplasmic structures that contribute to the granules population are eosinophil lipid bodies. These organelles constitute the products of catabolized arachidonic acid, active lipid mediators such as leukotriene C_4 (LTC_4), prostaglandin F_1 (PGF_1), prostaglandin D_2 (PGD_2), thromboxane A_2 (TXA_2) and a platelet activating factor (PAF) (18). These molecules possess proinflammatory properties and increase vascular permeability. Furthermore, they activate immune effector cells and induce smooth muscle constriction. All granules-associated eosinophil products are released in response to the numerous stimuli, delivered to exocytotic machinery through an array of receptors and surface molecules.

Ig receptors and members of Ig superfamily

CD4, CD16, CD32, CD33, CD47, CD48, CD50 CD82, CD86, CD89, CD101, HLA class1, HLA-DR, FcεR1

Cytokine receptors

CD25, CD116, CD117, CD119, CD120, CD123, CD124, CD125, CD131, CD213, IL-9R, IL-13Rα1, TGFβR,

Apoptosis, signaling and others

CD9, CD17, CD24, CD28, CD37, CD39, CD43, CD52, CD63, CD69, CD76, CD80, CD82, CD86, CD92, Siglec-8, CD165, LIR1, LIR2, LIR3, LIR7, TLR7, TLR8,

CD162, CD174, αd integrin, β7 integrin, CD11a, CD11b, CD11c, CD15, CD18, CD29, CD44, CD49d, CD49f, CD62L, CD156, CD162

Adhesion molecules

CD35, CD88, CD182, CD196, PAFR, LTB$_4$R, C3aR, CD191, CystLT1R, CysLT2R, fMLPR, CRTH2, Histamine 4R, CD192

Chemokine, complement and other factors

Figure 1. Membrane associated molecules of eosinophil leukocyte.

Adapted from Rothenberg, M. E., and Hogan, S. P. 2006. *Ann Rev Immunol.*

Membrane-associated molecules

Eosinophils express a number of cell surface receptors including immunoglobulin receptors, binding sites for lipid mediators, complement proteins, cytokines, chemokines, co-stimulatory and adhesion molecules. Eosinophils express specific members of the Fcγ immunoglobulin receptor superfamily. Under resting conditions eosinophils bear only FcγRII (CD 32) on their surface. Stimulation of eosinophils with IFN-γ induces expression of CD16 and CD64 (FcγRI), and further ligation of upregulated receptors with specific antibody causes a considerable release of lipid mediator LTC_4 (19). Eosinophilic membranes also carry a substantial number of receptors for IgE molecule (FcεRII and CD23). The binding of these receptors to specific immunoglobulins provokes cell activation, release of a platelet aggregation factor (PAF), EPO, and boosts eosinophil-mediated cytotoxicity (20). Receptors for the complement proteins C1q, C3a, C3b/C4b, (CRI), iC3b (CR3), C3d and C5a are also present on the eosinophil plasma membranes (21). Specific binding of complement receptors to their ligands upregulates the expression of adhesion molecules, increases chemotactic mobility and activates the generation of adaptive immune responses (22).

Other molecules that serve as innate immunity recognition sites are members of the immunoglobulin superfamily (IgSF), CD33-related Siglecs (Figure 2).

Human

sialoadhesin

CD 22 Siglec **2	MAG Siglec 4	Siglec15	CD33 Siglec 3	Siglec 5 CD 170	Siglec 6 CD 327	Siglec 7 CD 328	**Siglec 8** _	Siglec 9 CD 329	Siglec c10 _	Siglec c 11 _	Siglec c 14 _
*** Bas	Oligo D	ND	MyP N	Mo, N	Troph	NK Mo	**Eos**	Mo, N,D C	Bas, Mo	Mac	ND
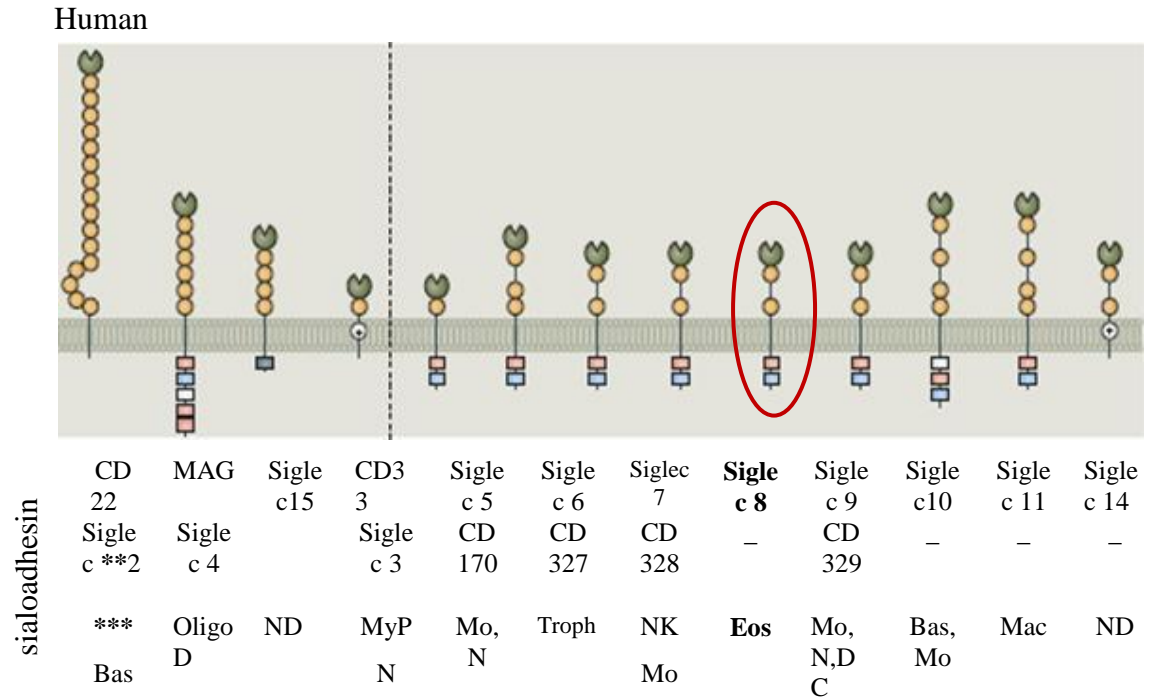
* - Common name; ** - Alternative name; *** - Expression

Mouse

Structure

Common name	Sialoa dhesin	CD22	MAG	Siglec 15	CD33	Siglec E	**Siglec F**	Siglec G	Siglec H
Alternative name	CD169	Siglec 2	Siglec 4	_	Siglec 3	_	_	_	_
Expression	Mac	Bas	Oligo D	ND	N	N, Mo	**Eos**	Bas	pDC
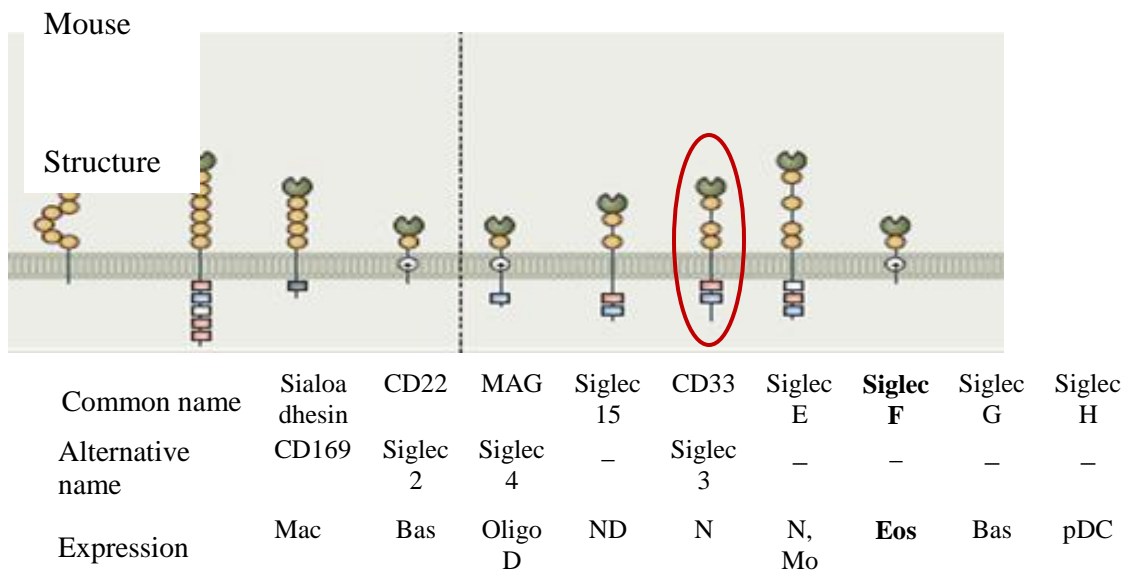
Figure 2. Human and mice isoforms of CD33-associated sialic acids immunoglobulin-like lectins (Siglecs)

The molecules, associated with the cells of eosinophilic origin marked into circles.

Adapted from: Crocker, P.R., Paulson, J.C., and Varki, A. 2007. *Nature Rev*

Immunol.

The sialic acid binding immunoglobulin-like lectins (Siglecs) function as recognition sites for sialic acids, sialoadhesins and peptidoglycans (23). In humans, there are nine members of CD33- related Siglecs family, whereas in mice there are only five CD33-related Siglecs (24). Most cell types of immune systems in humans and mice express one or more Siglecs on their membranes (25). Structurally, all Siglecs have an extracellular recognition domain, a transmembrane domain and an intracellular domain, which can bear different residues (Figure 2). Intracellular domains participate in downstream signaling processes, by inhibiting cell function (26). Studies on mouse and human Siglec molecules have revealed that there is specific expression of Siglec-8 on human eosinophils, while the Siglec-F is preferentially found on mouse eosinophils (27). Siglec-F molecules appear on the membranes of immature eosinophils in the bone marrow at a late stage of development, and remain in the mature state. This fact indicates that this molecule may serve as a specific marker for eosinophils for determination of cell maturity during development (28).

Among a battery of cell surface molecules, eosinophils bear the receptors for hematopoietic cytokines such as IL-5, IL-3 and granulocyte-monocyte colony stimulating factor (GM-CSF). These cytokines promote eosinophilopoiesis *in vivo*, prolong eosinophil survival and modulate eosinophils activation *in vitro* (29). Eosinophils cultured in the presence of IL-3 and/or GM-CSF enhanced the production of lipid mediators and release of cytotoxic proteins upon contact with specific stimuli. IL-5 was also shown to be essential for eosinophil chemotaxis

and continued existence in tissue by promoting the activation of their surface integrins and adhesion molecules (30).

The above-mentioned availability of active adhesion molecules indicates that eosinophils roll along the vascular endothelial cell layer, adhere to activated endothelial cells and reach the sites of inflammation through diapedesis. They express an array of chemotactic, adhesion and transcellular trafficking molecules on surface membranes, such as very late activation antigen (VLA), integrins β_1 and β_2 (CD11c, CD11b), L-selectin and the following immunoglobulin superfamily members: intercellular adhesion molecule-1 (ICAM)-1, CD58 and CD31 (2). All adhesion molecules strengthen the interaction between eosinophils and inflamed tissue, thus, they assist in delivery of these leucocytes to the effector site.

In addition to the functional role of adhesion molecules in eosinophil motility, there is a system of chemokines and their receptors that is essential for cell trafficking to tissue sites. Noteworthy is eotaxin, a very potent eosinophil-specific chemoattractant that was discovered during experimentation with a guinea pig model of allergic inflammation (31). The study also revealed that expression of eotaxin in the lungs was constitutive. Further studies involving the use of eotaxin$^{-/-}$ mice demonstrated the necessity of this chemokine for maintenance of basal levels of tissue eosinophilia (32). As a ligand for eotaxin signals eosinophils express the chemokine receptor CCR3, which can be either present on the cell membrane or be internalized into the cytoplasm (33). An

interchange between surface and internal expression of functional molecules may be an example of eosinophils' heterogeneity.

Eosinophils are morphologically and functionally heterogeneous depending on the state of maturation, cell cycle stage and presence or absence of activation stimuli. When stimulated, they undergo intracellular changes to their granules and secretory vesicles, leading to solubilizing of the granules' crystalloid core with a rest of content, and restructuring of the cytoskeleton (2). They also multiply immunoglobulin receptors, MHC class II molecules (HLA-DR) and integrins on their plasma membranes. In allergen sensitized individuals the majority of eosinophils (about 65%) undergoes general morphological changes in cell density, and become hypodense (34). It has been suggested that hypodense eosinophils manifest higher state of activation and capability of *de novo* synthesis of different cytokines, lipid metabolites and mediators.

Eosinophil development

The bone marrow derived hematopoietic stem cells (HSCs) are pluripotent stem cells, which give rise to all types of blood cells (Figure 3). Hematopoiesis is under the tightly regulated control of transcription factors including GATA-1, GATA-3, PU.1 and Ikaros. These transcription factors guide the stem cells to differentiate into subsets of common lymphoid (CLP) and myeloid progenitors (CMP) (35). The PU.1 transcription factor is present in cells of both lineages, and restricted fluctuation in its levels in combination with GATA-1 factor leads to the development of granulocyte-monocyte progenitors (GMP) (36). Further differentiations of GMPs are the outcome of continued expression of PU.1 and

downregulation of GATA-1 for the monocyte/neutrophil lineage (37). Whereas, the eosinophilic progenitors continue to produce GATA-1 and C/EBPα (38). The GATA-1 transcription factor is considered to be the major genetic regulator of committed eosinophilic progenitors. A GATA-1 gene knock out model resulted in mouse development devoid of eosinophils (39).

Other aspects aside from transcription factors are essential for eosinophilopoiesis. Hematopoietic cytokines IL-3 and GM-CSF provide eosinophils' progenitors with survival signaling. The role of GM-CSF in eosinophil hematopoiesis is well established. At the onset of generation of the two main lineages some HSCs clones upregulate the expression of the receptor for GM-CSF and commit to the GMPs stem cells (40). Functioning of the PU.1 transcription factor directly influences expression of receptors for hematopoietic cytokines. In developing granulocytes, the downstream signaling of the GM-CSF receptors maintains cell division and survival (41). Generally, the GM-CSF provides a directional as well as supportive function during granulocytopoiesis. It has been shown experimentally that GM-CSF alone does not maintain lineage commitment in the absence of gene regulators and other cytokines (42).

Another cytokine that plays a key role in eosinophilopoiesis is IL-5. Experiments with peripheral blood and bone marrow isolated $CD34^+$ stem cells have shown that small number of granulocyte-monocyte colonies contained about 5-10% of cells, expressing receptors for hematopoietic cytokine IL-5α chain (43).
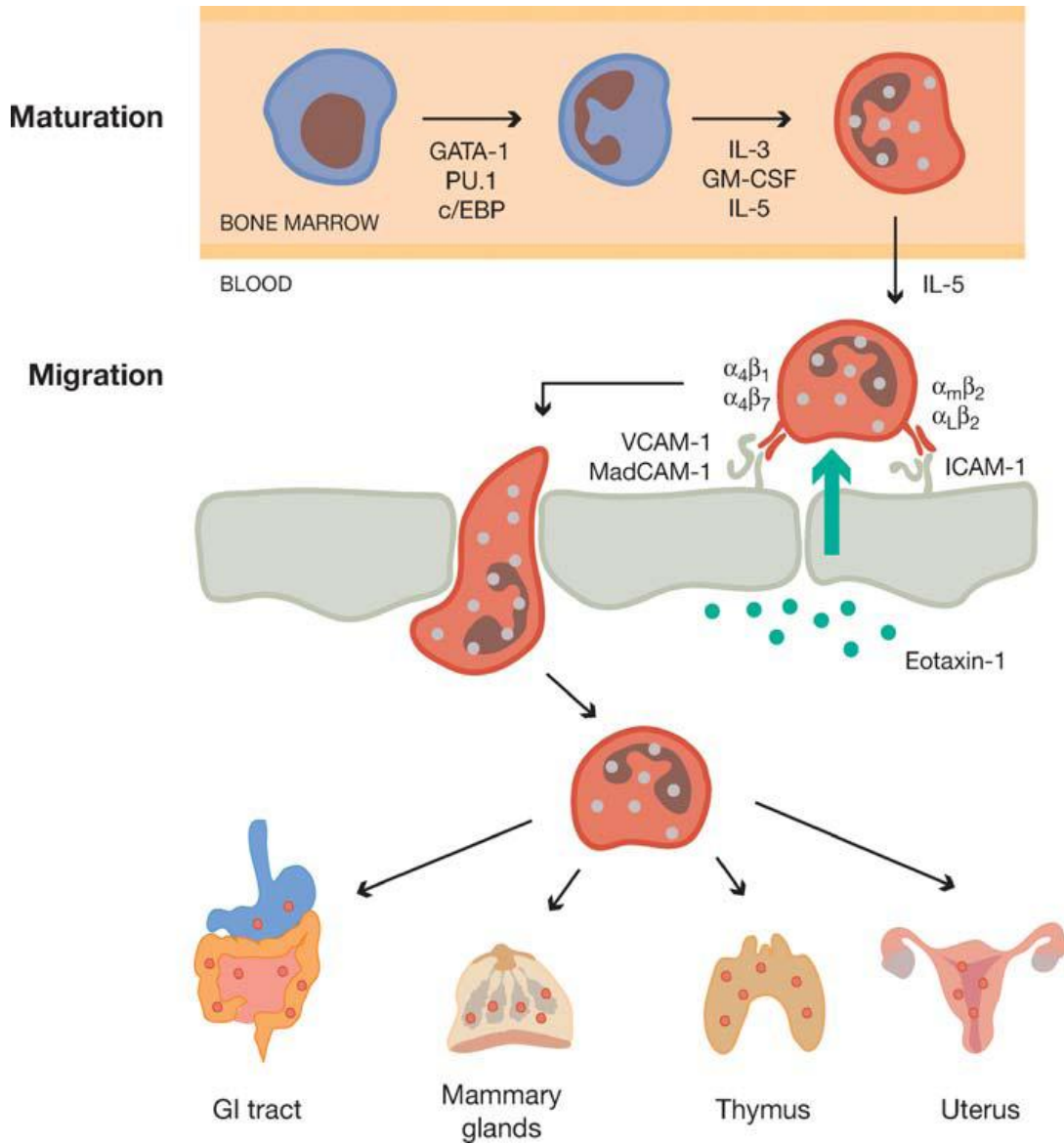
Figure 3. Stages of eosinophil development, recruiting and homing to the tissue.

Adapted from Rothenberg, M. E., and Hogan, S. P. 2006. *Annu. Rev. Immunol*.

These cells develop into committed eosinophilic progenitors under the influence of IL-5 (44). The evidence from the experiments with an IL-5 overexpressing mouse model (45) and IL-5 knockout mice (46) support the idea that IL-5 is of primary importance for eosinophil development, differentiation and survival in tissues. T-lymphocytes in human blood express baseline levels of IL-5, and the Th2 subpopulation has the potential to produce large amounts of this cytokine (47). IL-5 messenger RNA was also detected in cells, isolated from many organs in mice, but considerable levels were obtained from the lungs, thymus, bladder, uterus and spleen (48). In humans, IL-5 expression was also described in lung epithelial cells (49). These data indicate organs and peripheral sites that potentially may support eosinophil homing and maturation after they exit bone marrow.

At the final stages of cellular advancement, proeosinophils lose mitotic ability and synthesize functional molecules. Transcription factors and hematopoietic cytokines are implicated in expression of eosinophil-related products. During the process of eosinophil development and maturation several protein molecules such as granule-stored MBP as well as other signaling molecules are synthesized in response to hematopoietic cytokines (IL-5 and GM-CSF) and transcription factors (GATA-1, PU.1, and C/EBP isoforms) (50). Once eosinophils reach the final stages of maturity, they egress from the bone marrow and migrate to peripheral sites (Figure 3).

Mobilization of eosinophils from the site of hematopoesis to the peripheral tissue sites is achieved and enhanced by eotaxin-1 and eotaxin-2 signaling (51).

Eotaxin-derived chemotactic signals, delivered to bone marrow eosinophils, contribute to the eotaxin receptor CCR3 expression and stimulate precursors towards terminal maturation (52). The CCR3 ligation initiates Ca^+ mobilization within eosinophils and subsequent *de novo* synthesis of proteins and mediators (53). At this stage eosinophils also upregulate integrins and adhesion molecules. The interaction between eotaxin and its receptor in cooperation of IL-5 provides eosinophils with robust stimuli to exit the bone marrow and enter the blood circulation (54).

Eosinophil migration and homing

Upon maturation to fully developed cells, eosinophils circulate in the blood and prepare to migrate to the peripheral sites (Figure 3). Specific recruitment to the tissue involves margination, rolling, adhesion and diapedesis through vascular endothelial cells to reach the specific inflammatory site by chemotaxis (2). The entire process is facilitated by upregulation of key adhesion molecules. Constitutively non-activated eosinophils express a carbohydrate-reach adhesion molecule L-selectin, which interacts with capillary endothelial cells bearing E-selectin. This temporal contact allows the cells to roll along the blood flow and receive additional humoral stimulation from the site of inflammation (55). Perivascular lymphocytes, macrophages and endothelial cells release cytokines and lipid mediators, which may activate eosinophils, resulting in an increased affinity and expression of adhesion molecules on the eosinophils' surface. The most efficient activators of eosinophil recruitment are hematopoietic cytokine IL-5, non-specific cytokines IL-2, IL-4, IL-13, RANTES and a platelet aggregation

factor (PAF) (56). The peripheral chemoattractants eotaxins-1 and-2 together with IL-5 play a significant role in the upregulation of CCR3 receptor and additional stimulation of the cells (57). Other adhesion receptors that become activated under eotaxin/CCR3 signaling are the β1-integrin, VLA-4 (CDw49d/CD29), which binds to VCAM-1 on endothelial cells; another group of molecules are the β2-integrin receptors LFA-1 (CD11a/CD18), Mac-1(CD11b/CD18), and α X β2 (CD11c/CD18). The last one binds to ICAM-1 on epithelial cells (58). Integrins and adhesion molecules initiate more specific attachment of eosinophils to the vascular wall that enables them to extravasate to the surrounding tissue (59). The migration is guided by the concentration gradient of released chemotactic mediators and cytokines. The moderate concentrations of proinflammatory molecules preferentially prime eosinophils, whereas high concentrations cause eosinophils to undergo *in situ* activation and degranulation (60).

Distribution of eosinophils

The normal level of blood eosinophils ranges between 1-2% generally. They have a half life of 8 to 18 hours in the blood stream and have a preference to home to different tissues. A substantial number of eosinophils are found in the gastro-intestinal tract (GIT), mammary glands, uterus and thymus (61) (Figure 3). In mice, GIT eosinophils are detectable at the onset of late gestational stage and early postpartum period. The infiltration is independent of either the presence of any bacterial flora or allergic sensitization. The arrival and homing of eosinophils to the GIT is essentially regulated by the constitutive expression of eotaxin in the intestine, coordinated with secretion of the hematopoietic cytokines IL-5 and GM-

CSF (62). Eosinophils are detected in all parts of the normal GIT, but not in the esophagus and the tongue under normal conditions. They are predominantly found infiltrating the submucosal layer. Oral and esophageal eosinophils are more likely associated with severe diseases such as oral squamous cancer and eosinophilic esophagitis (82). The distribution and patterns of eosinophilic infiltration in mice were found to be similar to humans. Sensitization and challenge with airborne allergens did not influence the presence of eosinophils in the GIT (63). Multiple evidences suggest that gastrointestinal eosinophils in normal conditions secrete their granules contents (64).

In the female reproductive system eosinophilic infiltration is restricted to the mammary glands and uterus. The presence of eosinophils in the mammary glands is limited to the period of puberty, and associated with the increase in levels of constitutive eotaxin expression by the ductal epithelial cells (65). Overexpression of IL-5 and hypereosinophilia resulted in the retarded development of the mammary glands in mice with otherwise normal reproductive function, indicating the primary importance of physiological levels of eosinophils during ontogeny (66).

Eosinophilic infiltration of the uterus may have some modulatory effect in the female reproductive function. The prolonged interval between estrus, diminished birth weight and reduced time of implantation was observed in the IL-5 deficient mice, indicating the role of this cytokine on eosinophils in reproduction (67). It was demonstrated that eosinophil influx to the uterus and cervix depends on the level of estrogen, and fluctuates along with cyclic changes of estrogen:

progesterone ratio. The number of eosinophils increases during estrus and early pregnancy compared to other periodical changes in the female genital tract (68).

Another site of eosinophil homing is the thymus. Although the thymus has been repeatedly noted as a homing site for the eosinophils, the precise impact of these cells during thymic ontogeny has not been elucidated. Studies indicate the presence of immature eosinophils in mouse thymus, as detected by CD33/CD34 markers expression and electron microscopy (69). The thymic eosinophils were reported to be absent in the eotaxin deficient mice suggesting their recruitment to the thymus (32). A recent study by Throsby, M. *et. al.* (2000) revealed specific pattern of eosinophilic infiltration in the mouse thymus (70). In addition to the observation of physiological infiltration the influx of eosinophils was observed only upon the deletion of reactive thymocytes in reported model of acute negative selection. Molecular pathways that may contribute to the thymocytes apoptosis are yet to be investigated. In my study, the possible mechanism of interaction between eosinophils and developing thymic lymphocytes was examined.

Eosinophils and immune response

Eosinophils are *end cell* leukocytes with the capacity to execute a complete range of immune functions starting from innate antigen recognition up to effective parasite elimination (Figure 4). Communication between eosinophils and T-lymphocytes is essential to maintain adapted and effective immune response (ref). The eosinophils are attracted to the sites of inflammation by the Th2 type cytokines and chemokines secreted as a consequence of APCs and T-lymphocytes interaction (57). I will describe other potentially important functions of

eosinophils expressed during immune responses, especially allergic inflammation and tumors.

Antigen presentation is one of initial steps in cascade of immune response and eosinophils participate in this event. Throughout the constitutive expression of human leukocyte antigen DR (HLA-DR) eosinophils have been shown to present antigens (71). Purified peripheral blood eosinophils from healthy donors, incubated with soluble helminth antigens increase the surface expression of MHC class II molecules and prime naïve T-cells to produce IL-5 (72). During allergic inflammation eosinophils undergo activation of *de novo* protein synthesis and become a source of a range of cytokines (73). They secrete cytokines IL-1, IL-2, IL-4, and IL-10 capable of promoting of effector Th cells proliferation. Murine eosinophils at the site of inflammation stimulate T cells to produce large amounts of IL-3, IL-5 and IL-13. The hematopoietic cytokines further support the development and maturation of eosinophilic precursors in the bone marrow and their subsequent influx to the tissue (44). Thus, eosinophils at tissue sites are able to create a microenvironment that supports their own survival and function through the induction of hematopoietic cytokines production both in an autocrine and paracrine manner (74).

The IL-13 and IL-13R are key molecules in inducing mucus hyperproduction, neovasculogenesis and subsequent thickening of the epithelial basal membrane with tissue remodeling during allergic asthma (75). Thus, eosinophils through the production of IL-13 as well as release of cationic proteins, which directly affect
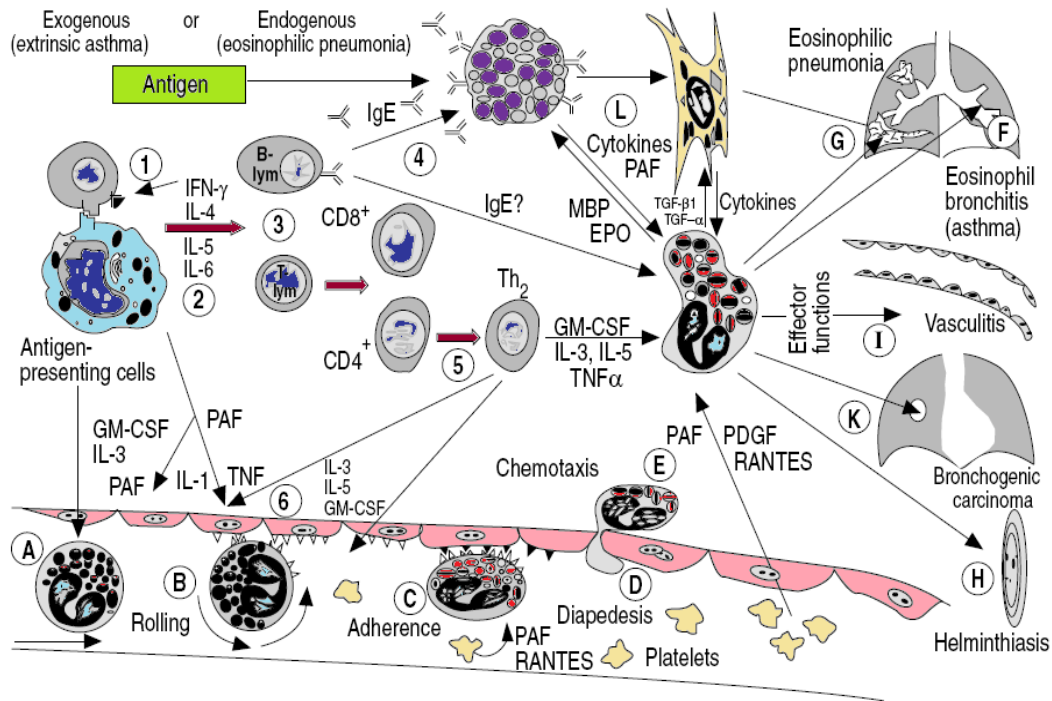
Figure 4. Putative functions of eosinophils in immunity and inflammation.

D – Diapedesis

E – Migration to the inflamed tissue

F – **D**estruction and damage of airway epithelium

G – Interstitial edema in eosinophilic pneumonia

H – Parasitic infection

I – Granulomatous tissue destruction or formation during eosinophilic vasculitis

K- **C**ontribution to the tumors elimination by toxic products

L- Intensification of inflammatory reactions through activation of tissue cells

1 – Antigen presentation
2 - APCs cytokines release
3 T-lymphocytes activation
4 IgE secretion
5 Th2 cells cytokine secretion
6 Induction of eosinophils mobilization to the site of inflammation, epithelial cells activation

Adapted from Kroegel, *et.al*. 1994. *Eur Respir J.*

neuro-muscular tone, are major contributing cells to the tissue remodeling in allergic airways inflammation (76). Strikingly, recruited eosinophils to the site of inflammation become a source of IL-4 cytokine, thus they further support the predominance of Th2 lymphocytes (77). Research has shown that eosinophils traffic to the regional lymph nodes; this was further elucidated in our laboratory when the experimental evidences suggested that lymph nodes infiltrating eosinophils modulate the immune response *in situ* by their constitutively expression of the enzyme Indoleamine 2, 3-dioxygenase (IDO) (78).

One more important immunogenic function is an optimal T cell stimulation delivered by TCR and co-stimulatory molecules litigation. Eosinophils have been shown to bear co-stimulatory ligands CD80, CD86 in a resting and stimulated state (79). In addition, eosinophils express an immune modulating action in allergic inflammation through providing CD40 co-stimulation, which is necessary for the switch in antibody production phenotype in B-cells and the support of Th2 cells predominance (80).

Eosinophils and cancer

Paul Ehrlich has identified the presence of eosinophilic infiltration within solid tumors and surrounding tissue soon after discovery of these cells in 1879 (81). However, the role it plays in a neoplasia-associated ailment is poorly understood. Eosinophils were found in many types of cancers. Tumor-associated tissue eosinophilia (TATE) is subdivided into two opposite groups: favorable and poor cancer survival prognosis, associated with high numbers of tumor eosinophils (82). Cormier *et.al.*, (2006) revealed that tumor infiltrating

eosinophils take part in the inflammatory response against cancer cells (5). They are actively recruited to demarcate the immune-active boundary between healthy and damaged tissue (83). In some cancer types tumor cells possess the ability to recruit these immune modulatory leukocytes to deviate their antitumor defense. Through this mechanism malignant cells escape T cell-mediated cytotoxicity responses (84). In cases of poor prognosis associated TATE, the tumor cells interact with the immune system in suppressive way to alter anti-tumor host response (85). This evidence suggests that eosinophils may be drawn as modulators of these mechanisms in such cases of neoplasia. Experimental observations showed that in non-small cell lung carcinoma, known by eosinophilia-poor prognosis association, the infiltrating eosinophils express IDO (86). This finding indicates that in cases of tumors with poor prognosis, eosinophils act to suppress T-cell immunity through production of immunoactive enzymes. Thus, in cases of malignancies, eosinophils actively interact with surrounding cellular compartments, expressing either protective or immune suppressive properties.

All existing evidences to date suggest that eosinophils, in either homeostatic or pathological conditions, play an active role in adaptation to changing microenvironments. Although eosinophils will remain well acclaimed as *end* cells in a parasite's elimination and in response to allergenic exposure, novel data strongly suggests that there is an emerging role for them in immune modulation in all tissue sites where they are present (87).

Immune-modulatory Function of Indoleamine 2, 3-dioxygenase

Immune modulation is an essential mechanism that allows the generation of highly adaptable and targeted responses to a variety of antigenic stimuli. Professional antigen presenting cells (APCs) such as macrophages, DCs and eosinophils act as major components to immune modulation during the course of allergic inflammation, tumor invasion and infectious diseases. The main features of immune adaptation are the ability to develop distinct populations of T-lymphocytes with variability of secreted cytokines, generation of natural regulatory T-cells and the induction of complex tolerogenic mechanisms. The term *tolerance* refers to a special state of the immune system where no tissue-destructive inflammatory response against a specific antigen is maintained in the absence of immune deficiency. The decision to induce tolerance or generate immunity requires the integration of diverse signals that APCs acquire while interacting with innate and adaptive components of the immune system (88). The cellular and humoral mechanisms, such as antigen presentation, cytokine secretion and delivery of apoptotic signals, are actively involved in tolerance development.

Among the mechanisms that may be generated to achieve non-responsiveness to antigens is clonal deletion of foreign and/or self-antigen specific T-cells. Recent literature provides a large number of observations that induced expression of tryptophan catabolizing enzyme Indoleamine 2, 3-dioxygenase (IDO) and

generation of immune active metabolites arrest proliferation of activated T-cells, thus modulating immune response (89).

Tryptophan is an essential amino acid consumed in the body for *de novo* protein synthesis and other metabolic functions; it is not synthesized by mammalian organisms and is delivered through the food chain (90). The breakup of this amino acid occurs in many organs of human body and there are two rate-limiting enzymes inducing tryptophan catabolism for downstream residues: Tryptophan 2, 3-dioxygenase (TDO) and Indoleamine 2, 3-dioxygenase (IDO) (Figure 5). TDO is a liver restricted enzyme with high substrate affinity, whereas IDO is expressed extrahepatically in many cell types, has less specificity for its substrate and plays a significant role during immune response (89). Both enzymes act during oxidation of the tryptophan indole ring, which is the first step in the tryptophan catabolism pathway (Figure 5). In contrast to TDO, which is a housekeeping enzyme and is not induced, IDO requires stimulation for the induction of mRNA expression and protein synthesis (Figure 5). Infections and inflammatory responses are common conditions, inducing IDO enzymatic activity in many cell types of human body.

During onset of infection/immune response and subsequent release of proinflammatory cytokines such as interferons (IFN), type-I (IFNs α/β) and type-II (IFN-γ) many cell types of the body react with a robust IDO synthesis and tryptophan catabolism (91). Even though the interferons are the most potent IDO inducers *in vivo,* cells of immune system express IDO also in response to combined stimulation with lipopolysaccharides (LPS) and TNF (92). Studies of
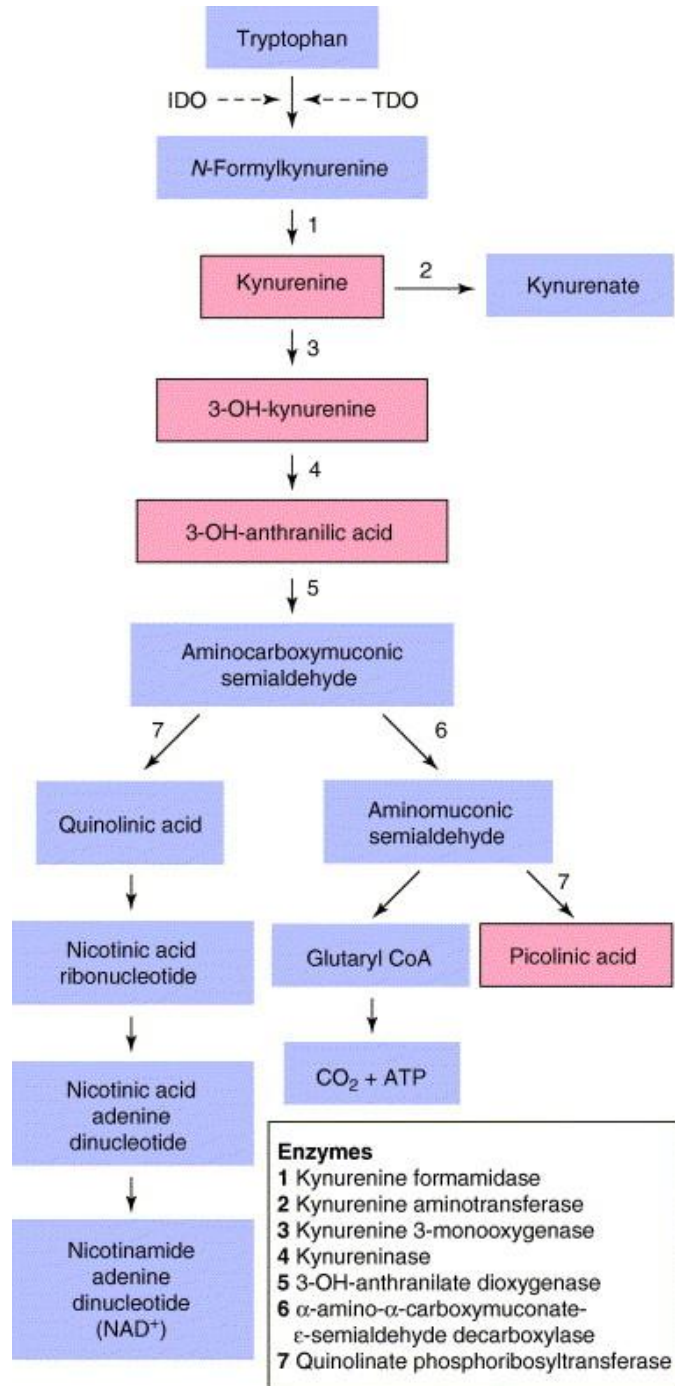
Figure 5. Kynurenine pathway of tryptophan catabolism in mammalian cells.

Adapted from Grohman, U. 2003. *Trends in Immunology*

tryptophan catabolism revealed additional IFN-independent IDO inducer. The ligation of the cytotoxic lymphocyte antigen-4 (CTLA-4) and co-stimulatory molecules CD80/CD86 was shown to be efficient in IDO initiation in IFN-γ deficient mice (93).

In contrast to an induced IDO production, several tissues employ constitutive expression of tryptophan consuming enzymes for *de novo* synthesis of bioactive molecules. Tryptophan catabolism is a source of essential functional molecules such as serotonin and melatonin in the nervous system, as well as cellular co-factor NAD+ in all cell types (94) (Figure 6). In immune privileged sites, such as reproductive system and CNS tryptophan catabolites are employed constitutively for the consumption of superoxide ions thereby playing a protective role (95). In recent years there has been an increasing interest to the function of this pathway in the immune system.

One of the first reported studies that proposed the immune modulatory activity of IDO pathway explored the expression of this enzyme in trophoblast cells during pregnancy and its protective role for the allogeneic fetus against maternal T-cells (96). Experiments in mice revealed that there are cells in immune system that are capable of producing large amounts of IDO either constitutively or upon stimulation (Figure 6). Specifically, immature dendritic cells were shown to have the capacity to express IDO constitutively (97). These DCs possess specific phenotype and express CCR6/CD123 markers (98). The subsets of conventional DCs, bearing CD11c and CD8α markers, plasmacytoid DCs (99) and macrophages are also the sources of immune-active IDO (100).
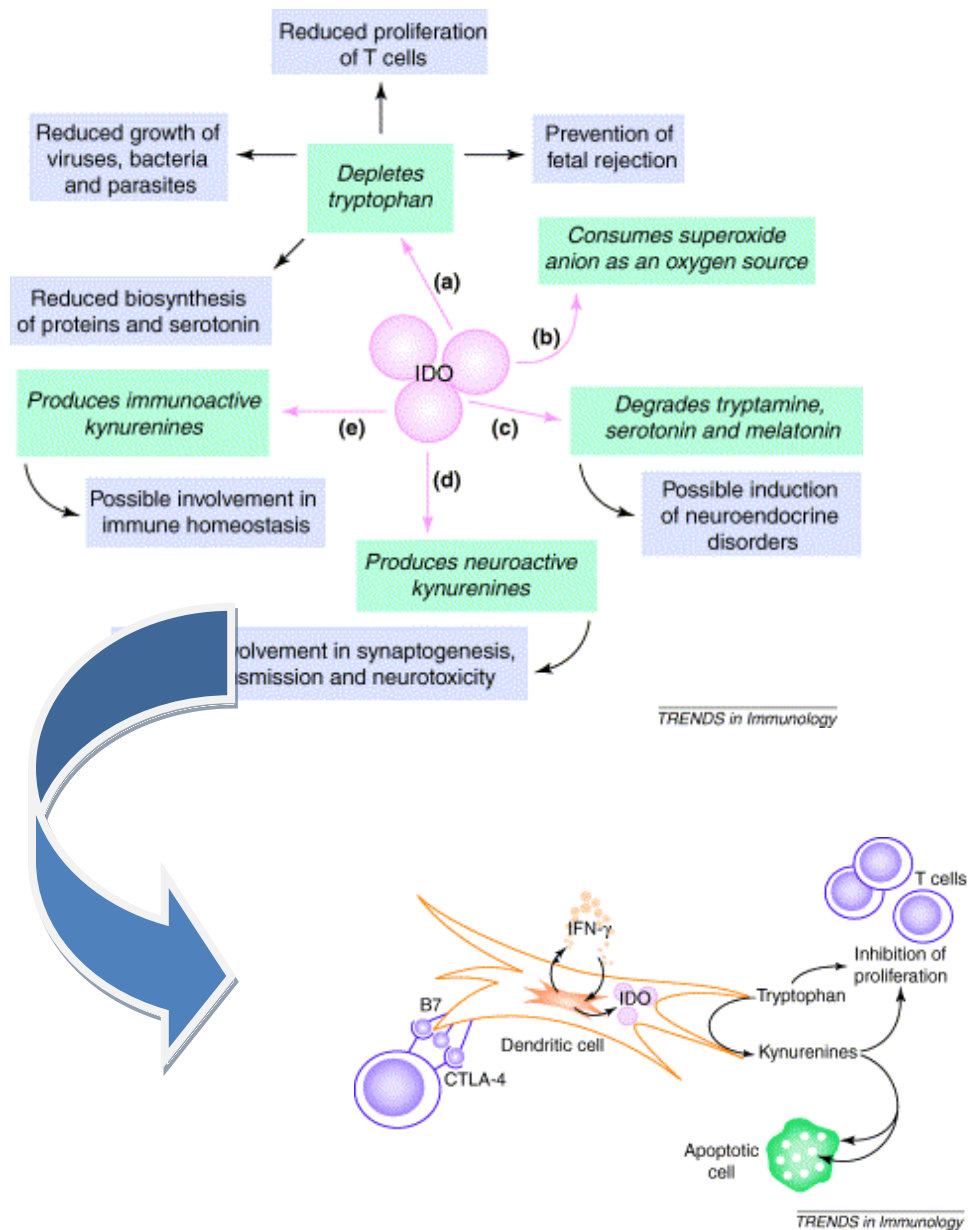
Figure 6. Effects of IDO induction pathways and possible roles in physiopathological conditions including a mechanism of IDO-based immunological tolerance.

Adapted from Grohman U., *et.al*. 2003. *Trends in Immunol.*

Thus, in the immune system the IDO production and function is associated with cell types capable of immune modulation.

Observations on the effects of excessive tryptophan catabolism on live cells demonstrated significant inhibition of cellular division and development. Two theories have been proposed to explain how tryptophan catabolism can modulate cell growth and immunity (89). The first theory speculates that extensive tryptophan catabolism suppresses T cell proliferation by significantly reducing the supply of this essential amino acid. The other theory postulates that downstream metabolites of tryptophan catabolism act to suppress certain immune cells by pro-apoptotic mechanisms.

Primarily, IDO studies have explored the effects of IDO induction in the experimental models of tumor growth inhibition and its antimicrobial effects that could be attributed to acute tryptophan starvation (101). However, in the body the local tryptophan content is continuously regulated by blood flow, which renders the concept of weak tryptophan concentrations. This argument shifted the emphasis in studies of IDO induced tolerance towards exploring the metabolic pathways that may cause proliferation arrest of T-cells. The downstream molecules of the KYN pathway, such as quinolinic and 3-hydroxyanthranilic acids, 3-OH-kynurenines have been demonstrated to be toxic to neurons and implicated in a range of some neuro- degenerative disorders (102). Besides CNS, substantial amounts of quinolinates are produced in the lungs and lymphatic system where they may affect immune responses.

This idea guided research towards experimental evidences of immune activity of tryptophan derivates. Further observations revealed the inhibition of T- cell proliferation in contact with derivates of KYN pathway in studies using lung transplant rejection in rats (103). In support of these findings the study by Fallarino *et.al.,* (2002) revealed the toxicity of quinolinic acid and 3-OH-kynurenine to the specific lymphocyte populations when injected into mice. These studies showed that some subtypes of T-cells, especially immature CD4/CD8 double positive thymocytes are more likely to undergo apoptosis by tryptophan catabolites (104). It is well known that clonal deletion of autoreactive immature thymocytes takes place in the thymus during negative selection. Pro-apoptotic molecules of this process have not yet been sufficiently investigated. Thus another focus of my study was to study the role of IDO in intrathymic negative selection.

Thymus: Structure and Function

The thymus is a primary lymphoid organ. The hierarchy of lymphoid organs is determined by their structure; the way antigens and lymphoid cells make their entry and exit from these organs, and what outcomes are generated as a result of particular interaction of an antigen with its specific T helper cells (105). T-cell receptor specific T lymphocytes develop in the thymus from the common lymphoid progenitors that emerge from bone marrow (106). The maturation of thymocytes progresses under the physiological control and does not require exogenous antigen presentation (107).

Anatomy of the thymus

The macroscopic structure of the thymus was described a long time ago. However, this organ did not attract critical attention because of the lack of considerable knowledge regarding its importance for the body functions (108).

By the end of the fetal period in mammals, the thymus is a broad, irregularly lobulated organ situated in the anterior mediastinum above the heart dorsal to the sternum and extending into the neck on top of the trachea with two small processes (109). The thymus is a very fast changing organ. At the time of birth the thymus achieves its greatest relative weight. Nonetheless, its absolute weight continues to increase, reaching 30 to 40 g at about the onset of puberty (109). Under the influence of shifting levels in the pituitary-adrenal axis hormones, starting with puberty, the function of the thymus declines (110). The increased concentrations of growth and sex hormones cause the major changes in release of the variety of humoral factor and intrathymic hormones that support the activity of the thymus (111). There are several intrinsic factors such as aging, genetic and humoral factors that can affect the immune competence of the thymus. With aging the prolipherative ability of thymocytes, as well as the capacity of the bone marrow to sustain the influx of new cells diminishes (112). Under the influence of genetic and humoral factors the thymic gland decreases in size and weight. The ultrastructural changes inside the organ display substitution of lymphoid compartments by deposition of adipose tissue. Thymic cellularity and density are also diminished (113). For a better understanding of thymic function I present morphological details of this organ.

A macroscopic examination of the thymus reveals two compacted symmetrical halves (lobes). The connective tissue capsule, consisting of two layers surrounds both lobes. The external layer covers the lobes and the internal layer penetrates the parenchyma to form either septae or trabecules (114). The trabecules divide the lobes into smaller irregular compartments (lobules). Each lobule has separate branch of arterial and venous vascularisation (115). Capillaries invade two main lobular compartments: the cortex and the medulla, and form a very dense network at the cortico-medullary junction. These compartments can be easily described; however the origin of populating cells has not been attributed to a particular type for a very long time.

The descriptive study of the thymus using microscopy at the beginning of the past century revealed the similarity between the cells populating the thymi and peripheral blood lymphocytes (116). Thymic cells were found to be distributed differently inside each lobule with the formation of two anatomical substructures. Any conventional histochemical stain, where the cortex appears usually as darker subcapsular area and centrally situated medulla is lighter stained, can easily visualize the main thymic anatomical compartments (117). The cortex is tightly populated by immature thymocytes and scattered cortical epithelial cells, whereas the density of the medulla is lower and it consists of diverse cell population along with semi-mature and mature thymocytes (118). In contrast to other lymphoid and non-lymphoid organs, which develop their stroma from connective tissue, the thymic stroma contains predominantly reticular and epithelial cells (119). Epithelial space inside of each lobule and perivascular spaces are separated from

each other by a closed, flat epithelial cell layer with a basal lamina that contributes to the blood-thymus barrier (114). The ultrastructure of thymic compartments is distinguished by several types of epithelial cells (Figure 7). Some of them are restricted to either cortex or medulla and have a diverse structure that has an impact on cell density. Microscopic investigations helped to distinguish cellular properties and ultra structures that led to thymic cell classification.

Morphologically all human thymic epithelial cells could be subdivided into 6 types (Figure 7). Type-1 cells form an almost continuous layer under the capsule and around the capillaries. Type-2 cells are large, have a pale nucleus with dark cytoplasmic inclusions and are situated predominantly in the outer cortex. Type-3 cells have unevenly shaped nucleus, cytoplasmic extensions and can be found in deeper cortex. Type-4 cells express high affinity to staining, have cytoplasmic processes and are located in the medulla whereas type-5 cells have moderate stain and situated predominantly in the cortico-medullary region. Finally, type-6 cells are almost the largest cells that are found in the thymus and are located in the medulla in proximity to the Hassall's corpuscles (120).
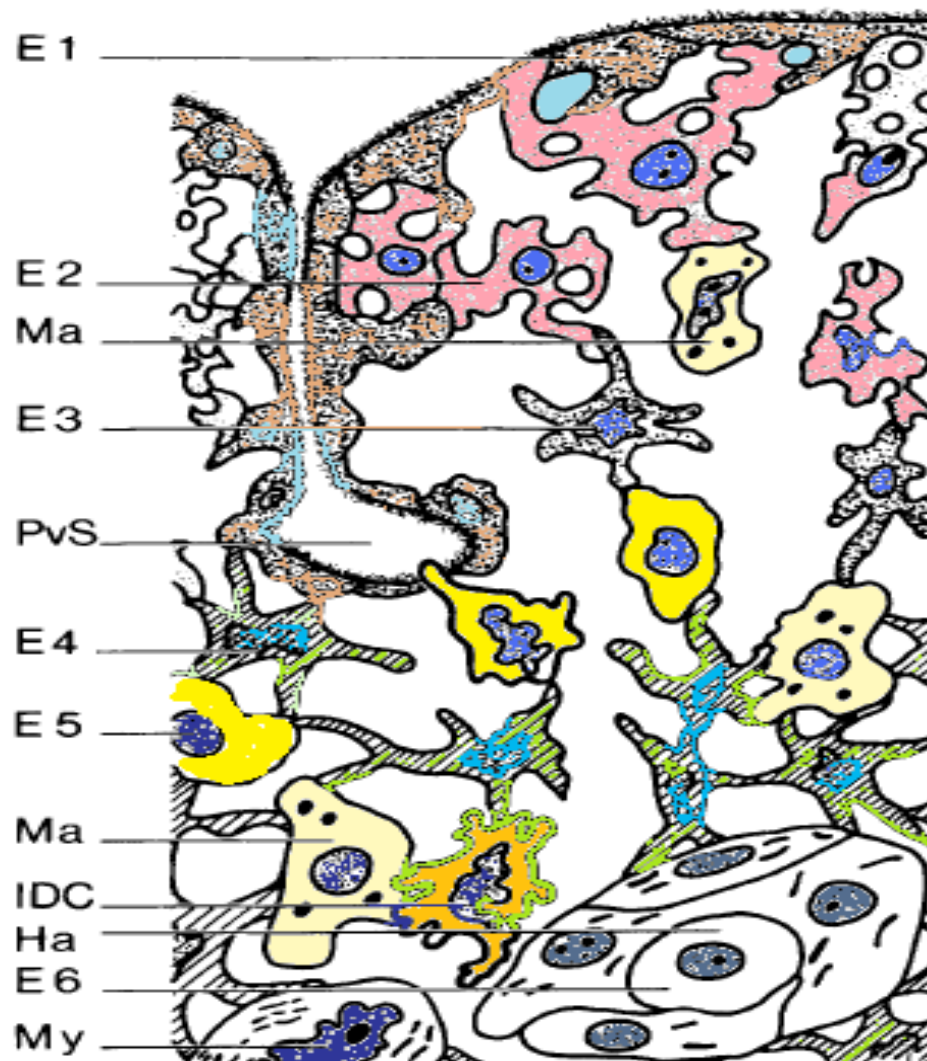
Figure 7. Schematic representation of thymic stromal microenvironment.

Thymus micro-environment composed of six types of epithelial cells *(El* to E6), macrophages *(Ma),* interdigitating cells *(IDC)* and myoid cells *(My).* The type 6 epithelial cells form Hassall's corpuscles *(Ha).* The type 2 and 3 epithelial cells are considered to represent the thymic nurse cells.

 Adapted from *Anatomy and Embryology* 1991.

Hassall's corpuscles are specific thymic structures that were first described in the 1840's by British pathologist Arthur Hassall as corpuscular bodies composed of agglomerated reticulo-epithelial cells in the medulla (121). They appear at a stage, when thymic functions are fully established, and are composed of hypertrophied reticular cells and clusters of mature thymic epithelial cells of types 4 and 6. (122). Hassall's bodies possess some histomorphological features, such as deposition of glycoprotein and mucopolysacharides inside the cells, as well as development of reticular fibers that makes them resemble the epidermal epithelium (123). In addition to epithelial cells, Hassall's bodies may include macrophages and granulocytes such as eosinophils (124). Hassall's corpuscles also represent a very common structure of the medullary compartment in the human thymus (122); however, they absent in mice.

Progression of thymocyte development and trafficking through the thymus is guided apart from subcapsular areas and cortex toward the medulla. The thymic stromal cells repertoire shapes a distinction between medulla and cortex. The medullary compartment continuously expands during thymic ontogenesis with accumulation of selected thymocytes at the latest stages of maturation (128). Medullary epithelial cells are attributed to types 4, 5 and 6 based on cellular density and they accept staining less intense than the cortical epithelial cells (114).

Thymic medullary epithelial cells represent a cell population with unique ability to present self-peptides along with MHC class-II molecules. This characteristic makes them critically implicated in the induction of central

tolerance (129). Besides medullary epithelium, different types of DCs are present widely in the medulla. They are professional APCs, capable of producing of large amounts of MHC molecules, which makes antigens more accessible during the selection (130). It should be noted that unlike other lymphoid organs, where stroma has only supportive purpose for the movement of cellular elements, the thymic stroma acts as an active element in thymus function. To understand better the functional implications of thymic ultrastructural components researchers have always questioned thymic embryogenesis.

Thymic development

The model of the thymic organogenesis was drawn from studies on mice embryos, which demonstrated the origin of thymic rudiment from the third pharyngeal patch endoderm and the third pharyngeal cleft ectoderm (131). At day 9.5 of intrauterine development, buds of two embryonic layers start the thymic premordium from positioning each other (132). The synergistic outgrowth of the ectodermal and endodermal cellular layers forms the thymic rudimental epithelial space. Growing on the opposite sites of premordium the embryonic cells differentiate into future cortical and medullary compartments. Further, usually at day 11.5-12.5 of embryogenesis, the rudiment separates from the pharynx. Throughout all developmental stages ectodermal and endodermal derivatives cooperate closely with neural crest mesoderm (133). The thymic vasculature, capsule and perivascular space have mesenhymal origin and have been shown to be essentially implicated in differentiation of thymic epithelial cells (134). Mesenchymal cells provide developing epithelium with an essential epidermal

growth factor and fibroblast growth factor signaling (135). The mesodermal cells influence not only the earlier stages of the thymic development; they guide the compartmentalization during the later morphological organization (136). Even though both ectoderm and endoderm contribute to development of thymus, the experiments using grafts from different parts of thymic premordium under the kidney capsule demonstrated that endodermal cells were sufficient for the advance of the functional thymus (137). Furthermore, additional experimental evidence suggests existence of common thymic epithelial cells progenitors with a potential to give rise to cortical and medullar epithelial cells (138). These observations deepened our understanding of thymic development.

The epigenetic approach helped to dissect regulation of thymus' developmental stages. The process of thymic organogenesis is genetically regulated by a variety of the transcription factors. The cooperation of the paired box genes 1 (pax1) and HelioboxA3 (Hoxa3) transcription factors is required for the generation of the pharyngeal patch endoderm (139). The expression of pax9 in pharyngeal patch endoderm is necessary for epithelial cells differentiation (140). Functioning of transcription factor Foxn1 starting at day 11.5 enables epithelial compartments to support the newly arriving lymphocyte progenitors (141). This event marks the thymocytes dependent stage of thymic development. Further the thymocytes support the proper epithelial differentiation and in response they receive humoral and cell-to-cell interaction with stromal elements (142). All observations of thymic maturation support the idea that proper structural development of this organ is superior for its functionality.

Even though the thymus anatomy has been well described a long time ago, it was not until 1960 when the thymus was rediscovered as a critical organ for the development of immune competence in experiments by Jacques Miller using thymectomized mice (143). Miller's work demonstrated that lack of a properly functioning thymus at birth affects the subject's health and immune defense later. One more important conclusion that could be drawn from the results of Miller's study was the ability of peripheral T-lymphocytes to generate an antigen specific immune response as well as display tolerance to self-antigens (144). The identification and reaction to a foreign or self peptide bound to the self MHC molecules in the secondary lymphoid sites by T-cells requires a functional αβ T-cell receptor (αβ TCR). As it has been mentioned earlier in this chapter, the thymus is a primary lymphoid organ that is specialized to support an arrangement and selection of functional TCRs on precursor cells (105). A developmental pathway that eventually results in the generation of competent T-lymphocytes starts in the bone marrow with the commitment of some hematopoietic stem cells to the lymphoid lineage. This decision to commit to CLP is regulated by transcription factors. The experiments on the mouse model demonstrated that transcription factor PU.1 alone is critically implicated in CLP commitment. The expression of the IL-7 receptor, which is a central event in the lymphoid lineage decision, depends on PU.1 function (145). Future lymphoid progeny has the phenotype of IL-7R$^+$ Lin$^-$ Sca-1^{lo} c-kit^{lo} at the stage of migration to the thymus (146). It has been shown that thymus-seeding CLPs retain a multiple lineage potential and only distinct genetic regulation results in proper development (147).

One of the essential genetic decisions, which settle on the thymic immigrants to T-cell development, is the activation of the Notch transcription factor signaling (148). This transcription factor regulates early and later events in thymocytes development (149).

Intrathymic T-cell development

Recent research has resulted in better understanding of intracellular the signaling pathways that control maturation of the thymocytes (Figure 8). However, T-cell development is not an autonomous progression. Thymic stromal elements not only home differentiating cells, but also present to them a complex specific microenvironment that plays a critical role during T cell development (150). A combination of cell-cell contact and soluble factors from thymic stromal cells provide signals to developing thymocytes, leading to proliferation, induction of differentiation, or cell death by apoptosis.

All developmental steps, completed by thymocytes are coordinated by chemokines, cytokines and signaling molecules (151). The system of chemokines and their receptors assists in maintenance of thymic compartments by providing cells' guidance. The T-cells progenitors enter the thymus through the enriched in capillaries cortico-medullary junction. The expression of the chemokines CCL21 and CCL25 by thymic epithelial cells (TECs) insures the settlement of progenitor cells in the subcapsular area of the cortex (152).

Arriving cells possess specific phenotype described with reference to the CD molecules as CD8/CD4/CD3 triple negative (TN) and $CD25^-CD44^+$ (153). The triple negative state is also subdivided into specific steps that are distinguished by

the coexpression of CD25 and CD44 into TN1 (CD25 $^-$ CD44$^+$), TN2 (CD25$^+$CD44$^+$), TN3 (CD25$^+$ CD44^{low}) and TN4 (CD25 $^-$ CD44 $^-$), where CD25 is IL-2Rα chain and CD44 is phagocytic glycoprotein (154). The CD44 functions as an integrins-like molecule and is important during migration and settling of progenitors in the thymus (155). At the TN stage 2 immature thymocytes initiate the arrangement of pre-TCR β-chains, proceed to the TN3 stage and become irreversibly committed to the T lineage (156). The assembly of TCR β- chain is an induced event, which begins with the expression of a recombination activating genes (RAG-1, RAG-2) and subsequent initiation of variable/diversity/joining (VDJ) regions gene rearrangement (157). Thymocytes that undergo productive TCR β-chain assembly, acquire the invariant pre-TCR α chain, are positively selected for further development and acquire TCR-accessory structures (158). A pre-TCR compound includes a non-covalently associated polypeptides referred to as CD3 complex (159). The next stage is characterized by changes in the thymocyte membrane molecules that signify transition to finalization of TCR arrangements.

Following a successful β- chain positive selection of pre-TCR, TN thymocytes express a transcription factor of early growth response family (Egr) and eventually become double positive immature cells with a CD8$^+$ CD4$^+$ CD3^{low} phenotype (160). This transition step is the hallmark, when immature thymocytes begin an extensive proliferation (161). At this stage actively dividing thymocytes develop a unique symbiotic complex with the thymic nurse cells. The nurse cells engulf and nurture exclusively double positive cells to support their extensive

mitotic activity (162). Proliferating thymocytes with productive TCR β-chain activate the synthesis of the mature α-chain. The abundant proliferation process assures the accumulation of a huge population of double positive thymocytes that could provide necessary variability of the arranged α/β TCRs for the sustenance of the peripheral pool (161). In mice, the maximum level of double positive thymocytes ready to undergo selection is reached between days 10 and 12 of postnatal development (163). Upon losing the proliferation capacity, double positive thymocytes move close to a positive selection process (164).

Generally, the thymocytes selection is a process of an intensive probation of a proper development of TCR, which would insure mature T- cells, leaving from the thymi for the periphery, are functional (self-MHC restricted) and self-tolerant.

Positive selection is a consequence of whether the TCR on the developing thymocytes is assembled properly and able to recognize a self-peptide in combination with a self-MHC molecule. The positive selection starts in cortical double positive thymocytes (Figure 8) (165). It has been shown that cortical TECs create a unique microenvironment through the expression of costimulatory and MHC molecules, which is explicit for positive selection (166). The MHC class I and II restriction in antigen recognition by future T lymphocyte is one of the features of positive selection.

The consequence of positive selection has two opposing outcomes: either survival signal for the cells through properly assembled TCR or death by neglect of those that cannot successfully recognize a self MHC-peptide complex (167). Various studies indicate that generally positive selection is initiated by low-affinity self-
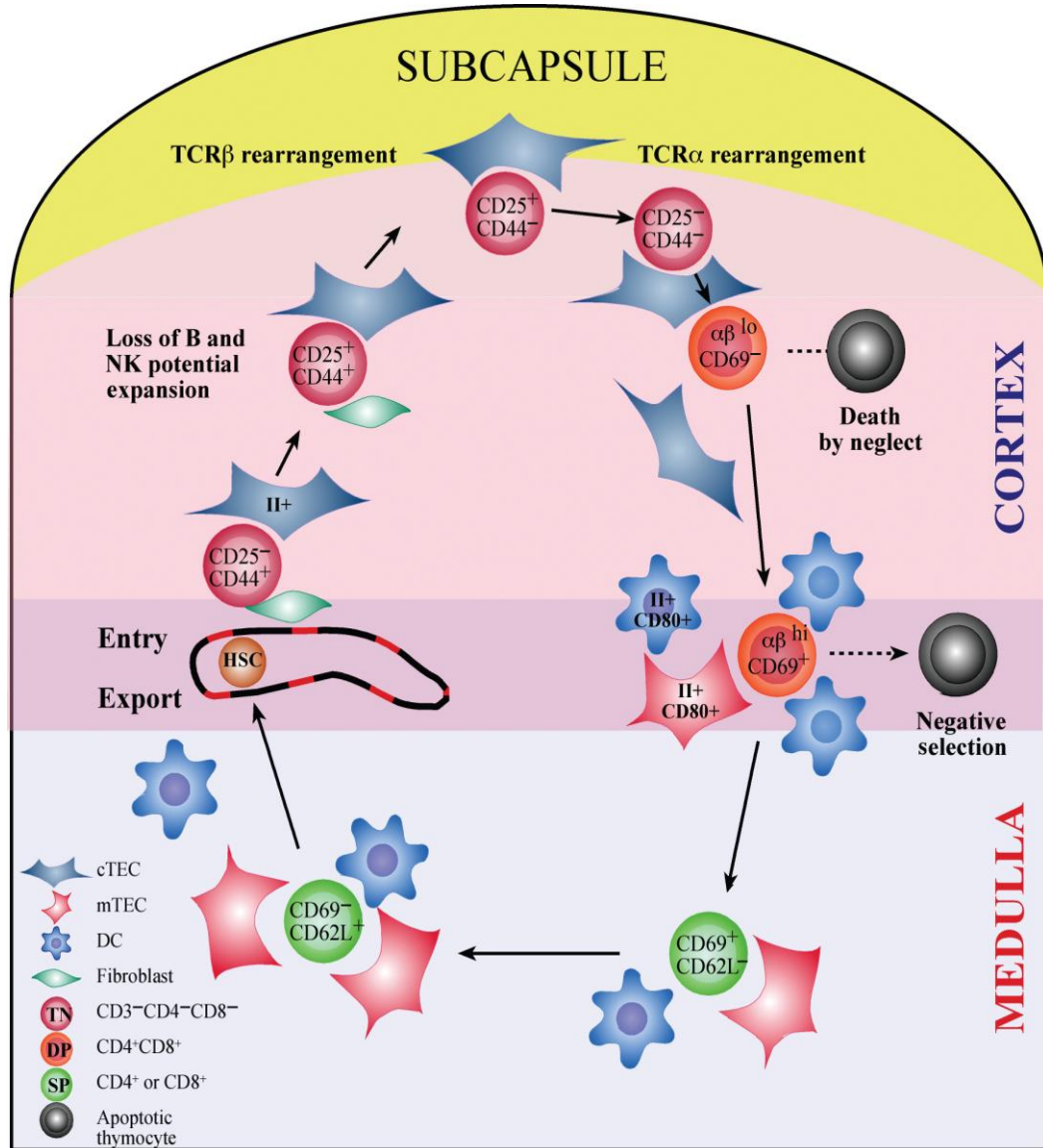
[1]**Figure 8. Thymic compartments, stages and specific cellular interactions, associated with the T-cell development in the thymus.**

Adapted from Gill, J., *et.al*. 2003. *Immunological Reviews;*

peptides with relatively rare accessibility (168). This choice assures peripheral T-cells of having a high affinity to foreign peptides that structurally resemble self-peptides, but are different (169).

Intrathymic development and selection instruct thymocytes in superior recognition of a variety of peripheral unfamiliar antigens as well as maintenance of tolerance towards self-antigens (170). The development of central tolerance is a pathway, which ensures the elimination of the positively selected thymocytes with strong affinity for their selecting MHC–peptide complexes termed *negative selection* (171). The semi-mature double positive thymocytes, which represent a cell population that is most susceptible to apoptosis, undergo negative selection (172).

Unlike positive selection, negative selection is not restricted to a single thymic compartment (Figure 8). It is initiated in the cortico-medullary junction, where positively selected thymocytes move under the influence of chemokine/receptor signaling (173), and continues in the medulla. Importantly, the medullary thymic microenvironment exhibits essential properties that support negative selection. Medullary epithelial cells have exceptional specificity for this cell type to present MHC class II molecules and induce thymocytes apoptosis independently of other cells (174). Several studies involving NOD mice and transgenic models demonstrated the unique presentation of self-antigens by MECs during self-tolerance induction (175). The percentage of *self*-presenting cells in the thymus is not significant, unlike their impact on selection outcomes (176). Even though the importance of epithelial cells for negative selection is

undeniable, the most efficient inducers of this feature in the thymus are bone marrow-derived MHC class II⁺ dendritic cells, which reside at the CMJ (177). The noticeable limitation of MECs for negative selection may be determined by insufficient expression of costimulatory molecules (178).

Observations from the experiments on mouse models demonstrated significant dependence of negative selection on additional stimulatory signaling through costimulatory molecules B-7/B-7.1(CD80/CD86) (179), CD40 (180) and leukocyte common antigen (CD45) (181). Unlike the cortex, thymic medulla is sufficiently infiltrated by costimulation-efficient cells such as DCs and macrophages. Eosinophils, possessing T-cell modulating potential, have also been shown to reside in the thymic CMJ and medulla (70). Possibly, they may provide additional costimulatory signaling for thymocytes selection through their expression of MHC and CD80/CD86 molecules.

The final steps in negative selection involve apoptotic processes that sustain the elimination of thymocytes, bearing self-reactive TCRs (182).The pro-apoptotic molecules are widely expressed in thymic negative selection. Activated cell autonomous death (ACAD) may be induced in thymocytes by metabolic withdrawal, too strong TCR stimulation, glucocorticoids receptor ligation, DNA damage, or a variety of other apoptotic stimuli. All cited mechanisms activate the pro-apoptotic intracellular pathways. Recent studies demonstrated a strong implication of pro-apoptotic Bcl-2 family proteins and NUR 77, an orphan steroid receptor, in maintenance of negative selection of thymocytes (183). However,

noted molecules appeared to be only complimentary for a complex cascade of molecular interaction in thymocyte apoptosis.

The apoptotic mechanisms employed to generate central tolerance in the thymus are distinct from those functioning during modulation of peripheral tolerance. In secondary lymphoid organs the peripheral tolerance is induced by extrinsic activation pathways, which mainly involve Fas/FasL interaction and tumor necrosis factor receptor (TNFR1)/tumor necrosis factor (TNF) ligation (183). During intrathymic negative selection Fas-associated death domain (FADD)-containing molecules, such as FAS, TNFR1 and TNF-related apoptosis inducing ligand (TRAIL), have an important role, but not essentially involved in thymocytes apoptosis (184). However, these data are very limited, controversial and requires further clarification.

Another potent mechanism of peripheral tolerance, the apoptosis of T-cells clones by Indoleamine 2, 3-dioxygenase (IDO)-induced tryptophan catabolism has recently emerged (96). It has been demonstrated that IDO production triggered by CD80/CD86 – CTLA-4 ligation in plasmacytoid dendritic cells facilitated the deletion of cytotoxic T-cells in the models of autoimmune diseases (185). Not only dendritic cells are the source of enzymatically active IDO. Some literature reported that eosinophils, present at the sites of peripheral immune modulation (86) and allergic inflammation (78), express enzymatically active IDO constitutively and thus may contribute to the tolerance induction. There are is no published data regarding to the induction of tryptophan catabolism via IDO activity during clonal deletion of autoreactive thymocytes in the thymus, although

some pre required molecules are widely expressed by thymic stromal elements and thymocytes. It would be of great interest to investigate whether eosinophils that naturally home to the thymus and express IDO constitutively may take part in the intrathymic selection process.

Hypotheses and study objectives:

Central hypothesis: Based on above evidence, I propose that the presence of eosinophils in the thymus at different time points during neonatal T-cell development has immune regulatory implications.

Specific Hypothesis:

Intra-thymic eosinophils constitutively express IDO and participate in thymic T-cell negative selection.

Aims:

To test my hypotheses I aimed to:

1. Reveal the pattern of eosinophilic infiltration in mouse thymus during consecutive time points of early and late postnatal development.

2. Elucidate the changes in thymic morphology and dynamics of the thymocyte selection process to show any correlations with eosinophilic infiltration.

3. Explore the expression of Indoleamine 2,3-dioxygenase message in mice thymi:

    a. Transcription of IDO gene into mRNA by reverse transcription and real time PCR.

    b. Presence IDO protein expressing cells in thymi.

    c. Expression of IDO protein by thymic eosinophils.

4. Reveal any relationship between pattern of eosinophilic infiltration, IDO expression and key stages of thymocytes development.

Chapter 2

Materials and Methods

Mice

Specific pathogen-free wild type newborn BALB/c mice were obtained from Health Sciences Laboratory Animal Services (HSLAS; University of Alberta, Edmonton, Canada) at days 1, 4, 7, 11, 14 and 21 postnatally. This strain of mice is known to be a good animal model with features reminiscent of human allergic asthma and is genetically more alert for eosinophil production (186). All mice were maintained in micro isolator cages and housed in a conventional animal facility. The cages within each animal colony were negative for viruses and other known mouse pathogens. Protocols and studies involving animals were conducted in accordance with the guidelines of the Canadian Council of Animal Care (187).

Histopathology

After intra-peritoneal injection of the anesthetics, (Ketamine (10% in dose 90 mg/kg) and Atravet (1% in dose 3mg/kg)) mice, taken at different ages, were sacrificed by cardiac puncture (187). Thymi were removed by thoracotomy. Each thymus was cleared of blood by washing in ice cold 1x phosphate buffered saline (PBS at pH 7.4-7.6) and immersed into 10% v/v formalin in phosphate buffer

(Sigma-Aldrich, Saint Louise, MO, USA). Following 24 hours of fixation, thymi were washed free of fixative with 1× PBS and gradually dehydrated through an ethanol series, starting from 70% up to ~ 100% concentrations before equilibration in xylene. Paraffin embedded 6 μm tissue sections were mounted on slides. Two independent methods were used to detect eosinophils in the thymus.

Histochemical staining

Thymic tissue sections were deparaffinized in two changes of xylene, for 2 minutes each. Next, the sections were hydrated step-wise in changes of alcohol. The starting solution was anhydrous alcohol in which the slides were immersed twice for 2 minutes followed by two changes of 95% and 85% solutions. After hydration to water, tissue was stained in working mixture of Wiegert's hematoxylin (Sigma-Aldrich, Oakville, ON, Canada) and Biebrich Scarlet (Ponceau BS, Fluka, Oakville, ON, Canada) solutions for 5 minutes. Next step involved the development of the nucleus in 1% acid alcohol solution (1% v/v concentrated HCl in 70% alcohol) with repeated examinations under the microscope. Usually it required about 5 to 7 immersions to achieve necessary result. Next, the slides were washed in 0.5% w/v Lithium carbonate solution, rinsed under the tap water for 5 minutes, and dehydrated in 95% alcohol followed by anhydrous Ethanol. Dehydrated slides were cleared in two changes of xylene and mounted in the xylene based Protocol mounting media (Fisher Scientific, Fair Lawn, NJ, USA). Expected results were achieved when the nuclei stained blue, and red blood cells and eosinophil granules stained red (188).

Development of eosinophilic allergic inflammation in airways

of mice for positive IHC controls

Following light anesthesia with Ketamine (75 mg/kg) and Acepromazine (0.6 x 10^{-2} mg/kg), group of 3 mice were immunized with an intraperitoneally (i.p.) injection of 0.9% sterile saline solution (0.5 ml) containing 10 µg of OVA and 2 mg of Al(OH)$_3$ on days 1 and 6. On day 12, after light anesthesia, mice were intranasally (i.n.) administered 50 µg of OVA (grade V; Sigma-Aldrich, Oakville, ON, Canada) dissolved in 25 µl of 0.9% sterile saline solution. The intranasal challenge was repeated on day 14 in equal dose (189). On the following day the mice were sacrificed by cardiac puncture. The lungs were removed by thoracotomy, washed of blood in the ice-cold PBS and placed into 10% phosphate buffered formalin for fixation. Further the tissue was processed in order, identical to the thymi. Paraffin embedded tissue was sectioned at 6µm and placed on slides. The sections were used as positive control for eosinophil identification by IHC.

Immunohistochemistry

Immunohistochemistry is a technique that involves direct detection of protein by binding with a specific antibody. Effectiveness of the immunohistochemistry can only be altered by epitope changes during fixation or inappropriate use of required reagents (190).

Eosinophils in the thymi were detected by binding of granules major basic protein -1 (MBP-1) epitope with specific rat anti-mouse monoclonal antibody, clone MT2-14.7.2 or MT2-14.7.3 antibodies. The antibody was generated by Dr. J. Lee's laboratory and purchased from the Mayo Clinic, Scottsdalle, Arizona,

USA. It is Sodium Azide free lyophilized preparation that was reconstituted in 1x PBS (pH 7.4-7.6) at room temperature to a stock concentration of 1mg/ml (1µg/µl). For the long term storage the mAb was kept at - 80ºC temperature. This primary antibody represents a rat anti-mouse immunoglobulin class G1, with a kappa light chain and required a corresponding rat IgG1 as isotype control (191).

Paraffin embedded thymic tissue was sectioned at 6 µm thickness on frosted, positively-charged slides (Fisher Scientific, Pittsburgh, USA). Slides were placed into xylene for deparaffinization with two changes of xylene for 2 minutes each. The next step utilized the compatibility of xylene and absolute alcohol to remove the rests of dissolved paraffin and replace it gradually with diluted alcohol to working buffer solution. Following two changes in anhydrous ethanol, the slides were submerged into series of 95, 85 and 70% alcohol solutions for hydration. The slides were then rinsed in 1x TrisHCl buffered saline containing 0.1% Tween 20 (TBST, pH 7.6). Target retrieval procedure was carried out by heating the slides in pH 6.0 ± 2.0 Target Retrieval Solution (DakoCytomation, Carpinteria, CA, USA) to a temperature of 95-99ºC in a conventional oven (192). The temperature was maintained for 20 minutes. The container of slides was removed from the heat source and allowed to cool at room temperature for 20 minutes in the same solution. Before proceeding to the next step, antigen retrieval solution was replaced by TBST in 3 sets of washes (5 minutes per wash). Endogenous peroxidase activity was quenched in Peroxidase Blocking Reagent Ready-to-Use (DakoCytomation, Carpinteria, CA, USA) for 10 minutes at room temperature (r.t.). For this and each following step, the slides were maintained in a humid

chamber to prevent the tissue from drying. After triple washing in 1xTBST, tissue on the slides was predigested with Pepsin solution Digest-All-3, (Zymed, San Francisco, CA, USA) in an incubator at 37ºC for 10 minutes, which was washed off in 3 rinses with TBST for 5 minutes each. To minimize possible nonspecific binding of the secondary antibody, which was raised in rabbit, 10% v/v normal rabbit serum (DakoCytomation, Glostrup, Denmark) in TBST was applied for 30 minutes at room temperature. Without washing the sections on the slides were covered by 200 µL of primary antibody, diluted to the optimal concentration of 2 µg/ml with the antibody diluent (Antibody Diluent with Background Reducing Components Ready-to-Use, DakoCytomation, Carpinteria, CA, USA), and incubated for 60 minutes at room temperature. Sections of mouse lungs sensitized to OVA and challenged intranasally mice were used as positive control for the primary antibody. An isotype control was carried out to evaluate the nonspecific binding of secondary antibody. Negative control slides were processed similarly, but the primary antibody was replaced with purified rat IgG, (Sigma-Aldrich, Saint Louise, MO, USA) at a concentration of 2 µg/ml diluted in the same antibody diluent. Rabbit anti-rat immunoglobulin, conjugated to horse radish peroxidase (HRP) (DakoCytomation, Glostrup, Denmark) was diluted to 13 µg/ml working concentration in 1.5% NRS and used as a secondary antibody. Following the application of the antibodies, the slides were kept for 60 minutes at room temperature and then washed 3 x 5 minutes in TBST. For visualization, the immunological reaction was developed with Diaminobensidine (DAB) chromogen. The peroxidase enzyme produced a colored reaction when incubated

with peroxides. The complex of HRP plus hydrogen peroxide acted as an oxidant for DAB that gave a very stable brown coloration of the positive signal.

The slides were incubated with the mixture of chromogen and substrate for HRP, diluted in reaction buffer. The reaction buffer was an imidazole-HCl containing solution (pH-7.5). The substrate for HRP was hydrogen peroxide. About 5 to 7 minutes were necessary to obtain brown color indicating positive antibody binding. A rinse of slides for 5 minutes in distilled water stopped the color development reaction. Diaminobensidine is a well known carcinogen, thus, all development procedures were performed in a fume hood and the rest of DAB reagent was discarded appropriately.

Washed slides were counterstained in Harris' hematoxylin (Sigma-Aldrich, Egham, UK) for 30 seconds and developed in 0.5% w/v lithium carbonate solution. Excess of hematoxylin was removed by rinsing in 1% acid alcohol and stained additionally with 0.1% methyl green solution for 2 minutes. The slides were then washed under tap water and quickly dehydrated in 95% and absolute alcohol, cleared in xylene and mounted with Protocol mounting media (FisherScientific, Fair Lawn, NJ, USA).

Quantification of eosinophils

To assess and compare eosinophilic infiltration of thymic tissue at different ages, total number of 5 organs was collected for each group. Each thymus was sectioned at different depths with 3 consecutive sections placed on each slide. Two slides of different depth from each organ were chosen randomly. Total 6 sections from one thymus and therefore 30 sections for the each age group were

assessed. Slides were analyzed under 40 x magnification on the bright light microscope with two perpendicular grids. Sections were scanned in systematic order according to the grid in two 90º dimensions avoiding overlapping of the power fields. Eosinophils were counted on 10 random 400x power fields for each section and totally on 60 power fields for each organ.

Calculation of the cortex to medulla ratio

The slides for the study were randomly selected and a total of 5 sections for each age group, taken at the different depth were assessed under the light microscope, connected to the Leica video camera. The areas of the cortex and medulla compartments were detected using OpenLab 3, 5 software and the ratios for corresponding areas of compartments were calculated after measurements, using MS Excell software.

Calculation of density of eosinophilic infiltration/μm^3

The slides for the density measurements were chosen randomly at different depths of each organ. The area of every thymic compartment was detected using OpenLab 3,5 software under the 20x magnification of the light microscope, linked to a Leica video camera. The total number of eosinophils was detected for the total area of a given tissue section and subsequently for each compartment separately. The average diameter of eosinophils was 6.957μm. The number of eosinophils in μm^3 (N) was calculated by the formula (193): N = number of eosinophils counted/area (μm^2) of tissue examined * 1000 μm/2* average diameter of an eosinophil + section thickness (μm). The density of eosinophilic infiltration was detected for each compartment separately.

Flow Cytometry

Study design

Whole thymic cells suspension

Control group   **IFN-γ**

treatment group

6, 12, 24 hours ⟵ **Incubation time** ⟶ **6, 12, 24**

hours
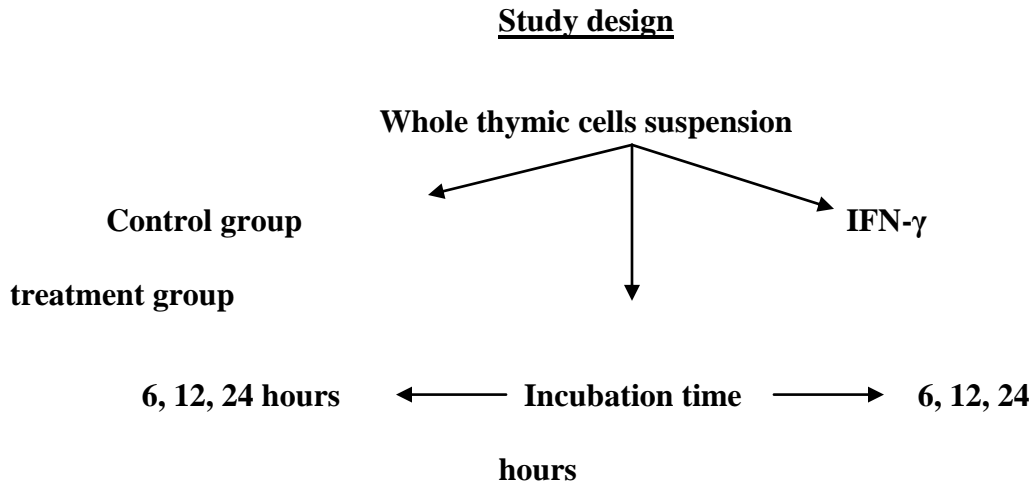
Staining procedure

Epitopes detected:

CCR3/Siglec F   **CCR3/Siglec F**

IDO   **IDO**

IDO/CCR3, IDO/Siglec F   **IDO/CCR3, IDO/Siglec F**

Preparation of single cell suspension from thymus

After removal by thoracotomy, thymi were placed on small Petri dishes (35x10 mm) containing ice cold Hank's Balanced Salt Solution (HBSS). The second set of Petri dishes, intended for cell recovery, was coated with Sigmacote® (Sigma-Aldrich, Oakville, ON, Canada) to prevent cell adherence. Working buffer was prepared using HBSS which was adjusted to mouse plasma osmolarity under control by microosmometry, using μ OSMETTE micro osmometer (osmolarity of mouse plasma is 308-312 mOSM) and 10% NaCl (194).

Tissues were first chopped with fine scissors and agitated continuously with pipetting for 10 min at room temperature in working buffer. Media containing free cells was strained through 400μm nylon mesh into a 50ml tube. Large stromal fragments were minced through a nylon mesh to separate the cells that remained attached to the connective tissue. The cells were collected by washing through the strainer with 5 ml of working buffer. Collagenase digestion was not used during the separation. Cell suspensions were centrifuged in an Eppendorf centrifuge at 1237 rpm or 300g for 7 min at 4°C (195). After the first wash, red blood cells (RBCs) were lysed in ammonium chloride based lysis buffer. Briefly, cells were resuspended in a mixture of working and lysis buffers in proportion of 1:10 respectively and incubated for 10 minutes on ice. To stop the reaction, at least 5 volumes of ice-cold working buffer were added. Cells were immediately washed by centrifugation and resuspension in working buffer, supplemented with 1.8 ml of pH 7.2 0.5M EDTA (Sigma-Aldrich, Saint Louise, USA) in 1 L to prevent rosette formation and clumping. Three subsequent washes were performed to prepare the cells for further analysis. Following the final wash, cell viability was assessed by Trypan Blue discrimination. The cell suspension in volume of 10 μL was diluted 1:100 v/v in 0.4% w/v Trypan Blue solution in a tube and incubated for 5 minutes at room temperature. The ratio of dead to live cells was calculated under the light microscope using a hemocytometer. Usually viability of the cells in this preparation was 92-95% and did not require dead cells separation (196). Cell culture media was prepared on the basis of RPMI 1640 media with HEPES modification (Sigma-Aldrich, Oakville, ON, Canada). Upon

the cells transfer, the culture media was warmed up to 37ºC in a water bath. Using aseptic conditions, 1×10^6 cells /ml of cells were resuspended into culture flasks containing prewarmed media and placed into an incubator at 37ºC in 5% CO_2 atmosphere (197).

Flasks containing the cells were divided in two groups: control (untreated) and Interferon gamma (IFN-γ) stimulated. Following 12 hours of recovery, recombinant murine IFN-γ (PeproTech Inc., Rocky Hill, NJ, USA) 10ng/ml of media was added to one group of cells to induce Indoleamine 2, 3-dioxygenase production. The cells were incubated at 37ºC under 5% CO_2 and harvested after 6, 12 and 24 hours of stimulation.

Bone marrow and whole blood cell suspension from IL-5 transgenic mice

After intra-peritoneal anesthesia with the mixture of Ketamine (10% in dose 90 mg/kg) and Atravet (1% in dose 3mg/kg) 6-8 weeks old IL-5/WT C57/BL6 mice were sacrificed by cardiac puncture. Blood was collected in a heparinized syringe and shaken to prevent clotting. Mouse hind legs were removed and freed from the soft tissue. Femoral and tibia bones were placed on Petri dishes with ice-cold working buffer. RBCs in whole blood were lysed as previously described.

The bone marrow was washed out of the bones by flushing with ice-cold working buffer in volume of 2.0 ml per bone using the 27 G needle and syringe. Clumps of cells were broken up by repeated pipetting up and down and strained through 400μm nylon mesh. Blood and bone marrow cell suspensions were collected in a 50 ml tubes and were centrifuged at 300 g for 10 min @ 4˚C and

resuspended in working buffer. Two washes in identical conditions were performed, and cell count using Kimura stain at 1:10 dilution was noted. Viability was assessed by 0.4% w/v Trypan Blue exclusion.

Cell labeling and detection of IDO using flow cytometry

For the detection of Indoleamine 2, 3-dioxygenase by eosinophils and other cell types in the thymus, cells of the whole organ were prepared in suspension and stained with fluorochrom conjugated antibody for intracellular IDO and specific surface markers. The specificity of surface marker antibody was analyzed on bone marrow and blood cell suspensions of IL-5 transgenic mice. For double labeling the combinations of fluorochrom conjugated antibodies were selected in a way that could ensure minimum of the emission spectrum overlap. For example, one molecule was bound by fluorochrome/antibody with far red emission spectrum (λ_{em} 668), whereas the second marker was conjugated with medium emission wave length (λ_{em} 578) fluorochrome. Some theoretical information could have explained my choice. Each detector of a laser scanner is designed to acquire a specific emission spectrum. All fluorochroms' emission spectrum exhibits a part extending towards longer wave length, which could be collected by different detector. In cases of fluorochrome combinations with partially overlapping emission spectrums it is necessary to perform a compensation procedure that tunes detectors to subtract the percent of signal from neighbor detectors (198). The selection of fluorochroms with non overlapping emission spectrums made it unnecessary to perform the compensation for my studies. It also insured a proper detection of double positive events. For IDO

detection by single labeling we chose the secondary antibodies, conjugated with different fluorochroms to improve the quality of detection and demonstrate consistence of results.

List of antibodies

Antibody	Host	Conjugate	Isotype	Clone	Concentration	Source
IDO	Mouse	N/C	Mouse IgG3	10.1	1.0 mg/ml	Chemicon, Billerica, MA, USA
Secondary	Goat	R-Phycoerythrin λ_{ex}496, 546, 565‡, λ_{em}578	IgG, Fcγ subclass 3 specific	N/A	1.0 mg/ml	Jackson ImmonoResearch West Grove, PA, USA
Secondary	Goat	Allophycocyanin λ_{ex}650, λ_{em}660	IgG, Fcγ subclass 3 specific	N/A	1.0 mg/ml	Jackson ImmonoResearch West Grove, PA, USA
IDO	Mouse	N/C	IgG	10.1	0.5μg/μL	UPSTATE Temecula, CA, USA
Secondary	Goat	Alexa 488 λ_{ex}495,λ_{em}519	IgG, H+L chain F(ab)$_2$ specific	N/A	2mg/ml	Invitrogen Eugene,OR, USA
Secondary	chicken	Alexa Fluor 647, λ_{ex}650,λ_{em}668	IgG, H+L chain	N/A	2mg/ml	BD Pharmingen San Diego, CA, USA
CCR3	Rat	Alexa Fluor 647, ,λ_{ex}650, λ_{em}668	IgG$_{2a}$	83103	0.2mg/ml	BD Pharmingen San Diego, CA, USA
Siglec-F	Rat	R-Phycoerythrin	IgG$_{2a,к}$	E50-2440	0.2mg/ml	BD Pharmingen San Diego, CA, USA
CD4	Rat	Alexa 488 λ_{ex}495,λ_{em}519	IgG$_{2a,'к}$	RM4-5	0.2mg/ml	BD Pharmingen San Diego, CA, USA
CD8	Rat	R-Phycoerythrin λ_{ex}496, 546, 565‡, λ_{em}578	IgG$_{2a,к}$	53-6.7	0.2mg/ml	BD Pharmingen San Diego, CA, USA

For immune fluorescent detection of CCR3/Siglec F epitopes in single/double staining, blood and bone marrow cells were resuspended in the flow buffer (see composition of the buffer in the Appendices) to achieve a count of $1x10^6$ in 200μL and transferred into 5ml tubes. To prevent non-specific binding of surface marker antibodies, samples were incubated with Fcγ receptor (CD16/CD32) blocking reagent for 30 minutes. Specific anti-Siglec F and anti-CCR3 antibodies were added to the cells without washing of the FcγRe block. The samples were incubated on ice for 45 minutes and 2-3 mls of working buffer were added at the end of staining to wash the cells. After washing by centrifugation at 300g for 5 minutes, cells were fixed in 1% paraformaldehyde for 15 minutes on ice. Finally, cells were washed in the working buffer and kept at 4ºC.

For thymic cell culture, following removal from the incubator, cell culture media was replaced by working buffer at room temperature. The proportion of dead cells was detected by Trypan Blue staining. When viability of the cell was lower than 85%, the separation of dead cells and debris were separated. Briefly, single cell suspension was layered over Ficoll-Paque™ PLUS (GE Healthcare, Uppsala, Sweden) and centrifuged at 1000 rpm for 25 minutes at room temperature (199). An interface between layers of Ficoll and working buffer contained the live cells, and dead cells were located at the bottom of the tube. After two washes, cell count was performed using Kimura stain. The cell suspensions were divided into two groups: the first one for the surface markers (CCR3/Siglec F) detection; the second was separated for evaluation of intracellular molecules. For CCR3/Siglec F labeling the thymic cell suspensions

were stained according to the protocol, presented for the blood/bone marrow cells. The cells in the second group were employed for intracellular IDO detection and combined IDO/Siglec F or IDO/CCR3 staining. These samples have undergone fixation in 4% paraformaldehyde in PBS on ice for 15 minutes. To terminate the fixation paraformaldehyde was replaced by the working buffer, containing 20mM Glycine (Fisher BioReagents, Fair Lawn, NJ, USA) and removed in 3 washes. Further, the cells were permeabilized by resuspending in the flow buffer with 0.1% Saponin for 30 minutes on ice. Single cell suspensions in the permeabilizing flow buffer were diluted to reach a concentration of 1×10^6 cells per 200µL and loaded into two sets (Control and IFN-γ) of 5 ml flow tubes. Primary anti-mouse IDO antibody was added first at a dilution of 1:200 accompanied by corresponding isotype control immunoglobulin solution at the same concentration. To ensure sufficient binding the cells were incubated for 120 minutes on ice, followed by the wash in the permeabilizing buffer. Secondary antibodies (1:200 dilution) were added to the cells and incubated for 60 minutes. Washing was performed by centrifugation of the cells at 300 g for 5 minutes followed by resuspension in the permeabilizing buffer. For double labeling, antibodies to the cell surface molecules (Siglec F or CCR3) were added and incubated for 45 minutes on ice in the dark. The combination of fluorochrom labels were selected to achieve non overlapping emission fluorescence for proper double staining analysis. Cells were washed in the permeabilizing buffer followed by the flow buffer. After the final wash the cells were resuspended in 400-500µL of the flow buffer for the analysis. Acquisition of flow cytometry data was carried

out on FacsCalibur scan machine according to manufacturer's instructions and analyzed using CellQuest software.

RNA Extraction

Whole thymi were used for total RNA extraction to detect the presence of transcribed mRNA for IDO gene. Organs, extracted during thoracotomy, were rinsed off blood in the ice cold PBS (pH 7.4-7.6) and flash frozen in liquid Nitrogen and powdered to enhance RNA yield. Further, RNA was isolated using microcolumn technique supplied by QIAGEN RNeasy MiniKit (QIAGEN, Hilden, Germany). Lysed tissue was homogenized with QIAGEN QIAShredder (QIAGEN, Valencia, CA, USA). Even though it is not necessary, according the QIAGEN protocol, to inactivate possible genomic DNA contamination, DNAse A (Invitrogen, Burlington, ON, Canada) treatment was routinely performed during on column RNA isolation using the QIAGEN protocol. Quality of isolated RNA, such as the presence of DNA contamination and RNA damage was assessed by electrophoresis on 1.4% Agarose gel in TAE, stained with 0.05% Ethidium Bromide (200). The concentration of RNA in samples was monitored, and the sample purity indicator (260/280 ratio) was determined by spectrophotometry at 260nm (201). Samples with absence of genomic DNA contamination, showing a S28/S18 ratio of at least 1.5:1, and purity measurement reading at $OD_{260nm}/OD_{280nm} = \sim 1.4 - 1.9$ were considered acceptable for reverse transcription (202).

Primer Design

Specific primers for detection of mRNA for Indoleamine 2, 3-dioxygenase were designed using Primer -3 software (http://frodo.wi.mit.edu/cgi- bin/primer3 /primer38_www.cgi) (NIH Genebank Access No. NM_008324, http://www.ncbi. nlm.nih.gov/sites/entrez). The primers were blasted against highly specific sequences in mouse genome by search over the website of the National Center for Biotechnology Information (NCBI) megaBLAST (http://www.ncbi.nlm.nih.gov/blast/Blast.cgi).

RT-PCR (203)

Reverse transcription of RNA was performed using 1µg of total RNA in the presence of random hexamer oligo (dT)$_{12-18}$ primer (Invitrogen, Burlington, ON, Canada), and Moloney murine leukemia virus reverse transcriptase (Invitrogen, Burlington, ON, Canada),. The mixture of 1µL of the primer (500µg/ml), and RNA (1µg/µL) in RNase-free water was kept in a thermocycler (M-J Research, Watertown, Mass.) at 65ºC for 5 minutes for annealing and was immediately placed on ice. Eight µL of master mix (see Appendix A for ingredients) were added to each tube. The reactions were incubated for 50 minutes at 42ºC, followed by inactivation at 70ºC for 15 minutes. The cDNA was stored at -70ºC for long term storage or at -20ºC for short term.

The cDNA amplification reactions with IDO-specific primers were performed in 25 µL volume. The reaction Master mix ingredients and concentrations are cited in Appendix A. A volume of ≥ 1µL of cDNA was added to each tube, followed by 2 units of Platinum® Taq DNA Polymerase (Invitrogen,

Mississauga, ON, Canada) immediately before the amplification. Reactions were carried out in a BioRad Thermal iCycler (BioRad, Foster City, CA, USA) with 96- well reaction module. Conditions for each step were as follows: step 1: 4 min at 94ºC, step 2: 30 sec at 94ºC, step 3: 30 sec at 58.6ºC, step 4: 1min at 72ºC, step 5: repeat steps 2-4 for 35 cycles, step 6: 10 min at 72ºC, step 7: 4ºC for ∞. The products along with 0.5 Kb DNA ladder (Invitrogen, Mississauga, ON, Canada) in a volume of 10 μL were loaded on 1.4% Agarose in TAE gel, stained with 0.05% Ethidium Bromide (Sigma-Aldrich, Saint Louise, USA). Separation was performed by horizontally loaded gel electrophoresis at 90 V for 45 minutes. Products were visualized under UV light transilluminator using AlfaImager 2200 visualization system and pictures were adjusted using the AlfaImager 2200 software.

Semi-quantitative real time PCR (204)

Intron-spanning primers were designed using Primer Express software (Applied Biosystems, Scorsby, VIC, Australia). Reverse transcribed RNA samples were diluted 1:5 and quantitated by real time PCR, using QuantiTect SYBR Green Master Mix(Qiagen) on the ABI PRISM 7900HT (Applied Biosystems). Melting curve analysis was used to assess the specificity of the assay. Copy numbers were determined by 10-fold serial dilutions of plasmid standards and normalizedto the reference gene elongation factor 1α.

Statistical analysis (205)

In order to assess the changes of a variable, which represents the mean for several groups, such as an eosinophilic infiltration in the thymi of mice at

different ages (inference for the groups' means of variable) the one-way analysis of variance (ANOVA) test was performed. In a case the p-value indicated a statistically significant difference between the groups, the paired multiple comparison post-hoc testing was performed using the Tukey's test. The one-way was also carried out for all inferences, where the comparison of the means from different groups was necessary. In cases of inferences, where the two or more variables have changed affecting each other, the two-way analysis of variance (two-way ANOVA) was performed. For the inferences from the means, which represented the responses to the different treatments (Control and Treatment groups) in a matched pairs design of the study, the paired t-test was applied. The p-values were abbreviated as follows: p-value < 0.05 - *; p-value < 0.01 - **; p-value < 0.001 - ***.

Chapter 3

Results

Characteristics of eosinophilic infiltration in thymus:

Eosinophils in thymic tissue were identified in fetal organs at day 17 of gestation and postnatally at days 1, 4, 7, 9, 11, 14 and 21 by immunohistochemical staining using rat anti-mouse MBP-1 antibody as described in Chapter 2. The conventional histochemical technique in Luna modification in neonatal mouse thymus, resulted in nonspecific staining of the cytoplasm of different cells, and therefore, was inappropriate for use (188).

The positive signals for MBP-1 were revealed as cytoplasmic stain and were compared with isotype and positive control sections (Figure 9, A., B.). Eosinophils (MBP-1^{+} cells) appeared in the thymus at day 1 as solitary cells within surrounding the organs connective tissue and this pattern remained unchanged by day 4 (Figure 10, A., B.). At day 7, eosinophils were located in the cortico-medullary boundary interspersed between the highly populated by thymocytes cortex and the hypodense medulla (Figure 10, C., D). This eosinophil-infiltrated region was clearly detectable on the sections mainly in the areas between appearing dark-blue on hematoxylin stain cortex and medulla, which showed distinct less intensive staining with hematoxylin due to the paucity of cell numbers and diversity in cell population. In addition, pattern of eosinophilic

distribution in trabecules and cortex was found to be characteristic for this age (Figure10, E). Eosinophils were predominantly located in deep cortex rather than in the subcapsular areas (Figure 10, E). The distribution of eosinophils within these compartments at early ages may indicate their ability to penetrate through the connective tissue capsule, interlobular septae as well as emergence from local blood flow. The eosinophils had very distinct intracellular morphology with bilobed nucleus, as seen on high power magnification (Figure10.B).

At day 11, a marked increase in eosinophilic infiltration was observed mainly in the cortico-medullary junction (CMJ) and medulla, whereas there were fewer eosinophil numbers observed within cortex and connective tissue. Clusters of eosinophils as well as scattered cells located in the CMJ were characteristic feature of day 11 infiltration of the thymus (Figure 11C., D). At this age the mature solitary eosinophils were still seen in deep cortex and connective tissue compartments (Figure 11 A., B), however in fewer numbers than those seen at day 7 and 9. Numbers of MBP-positive cells decreased by day 14, compared to day 11(Figure 12 A., B.). There were no accumulations of cells observed at day 14 within tissue sections. Eosinophils were seen scattered along the cortico-medullary areas and in the deep cortex. Fewer cells were identified in the connective tissue and in the medulla (Figure 12, A., B.). Thymuses at day 21 were infiltrated by eosinophils significantly, predominantly within medulla and cortico-medullary region compared to earlier ages. The cells were mainly scattered in the medulla regions and rarely formed small groups (Figure 12. C., D). In large

numbers eosinophils were seen along the perivascular spaces, but significantly

fewer of them were found in the connective tissue (Figure 12, E., F).
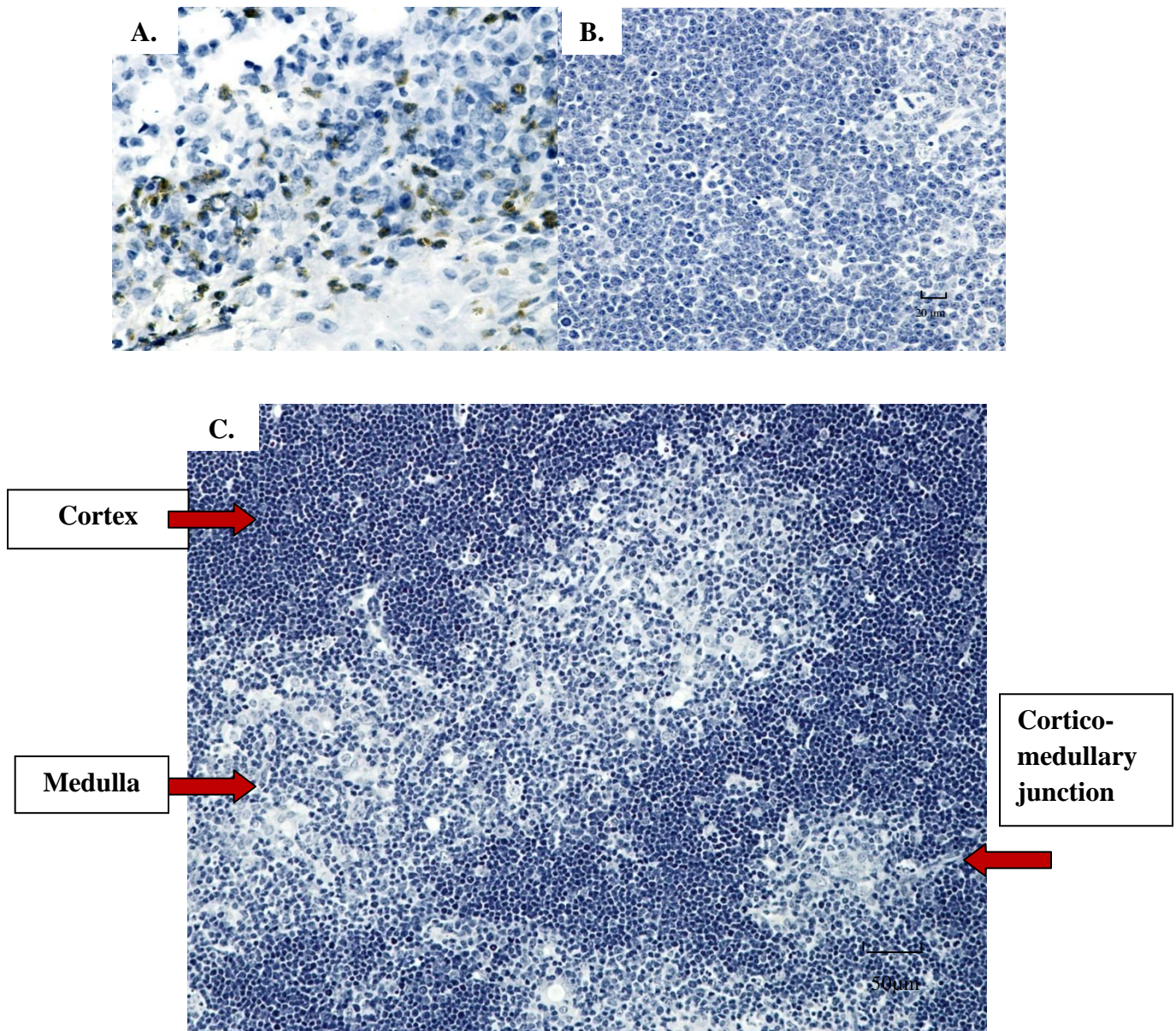
Figure 9. Identification of eosinophils on the tissue sections by IHC using rat anti-mouse MBP-1 antibody.
The lung of OVA sensitized and challenged mouse were used as positive control samples (**A.**). The isotype control was carried out using corresponding subclass of rat IgG on identically processed thymic sections to insure specific binding of secondary antibody (40x magnification, size bar 20µm), (**B**). Figure **1. C** depicts thymic compartments on the tissue sections under the 20x magnification, size bar 50µm.
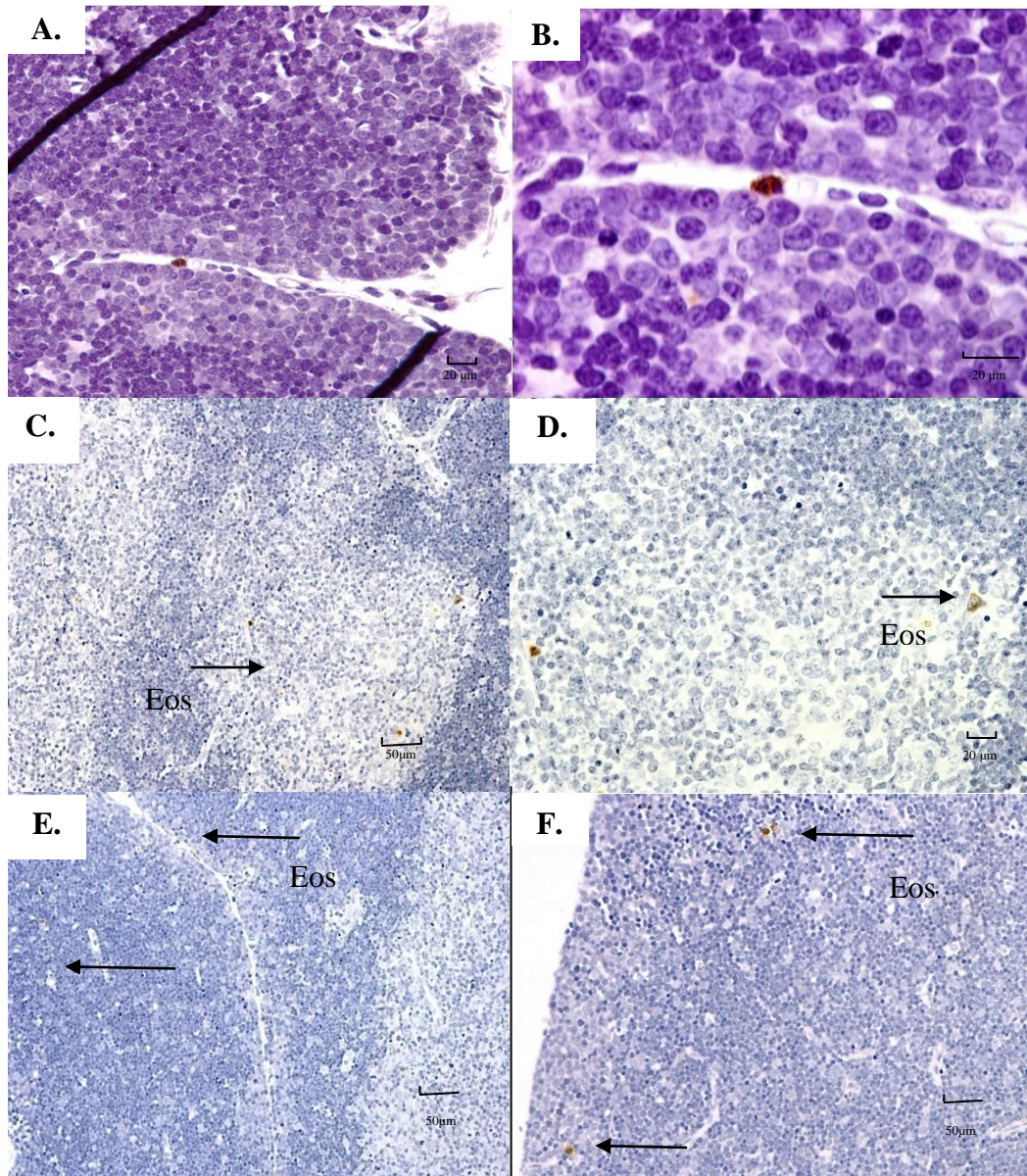
Figure 10. Detection of eosinophils on thymic tissue sections using rat anti-mouse MBP-1 antibody.
A. Solitary eosinophils were seen on the sections from day1 thymi (40 x magnification, size bar 20µm)**. B.** Repeated image of the eosinophil at day 1 thymus (100 x magnification, size bar 20 µm). **C.** Eosinophils present in the CMJ of the thymus at day 7 (20 x magnification, size bar 50 µm). **D.** Eosinophils scattered around the CMJ at day 7 (40 x magnification, size bar 20 µm). **E.** At day 7 eosinophils were found in the deep cortex and trabecules. **F.** Day 7 eosinophils are in a deep cortex (20 x magnification, size bar 50 µm).
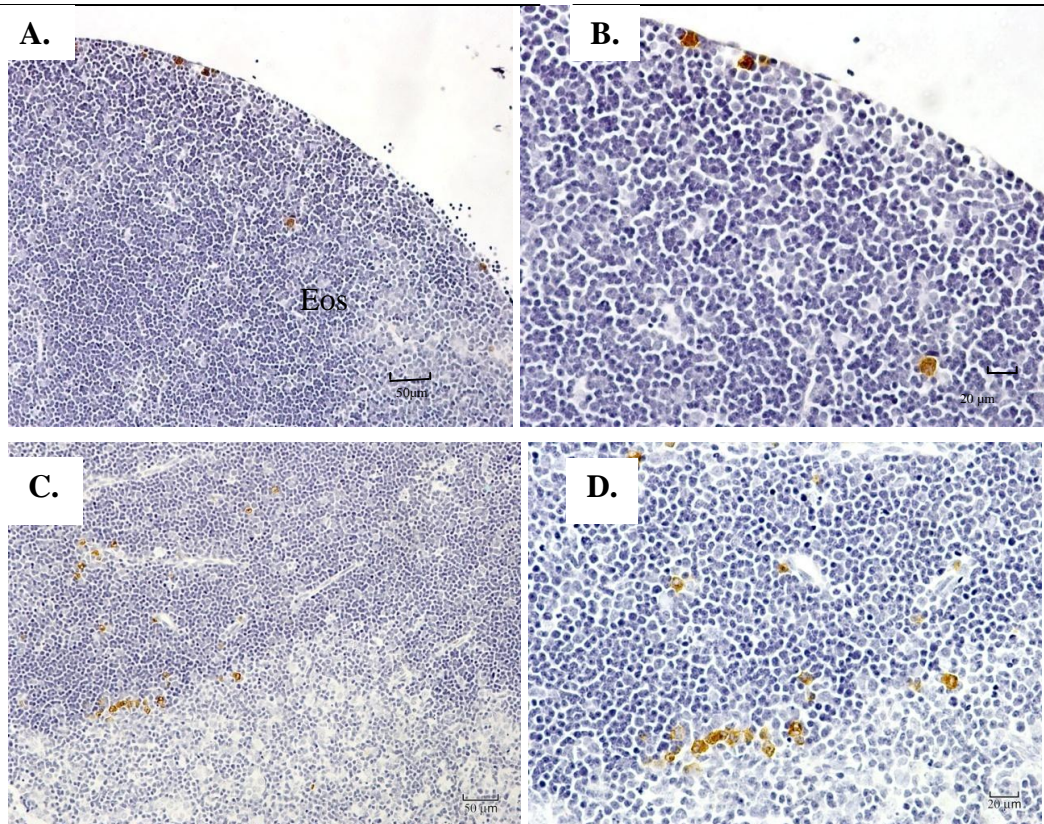
Figure 11. Detection of eosinophils within thymic tissue sections using rat anti-mouse MBP-1 antibody at day 11.
Eosinophils were revealed as cells with brown colored cytoplasmic stain and bilobed nucleus under bright light microscopy. **A.** Solitary cells were found in the deep cortex and subcapsular areas. **C.** Clusters of eosinophils were observed in the CMJ and in the perivascular spaces (20 x magnification, size bars 50 µm). Images **B** and **D** represent a higher magnification (40 x, size bars 20 µm) of pictures **A** and **C**.
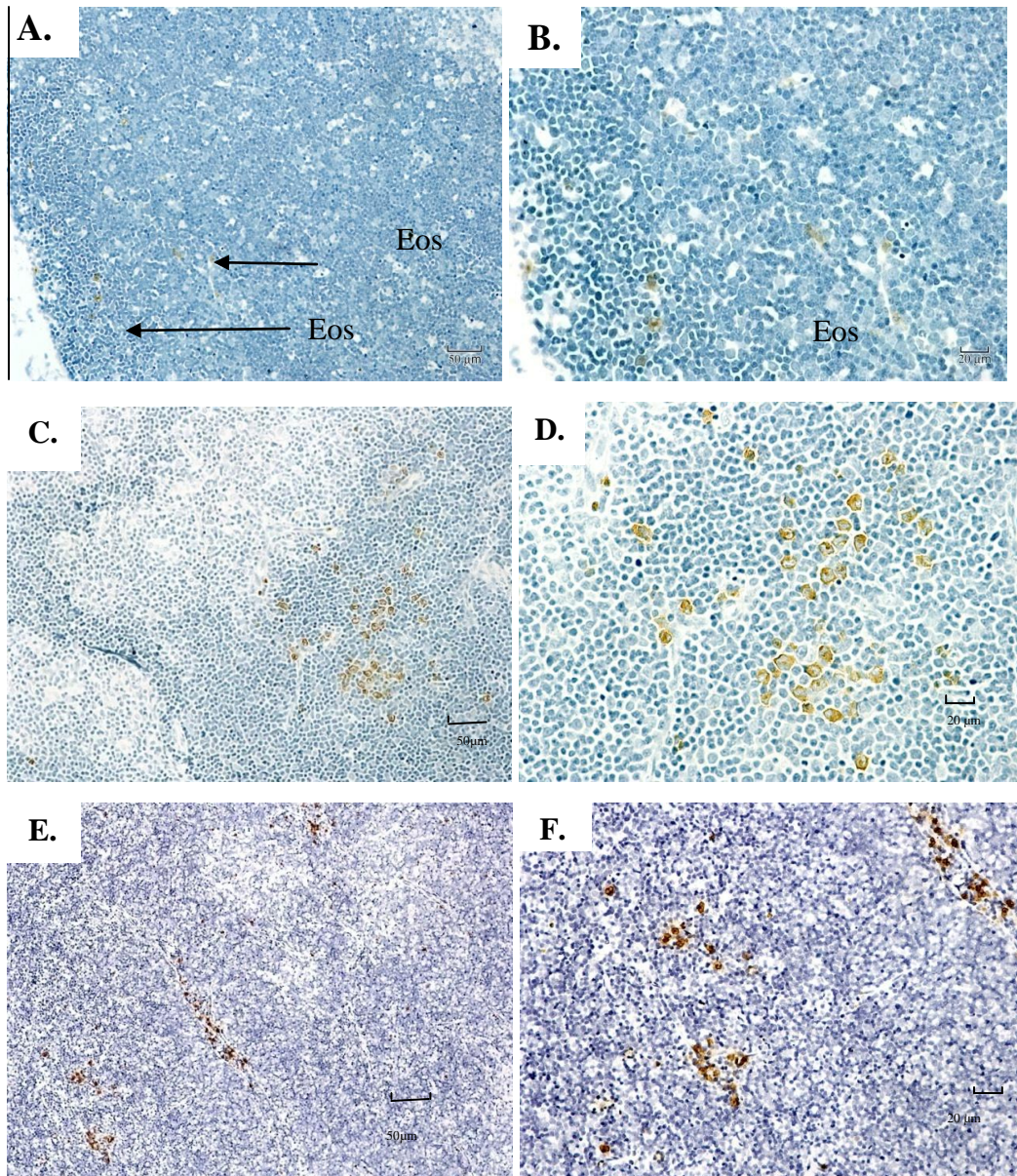
Figure 12. Detection of eosinophils within thymic tissue sections using rat anti-mouse MBP-1 antibody.
A. At day 14 the thymi contained fewer eosinophils than at day 11. The scattered cells were located in deep cortex and CMJ. No aggregated eosinophils were observed (20 x magnification, size bar 50µm). **C.** Day 21 thymi were significantly infiltrated by eosinophils in CMJ. Clusters of eosinophils were located in perivascular space and CMJ (20 x magnification). The pictures **B., D., F** are paired pictures under 40 x magnification of **A, C** and **E,** (size bar 50µm).

Eosinophils were enumerated on 3 to 4 consecutive tissue sections, prepared from different depths of the thymi. Slides were chosen randomly, and equal area of tissue was assessed for each thymus (see Chapter 2 for details). A summary of eosinophilic infiltration in absolute numbers is presented in Figure 13 (A). The difference in numbers of eosinophils between groups of days 1, 4 and 7 thymi was not significant (ANOVA, p-value > 0.05). At day 9 the infiltration increased not significantly, compared to days 1, 4 and 7 (p-value > 0.05). The eosinophil count revealed that at day 11, eosinophilic infiltration increased significantly compared to days 1, 4, 7 and 9 (ANOVA, p-value < 0.01). At day 14, a non-significant drop in numbers of cells was observed (ANOVA, p-value > 0.05) compared to days 1, 4, 7, 9 and 11. By day 21, eosinophilic infiltration increased 10 fold that was statistically significant (ANOVA, p-value < 0.01) compared to all younger age groups (Figure 13, A.).

Observations made in this study and others, (206) have suggested that the thymus is a rapidly changing organ. Early after the birth (days 1 - 4), the thymus is populated mainly by CD8/CD4 double negative (DN) thymocytes, which reside in cortex. Morphological measurements at this age reflected predominance of tightly populated by thymocytes cortex over less developed medulla with a maximum in cortex to medulla ratio (C: M ratio) of 4.75 ± 0.23 at day 1 (Figure 13, B.). This was statistically significant compared to all later ages: 4, 7, 9, 11, 14 and 21 days (p-value < 0.01). With the increase in numbers of positively-selected $CD4^+CD8^+$ thymocytes that migrated towards medulla (161), a significant decrease (3.65 ± 0.07) in C: M ratio was observed between days 4 and11 (p-value

< 0.05) (Figure 13, B). At this stage no significant rise in eosinophil numbers was observed (see Figure 13, A). By day 11, when the first shift in eosinophils' count was observed, the percentage of double positive thymocytes reached its maximum (163) resulting in further expansion of medulla (C:M 3.34 ± 0.3). A second rise in eosinophilic infiltration at day 21 correlated with a significant decrease (1.85 ± 0.12) in C: M ratio compared to early ages 1, 4, 7, 9, 11, 14 days (p-value < 0.001).

A.
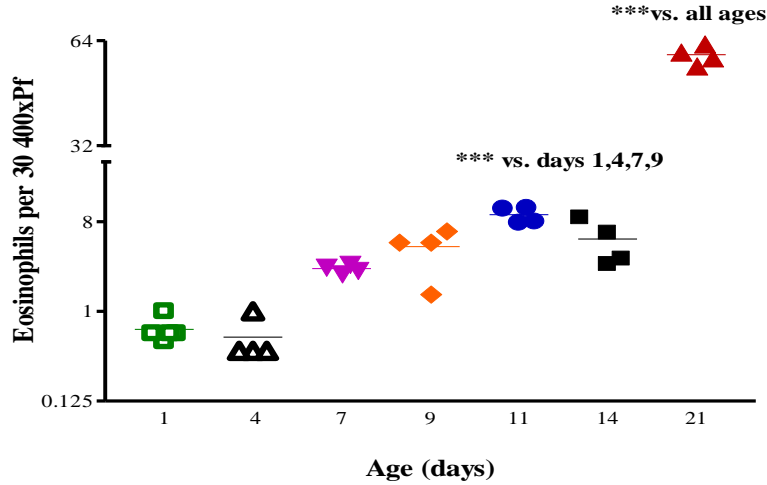
B.
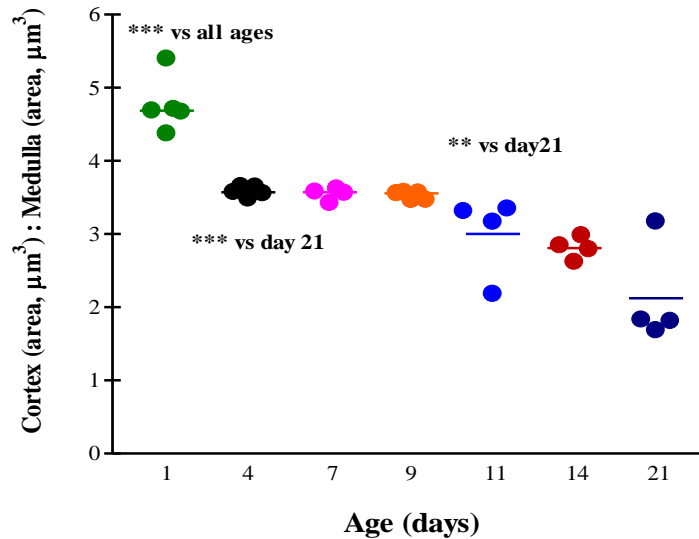
Figure 13. Summary of the detection of eosinophils within on tissue sections and its correlation with changes in thymic morphology.
Absolute number of eosinophils was calculated on identical area of the tissue sections under a 40 x objective. The highest number was observed at day 21 vs. all other ages (p-value < 0.001) and at day 11 vs. earlier ages (p-value < 0.001). The Y axis represents values as a log2. **B.** Cortex to medulla ratio was determined after measuring compartment areas on randomly selected tissue sections (n = 5 for each age) using OpenLab software.

Allocation of eosinophils throughout the period examined is presented in Figure 14A. To examine the relationships between various compartments, infiltration and age of the mice, a two-way ANOVA statistical analysis was performed. The results showed that infiltration of different compartments varied significantly depending on age (p-value < 0.001) (Figure 14, A) and the value of each compartment separately was significantly different from each other throughout examined period (p-value < 0.001). The presence of eosinophils in the CMJ was predominant starting day 7 during examined time-period and contained between 38 ± 9 and $60 \pm 8\%$ of all eosinophils, found within tissue section area. The age of mice significantly affected the infiltration of different compartments. The percentage of eosinophils in the connective tissue was the highest at day 4 ($50 \pm 9\%$) and the lowest at day 21 ($6 \pm 1.2\%$) of total MBP-positive cell counts on the tissue sections (Figure 14, A.). The medulla was significantly infiltrated at day 11 compared to all other age groups (one-way ANOVA, p-value < 0.05). Eosinophil infiltration of cortex was the highest at day 7 and composed $29 \pm 0.8\%$ of total eosinophils count within tissue section on a slide (one-way ANOVA, p-value < 0.05).

A.
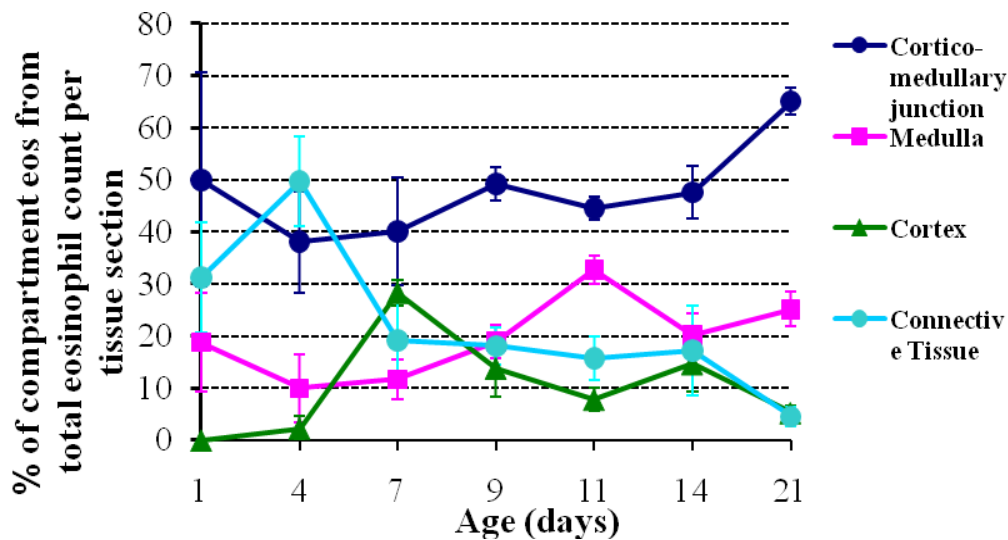
B.
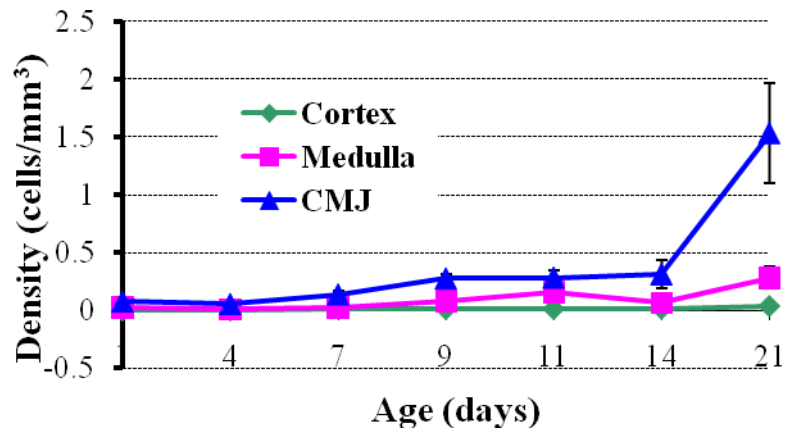
Figure 14. Distribution and density of eosinophils in thymic compartments.
A. The absolute number of eosinophils was calculated for each compartment on 20 sections totally for separate age group. Percentage was estimated taking the total cell count for the tissue section as 100%. **B.** Distribution of eosinophils was significantly affected by variability within compartment variable and was significantly higher in the CMJ starting day 7. Area of each compartment was determined on the randomized tissue sections sliced from different depth of the organs n=5 for each age group. In total 4 sections per one thymus were assessed. According to the equation, presented in Chapter 2 the density of eosinophils in the CMJ was significantly higher compared to the medulla at days 9, 14 (p-value < 0.01) and 21 (p-value < 0.001).

Density of eosinophilic infiltration (cells/mm^3) varied with age significantly depending on the compartment examined (Figure 14, B) (two-way ANOVA, p-value < 0.001). In cortex eosinophil density did not vary significantly throughout all ages and did not exceed 0.1 cell/mm^3 (one-way ANOVA). There was a significant increase in the density of eosinophils in the medulla at day 21 (0.35 ± 0.09 cells/mm^3) compared with days 1, 4, 7, 14 (one-way ANOVA, p-value < 0.05), but was not significant compared with day 11 (0.16 ± 0.023 cells/mm^3, one-way ANOVA, p-value > 0.05). Density of infiltration in cortico-medullary junction was significantly higher at day 21 compared with all early ages (one-way ANOVA, p-value < 0.001). The results demonstrated that presence of eosinophils in CMJ was significantly higher compared to cortex and medulla during all examined period and reached its maximum 1.5 ± 0.43 cells/mm^3 at day 21 (two-way ANOVA, p-value < 0.001). At days 7, 9, 14 and 21 the eosinophils' density in the cortex and medulla was significantly lower than in cortico-medullary boundary (one-way ANOVA, p-value < 0.01). However, at day 11 the density in medulla increased and almost reached the level of infiltration of CMJ in comparison with all other ages (Figure 14, B). However, this shift was not significant (one-way ANOVA, p-value > 0.05).

Phenotyping of Eosinophils based on CCR3/Siglec F Expression

Detection of eosinophils in cells suspension was performed using flow cytometry by identification of the CCR3 and Siglec F molecules expressed in eosinophils and employed as cell markers, as was described previously (207).

A.

B.

C.
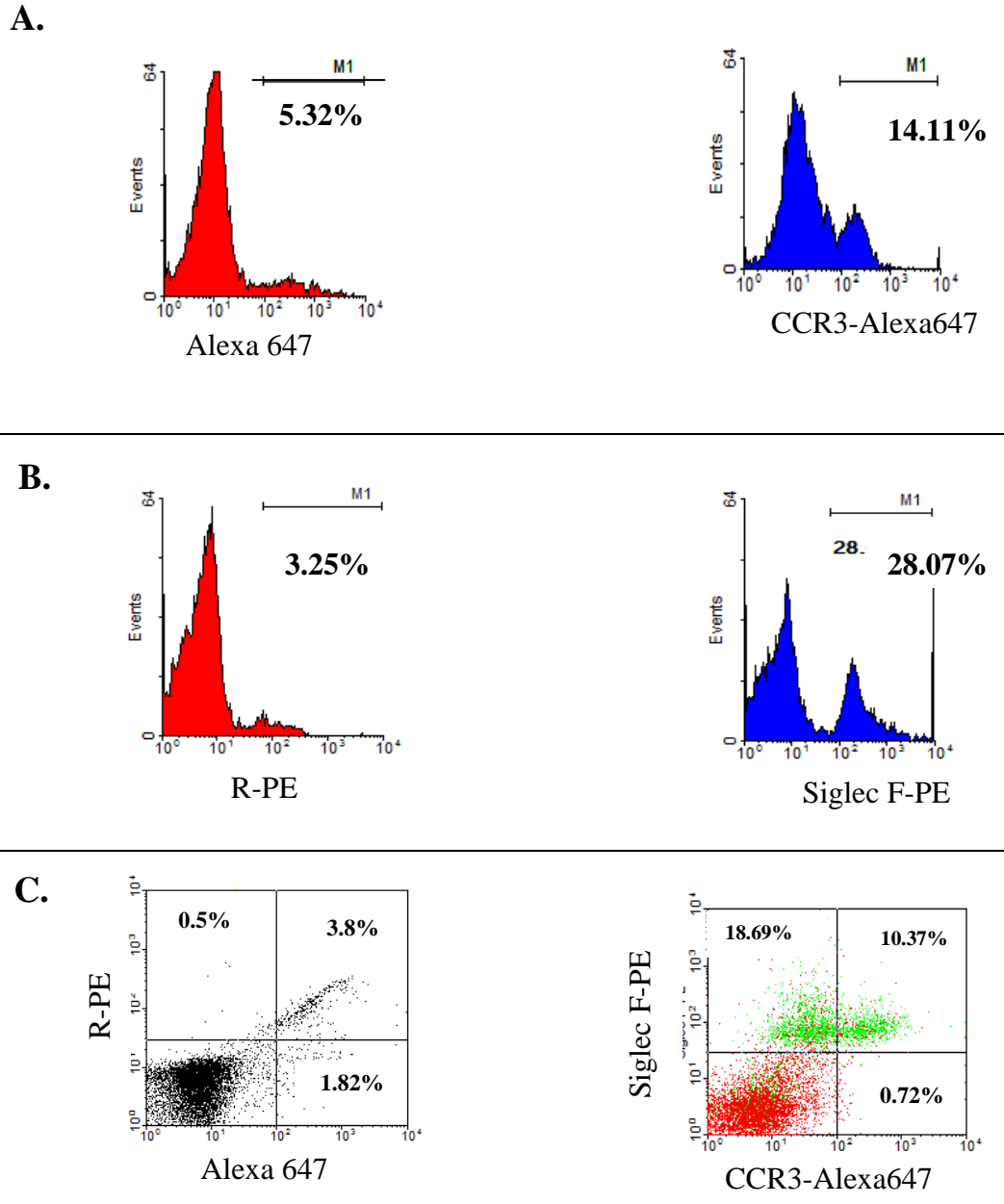
Figure 15. Positive control and antibody adjustment for detection of CCR3/Siglec F double positive eosinophils by flow cytometry using IL-5 transgenic mice bone marrow cell suspension.
A. Detection of CCR3 positive cells, stained with Alexa 647 conjugated anti-mouse CCR3 antibody. **B.** Detection of Siglec- F positive cells using R-PE conjugated anti-mouse Siglec-F antibody. **C.** Coexpression of CCR3 and Siglec-F markers; mature eosinophils are double positive and immature are Siglec-F single positive cells, localized in the left upper quadrant of the dot plot.

CCR3 molecules are abundantly expressed on eosinophils after exposure to eotaxin signaling and are mainly markers mature eosinophils (208). Siglec F molecules are characteristic for mature as well as immature eosinophils that reside in hematopoietic tissue (209). We used the bone marrow of interleukin – 5 (IL-5) transgenic mice (45) as a positive control to show the coexpression of Siglec F/CCR3 molecules. My results showed that bone marrow contained only 11% of CCR3$^+$ cells (Figure 15, A), whereas Siglec F$^+$ cells contributed to about 25% of total bone marrow cell population (Figure 15, B). The acquisition of the double stained cells (Figure 15, C.) indicated the presence of two eosinophilic cell populations: immature Siglec F$^+$ and mature CCR3$^+$/Siglec F$^+$ cells (208). The proportion of cells detected by Siglec F single labeling (28.07%) corresponded to the sum of percentages of double positive events from the upper right quadrant and single positive from the upper left portion of the dot plot (Figure 15, C).

Siglec F expression

The whole thymic cell suspensions were subjected to flow cytometry analysis to define the presence and numbers of eosinophils at different ages using R-PE conjugated anti mouse Siglec F antibody (see Chapter 2 for details) (28). The Siglec F expression was assessed in two groups of cultured cells, namely, control (untreated) and mouse IFN-γ-treated (Figure 16), collected after 12 hours of stimulation. The summary of the results, obtained in two separate experiments for ages 7 and 14 days as well as for four independent experiments for ages 11 and 21 days presented on the bar graph as mean ± SEM where applicable (Figure 17). Results showed that at age 7 days mouse thymus contained 1.6% of Siglec F$^+$ cells

Age	Control	IFN-γ +
7 days	12h C — 1.23%	12h IFN — 1.94%
11 days	12h C — 2.5%	12h IFN — 3%
14 days	12h C — 1.67%	12h IFN — 1.16%
21 days	12h C — 3.7%	12h IFN — 1.39%
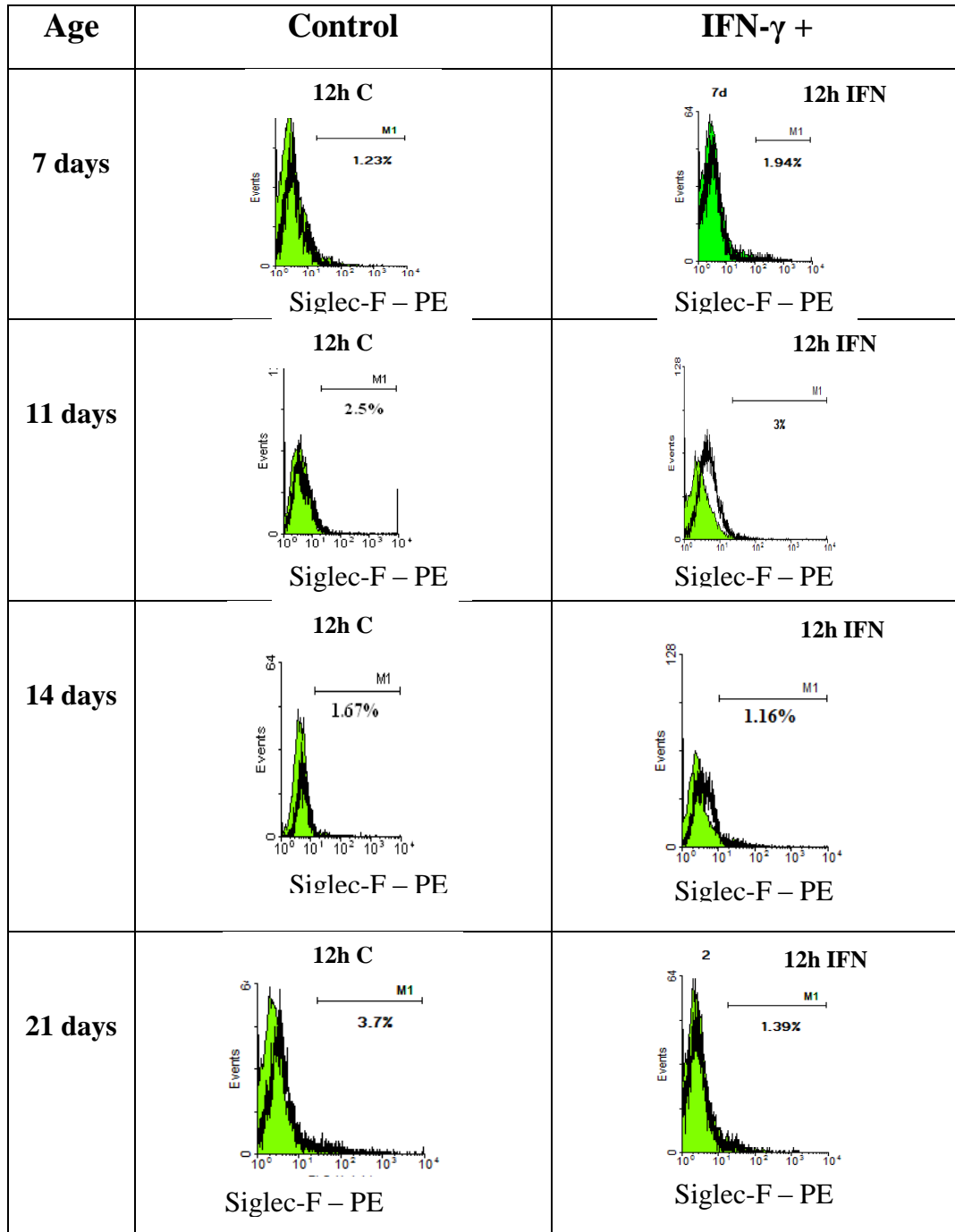
Figure 16. Differential expression of Siglec F on suspended whole thymic cells in control and IFN-γ-treated groups.

Cells were harvested after 12 hours of culturing in presence or not of IFN-γ and analyzed for Siglec F expression using R-PE conjugated anti-mouse antibodies without permeabilization. Green areas on the histograms show the binding of the isotype control. The percent of positive events, presented on histograms, is the difference between isotype control and experimental values.
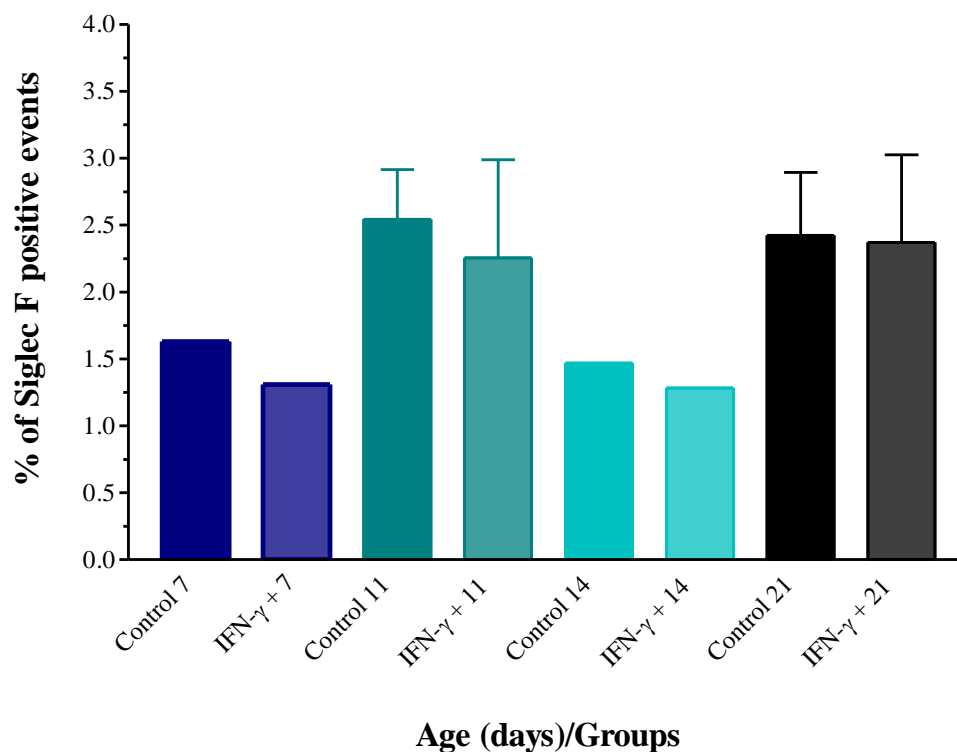
Figure 17. Summary of Siglec F expression by thymic cells in Control and IFN-γ treated groups for days 7, 11, 14 and 21.
Whole thymic cells in suspension were harvested after 12 hours of treatment and stained with anti-mouse Siglec F R-PE conjugated antibody and analyzed by flow cytometry. The bars on the graph represent mean ± SEM for ages 11 and 21 days. For ages 7 and 14 days bars display average of two independent experiments. There was no statistically significant difference between control and treatment groups for ages 11 and 21 days (paired t-test, p-value > 0.05).

in control group and about 1.3% in the treatment group (SEM was not applicable because of small sample size).

At day 11, specific fluorescent signals were determined on 2.6% ± 0.7% of cells in the control group and 2.25 ± 1% in the IFN-γ + group. At day 14, the percent of Siglec F$^+$ events dropped to 1.5% in control and 1.3% in the treatment groups. At day 21, the number of eosinophils increased again to about 2.3 ± 0.7% in control and to 2.2 ± 1% in IFN-γ + groups. The statistical analysis to show the age-related difference in Siglec F positive cells was not performed because of differences in sample size between ages. The paired t-test showed no significant difference in Siglec F expression between control and treatment groups for ages 11 (p-value 0.673) and 21 days (p-value 0.835).

CCR3 expression in thymus

In order to confirm the presence of mature eosinophils in the thymus, cultured cells from control and IFN-γ-treated groups were analyzed for CCR3 expression using Alexa 647-conjugated anti–mouse antibody (see Chapter 2 for details). The histograms were randomly selected to demonstrate difference in fluorescence compared to isotype controls (Figure 18). The results were obtained in four independent experiments for day 7, two experiments for day 14 and four experiments for age groups 11/21 days. At day 7 CCR3 was expressed on 9 ± 0.35% cells, 7.7 ± 0.2% at day 11, 6.3 % at day 14, and 6 ± 0.2% at day 21 in control group (Figure 19). The difference in percentage of CCR3 positive cells between all age groups was not statistically significant (ANOVA, p-value 0.365) for the control samples. The results of CCR3 detection in the stimulated group
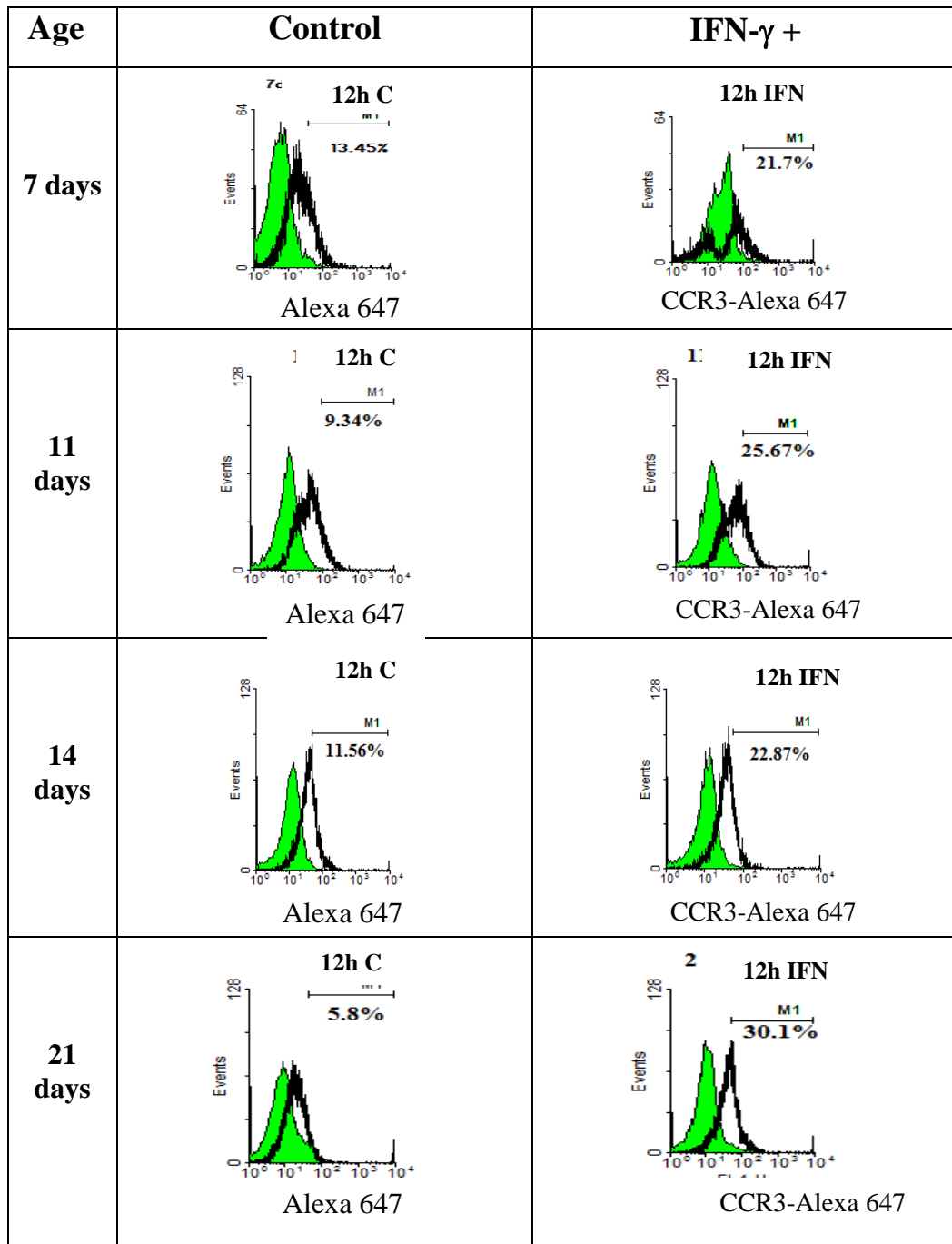
Figure 18. Expression of CCR3 in whole thymic cell suspension in the control and IFN-γ stimulated groups.

Cell suspensions were harvested after 12 hours of incubation. Non permeabilized cells were labeled with Alexa 647 conjugated anti-CCR3 antibodies or corresponding isotype control. The fluorescence was acquired using FACS-Calibur cytometer and WinMDI software. Green areas on the histograms depict binding of the isotype control. Percent of positive events represented the difference between experimental and background fluorescence.
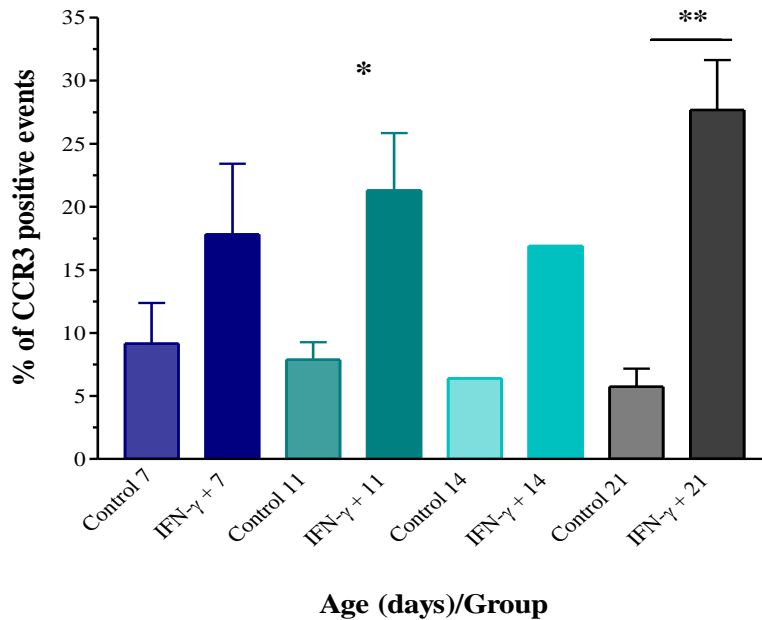
Figure 19. Summary of CCR3 expression by thymic cells in Control and IFN-γ-treated cells for days 7, 11, 14 and 21.
Cells, isolated from whole thymi in suspension were harvested after 12 hours of culturing, immune labeled with anti-mouse CCR3 Alexa 647 conjugated antibody without permeabilization and analyzed by flow cytometry. The effect of the IFN-γ treatment on CCR3 expression was determined by performing paired t-test. At day 7 the difference in CCR3 positive cells between control and IFN-γ stimulated samples was not statistically significant (n = 4, p-value > 0.05). For day 11 thymi obtained values were significantly higher in the treatment group compared to control (n = 4, p-value < 0.05). The difference between control and treatment was also significant at day 21 (n = 4, p-value < 0.01). Comparison was not carried out for day 14 samples due to small sample size (n = 2).

*- p-value < 0.05.

** - p-value < 0.01

revealed significant upregulation of eotaxin receptor by IFN-γ compared to the control group at days 11 (paired t-test, p-value 0.042) and 21 (paired t-test, p-value 0.012) (Figure 19).

Percent of positive cells after stimulation was 22 ± 4% at day 11 and 28 ± 2% at day 21. The difference between groups observed at day 7 was not statistically significant (paired t-test, p-value 0.067) and the test for day 14 was not performed due to small sample size. At day 7, the percent of CCR3$^+$ cells in stimulated group was 17 ± 7% and 16% on day 14. The difference in CCR3 expression between all ages in IFN-γ + groups was not significant (ANOVA, p-value 0.647).

Phenotyping of thymocytes

In order to link the pattern of the eosinophilic infiltration with key stages of thymocytes development we phenotyped the cells in whole thymic suspensions using CD4 and CD8 markers, and idenified four subpopulations of thymocytes differing by expression of these molecules: CD4$^-$/CD8$^-$, CD4$^+$/CD8$^+$ and two populations of single positive cells (CD4$^+$ and CD8$^+$) (Figure 20). Five independent experiments were performed for each age group. At the age 1 day postnatal the thymi were mainly populated by immature double negative thymocytes (55 ± 10%). By day 4 the percent of CD4$^-$CD8$^-$ cells decreased considerably and composed only 12 ± 1.5% of total cell count. During this time period, the number of double positive thymocytes increased significantly from 22 ± 6% at day 1 to 50 ± 12% at day 4. Next time period from day 4 to day 11 was charachterised by a steady rise of percentage of CD4$^+$CD8$^+$ cells. The maximum

Age	Isotype controls	Experiments
Day 7		
Day 11		
Day 14		
Day 21		
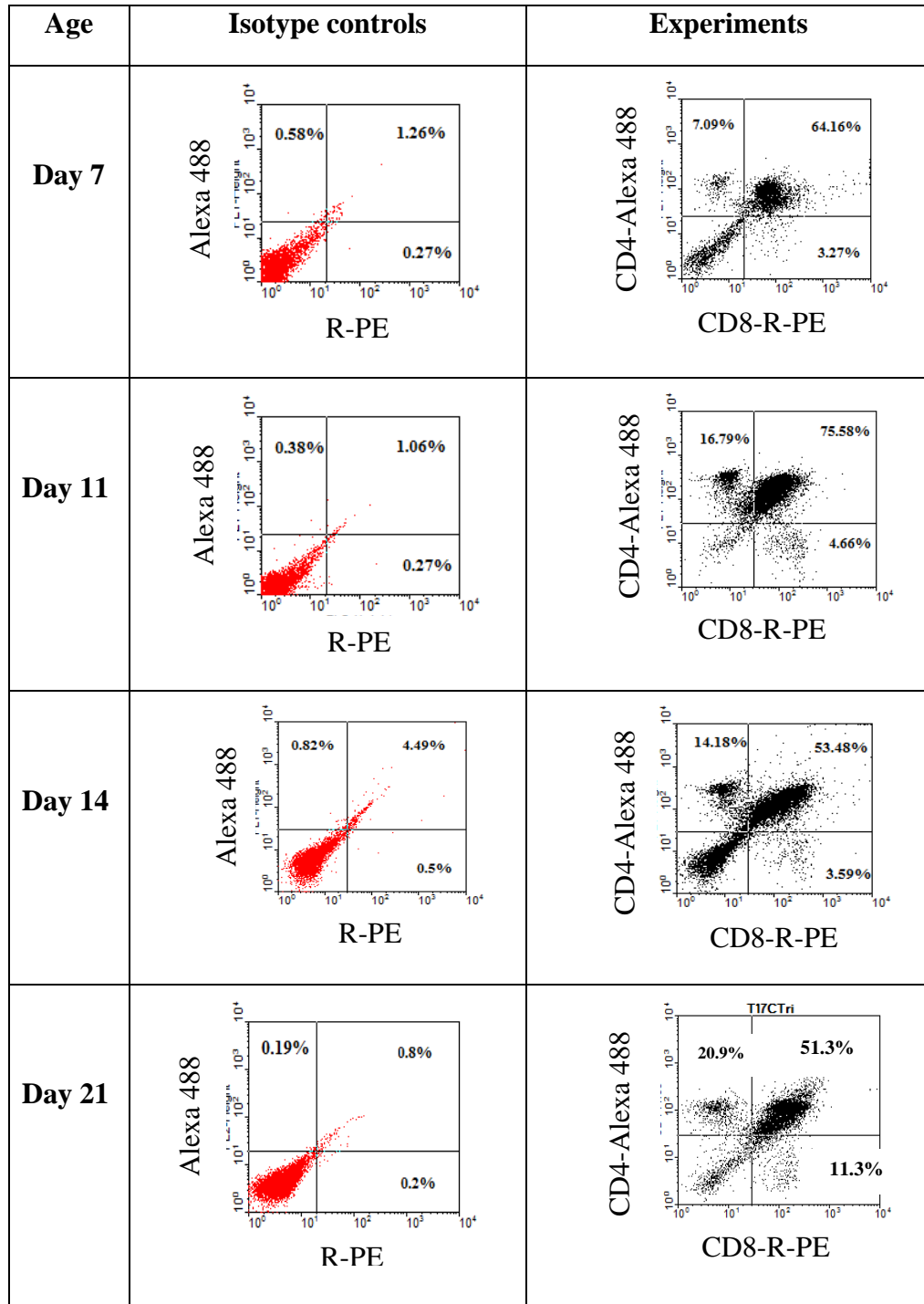
Figure 20. Phenotyping of thymocytes by CD4/CD8 expression in murine thymi at days 7, 11, 14 and 21 of postnatal development.
Non permeabilized thymic cells in suspension were immune labeled by Alexa 488 conjugated anti-CD4 and PE conjugated anti CD8 antibodies. The dot plots in the Experiments column display the percent of positive events without the subtraction of the percentage of cells with background fluorescence.
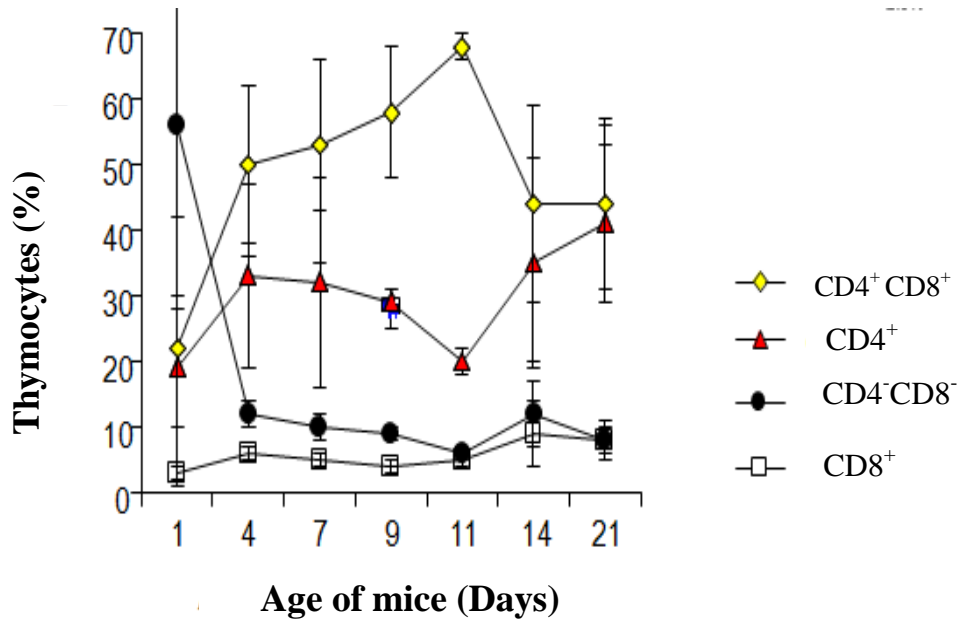
Figure 21. Summary of thymocyte phenotyping by coexpression of CD4 and CD8 molecules.
Cells, isolated from whole thymi were labeled with Alexa 488 conjugated anti - CD4 and R-PE conjugated anti - CD8 antibodies, followed by 4% paraformaldehyde fixation. All experiments were carried out with corresponding isotype controls to detect background fluorescence and non-specific binding of antibodies. Fluorescence was detected using FACS-Canto laser cytometer and row data were analyzed by CellQuestPro software. Five independent experiments were performed for each age group. The data are presented as mean ± SEM.

percentage of immature double positive thymocytes ($70 \pm 2.6\%$) that undergo selection processes and are thought to be susceptable to KYN induced apoptosis, was observed at day 11.

Thymi of day 11 age group also revealed the first significant influx of eosinophils (Figure 13, A.). At day 14 a decrease in numbers of $CD4^+/CD8^+$ thymocytes was observed ($42 \pm 12\%$ of total cell counts). In the next age group (21 days) $CD4^+CD8^+$ thymocytes comprised $41 \pm 10\%$, $CD4^+$ cells were at $40 \pm 9\%$ and $CD8^+$ accounted for $10 \pm 5\%$. A summary of thymocytes phenotyping, performed in this study is presented in Figure 21.

Phenotyping of eosinophils in thymus

Detection of Siglec F^+, Siglec $F^+/CCR3^+$ and $CCR3^+$ cells in whole thymic cell suspension was carried out following the confirmation of antibody specificity for eosinophilic markers using the technique described in the Chapter 2. All experiments were performed with corresponding isotype controls for detection of the background fluorescence. Analysis of dot plots for single- and double-positive events revealed the presence of two eosinophilic cell subpopulations, which were Siglec F^+ and Siglec F^+ $CCR3^+$ (207) and located in upper left and upper right quadrants (Figures 22-25, A., B.). The events in these quadrants were selected into regions, gated and plotted against the side and the forward scatter characteristics to display corresponding characteristics of the cells. The summary of the results is presented on Figure 22, parts C.D.E for day 7, Figures 23, C.D.E. for day 11, Figures 24, C.D.E for 14 days and Figure 25, C.D.E for 21 days old mice. The dot plots showed that cells, gated on the upper part of the dot plots in
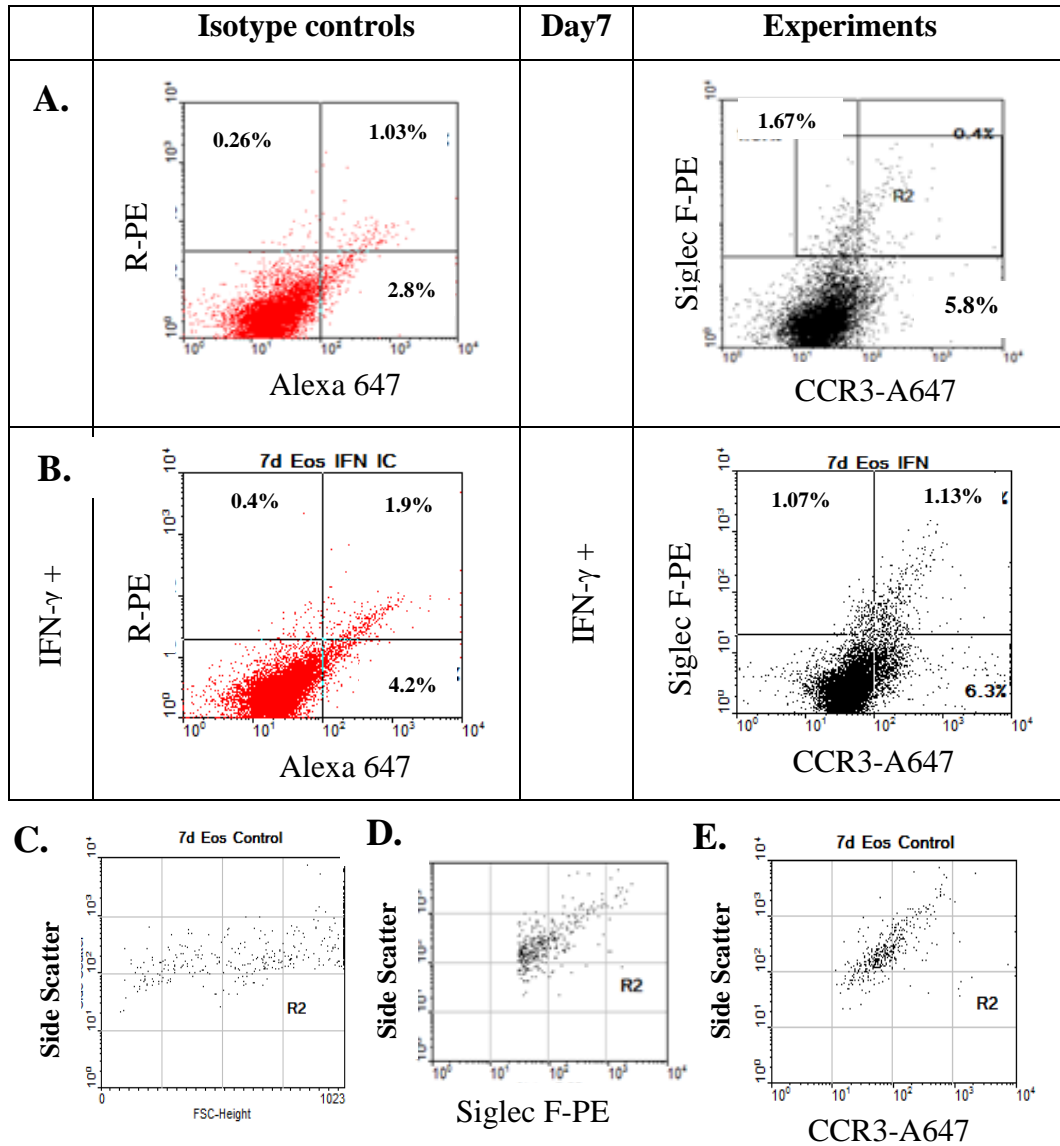
Figure 22. Eosinophils subpopulations in whole thymic cell suspension at day 7.

Cells, isolated from whole thymi were cultured for 12 hours in presence of IFN-γ (treatment group) and in culture media (control group), harvested, fixed/permeabilized and labeled with R-PE-conjugated anti-Siglec F and Alexa 647-conjugated anti-CCR3 antibodies. The percentages displayed on the dot plots in the Experiments column were calculated by subtraction of background fluorescence in isotype controls. **A.** Control group. **B.** IFN-γ treated group. **C.** A dot plot displaying the cells from upper left and upper right quadrants selected into region2 (R2) and plotted against forward and side scatter characteristics. **D.** Siglec F^{+} cells from Region 2, plotted against side scatter. **E.** CCR3^{+} and CCR3^{−} populations from Region 2, plotted against side scatter.
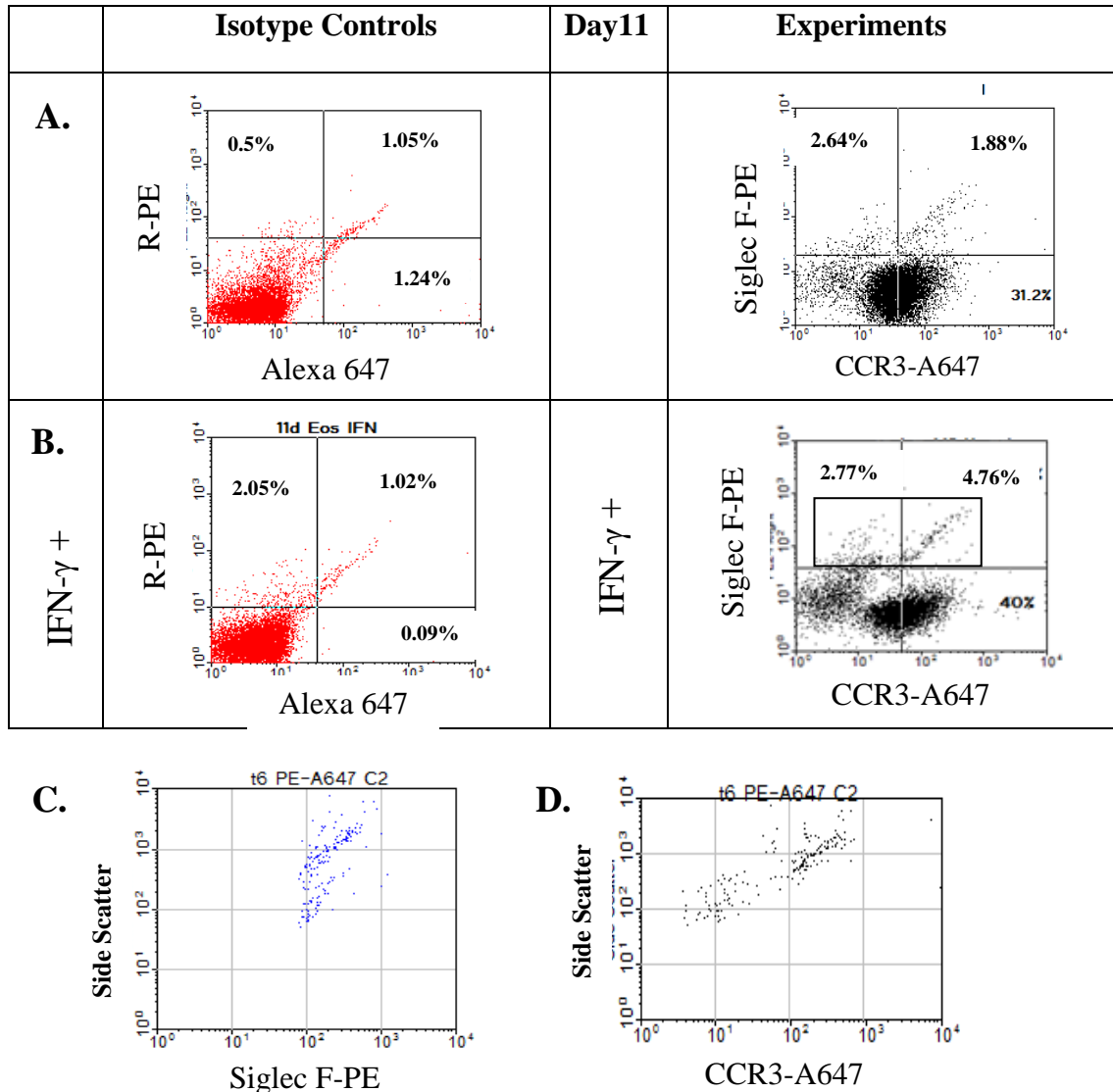
Figure 23. Eosinophils in whole thymic cells suspension at day 11.
Cells, isolated from whole thymi had been cultured for 12 hours in presence of IFN-γ (treatment group) and in culture media (control group), harvested, fixed/permeabilized and labeled with R-PE-conjugated anti-Siglec F and Alexa 647-conjugated anti-CCR3 antibodies. The percentage displayed on the dot plots in the Experiments column were calculated by sutraction of the percentage of positive events in isotype controls. **A.** Control group. **B.** IFN-γ treated group. **C.** Dot plot displaying the cells from upper left and upper right quadrants, selected into region2 (R2) and plotted against forward and side scatter characteristics. **D.** Siglec F$^+$ cells from Region 2, plotted against side scatter.
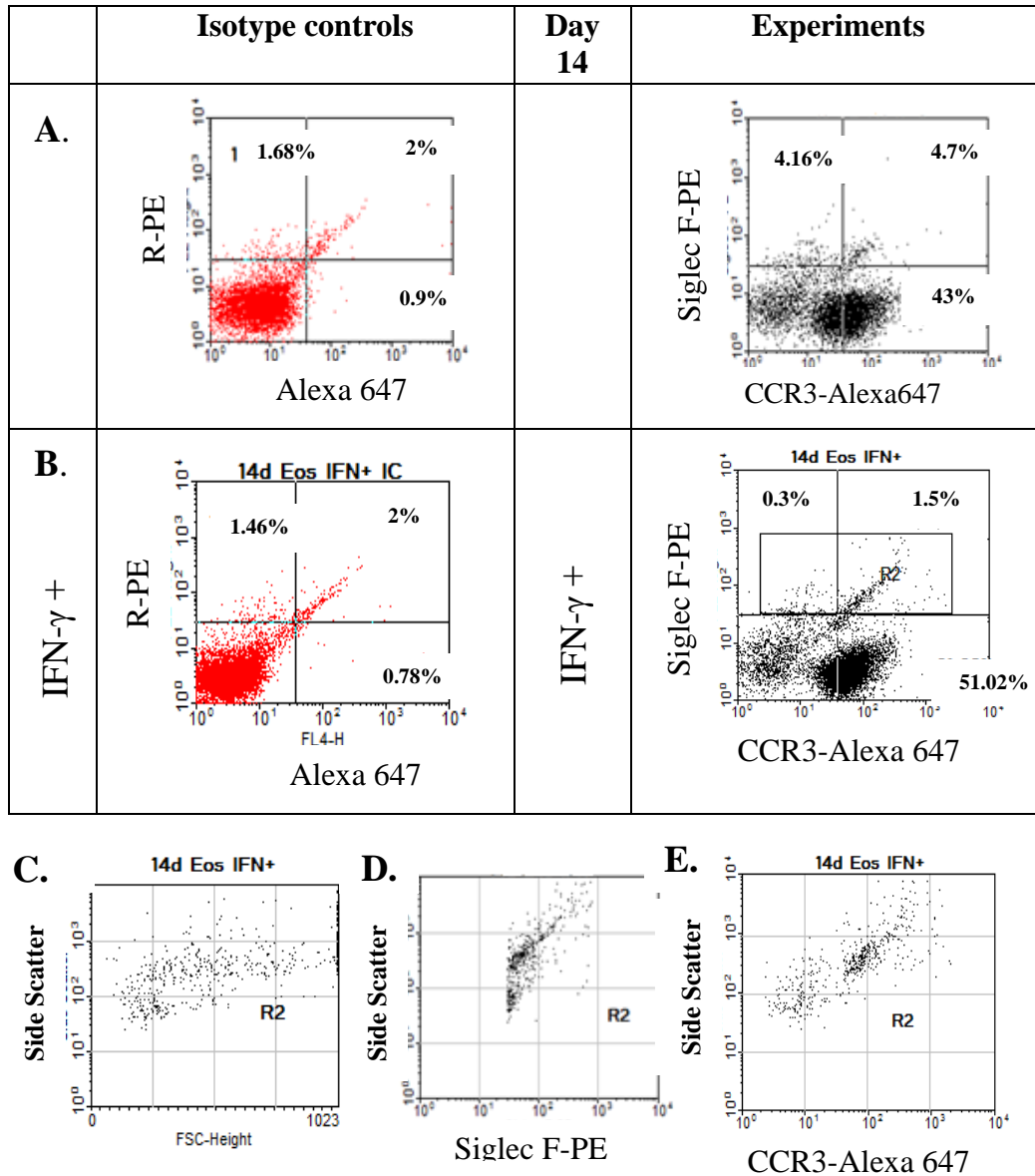
Figure 24. Eosinophils phenotype at day 14.
The cells, isolated from whole thymi were cultured for 12 hours in presence of IFN-γ (treatment group) and in culture media (control group), harvested, fixed/permeabilized and labeled with R-PE conjugated anti-Siglec F and Alexa 647 conjugated anti-CCR3 antibodies. The percentage displayed on the dot plots in the Experiments column were calculated by subtraction of background fluorescence. **A.** Control group. **B.** IFN-γ treated group. **C.** A dot plot displaying experimental results the cells from upper left and upper right quadrants were selected into region 2 (R2) and plotted against forward and side scatter characteristics. **D.** Siglec F$^+$ cells from R 2, plotted against side scatter. **E.** CCR3$^+$ and CCR3$^-$ populations from R 2, plotted against side scatter.

	Isotype Controls		Day 21	Experiments
A.				
B. IFN-γ +			IFN-γ +	

Figure 25. Eosinophil phenotype at day 21.
Cells, isolated from whole thymi were cultured for 12 hours in presence of IFN-γ (treatment group) and in culture media (control group), harvested fixed/permeabilized and labeled with R-PE conjugated anti-Siglec F and Alexa 647 conjugated anti-CCR3 antibodies. The percentage displayed on the dot plots in the Experiments column were calculated by subtraction of the background fluorescence. **A.** Control group. **B.** IFN-γ treated group. **C.** On the dot plot displaying experimental results the cells from upper left and upper right quadrants were selected into region2 (R2) and plotted against forward and side scatter characteristics. **D.** Siglec F^{+} cells from R 2, plotted against side scatter. **E.** CCR3^{+} and CCR3^{−} populations from R2, plotted against side scatter.

A.
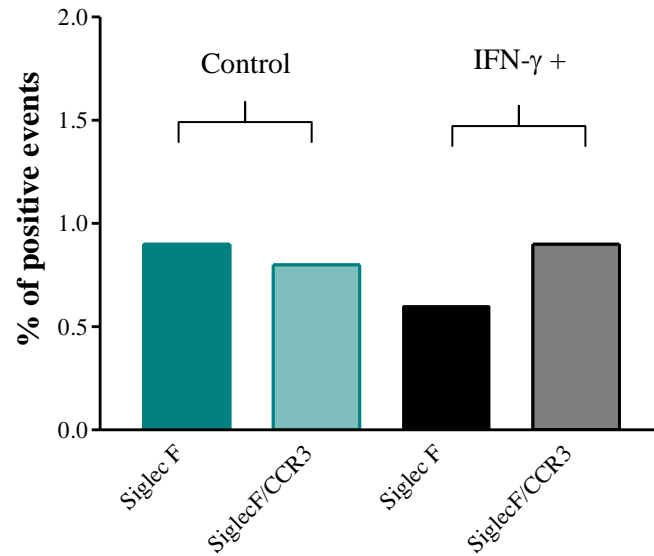
B.
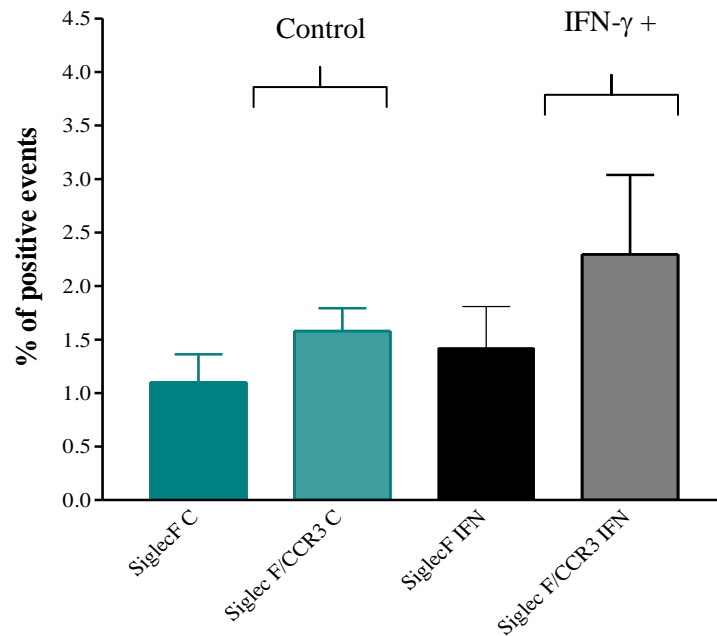
Figure 26. Summary of eosinophil phenotyping in thymic cell suspension by flow cytometry.
A. Day 7 data were collected in two independent experiments. Bar indicates the average value for the percent of positive events. SEM is not applicable due to small sample size. **B.** Day 11. Bars indicate mean ± SEM (n = 4). The difference between CCR3/Siglec F double positive events between Control and IFN-γ+ groups was not significant. (Paired t-test, p-value 0.447).

A.

B.
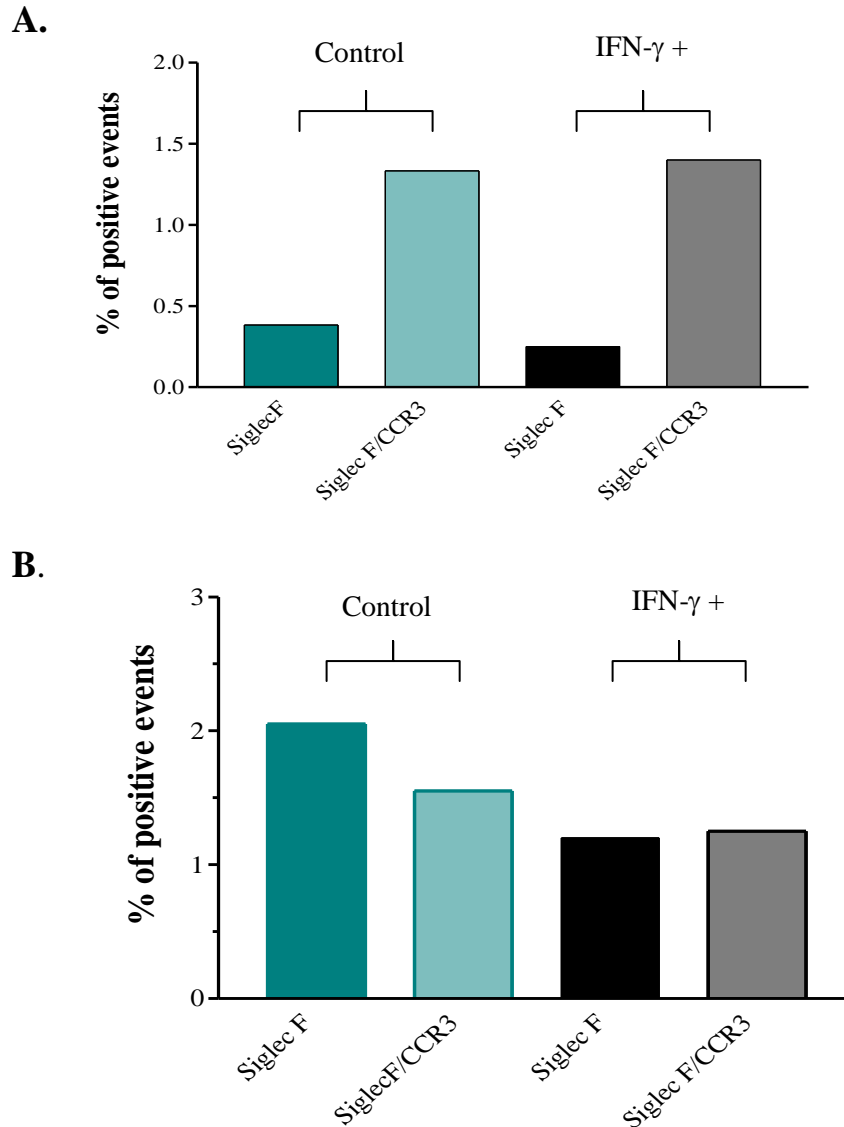
Figure 27. Summary of eosinophils detection in whole thymic cell suspension by flow cytometry.
A. Day 14. **B.** Day 21. For all experiments thymic cells in suspensions from Control and Treatment groups were double-labeled by anti-mouse Siglec F R-PE and anti-mouse CCR3 Alexa 647 conjugated antibody (see Materials and Methods). Data are presented as the percentage of Siglec F single positive and Siglec F/CCR3 double positive events. Two independent experiments were carried out for both age groups. The statistical analysis was not performed due to small sample size.

all ages have similar side scatter and forward scatter characteristics and exhibited properties of granulocytes that fluctuated in size and showed small differences in granularity.

Siglec F $^+$ cells were consistently smaller in size and had less developed granules that may be attributed to their immaturity (27). At day 7, the single positive events comprised about 0.9% of total cell count in control group compared to 0.6% in the treatment group. The percent of the double positive events was 0.8% for the control group and 0.9% for the IFN-γ^+ group. Results were obtained in two separate experiments and the summary is presented in Figure 26, A. There were 1.7% of eosinophils detected in the control experiments from day 7 animals. On day 11 1.1 $\pm$ 0.3% of total cells counts were Siglec F$^+$ events in the control group and 1.4 $\pm$ 0.4% in the IFN-γ treated group, and the difference between these two groups was not significant (paired t-test, p-value = 0.577). Double positive cells represented 1.6 $\pm$ 0.2% of the control preparation and 1.4 $\pm$ 0.4% in the IFN-γ^+ group respectively. Differences between control and treatment groups in Siglec F$^+$CCR3$^+$ cells at day 11 were not significant (paired t-test, p-value = 0.447).

The summary is displayed on Figure 26 B, n=4. At day 11 eosinophils composed 2.7 $\pm$ 0.2% from total thymic cells. At day 14, a decrease in numbers of eosinophil was observed in comparison with day 11 counts, where a composition of Siglec F$^+$ cells was 0.4%, and Siglec F$^+$CCR3$^+$ cells 1.3% in the control group. Among the IFN-γ treated cells there were 0.2% of single (Siglec F$^+$) and 1.3% of double (CCR3$^+$/Siglec F$^+$) positive events detected (Figure 27, A, n=2). As

followed, the percent of eosinophils in cell suspensions at day 14 composed 1.7%

from total thymic cells. At day 21, the numbers of eosinophils increased. In the

thymic cell suspension there were 2.1% of Siglec F^+ immature eosinophils and

1.5% of Siglec F^+ $CCR3^+$ mature cells in the control group. In the IFN-γ^+ group

there were 1.5% of Siglec F single positive and 1.6% of Siglec F/CCR3 double

positive events. The total eosinophil number (mature and immature) composed

3.1% in the treatment group and 3.6% in the control (Figure 27, B, n=3).

Detection of Indoleamine 2,3-dioxygenase in thymic cells by flow cytometry

Although some literature proposed that cells potentially expressing the

enzyme Indoleamine 2, 3-dioxygenase may be a feature in the thymus (89), there

are no documented reports to support this notion. I examined the presence of cells

that may potentially express the IDO protein, by using specific anti-mouse

antibody and secondary fluorochrome conjugated antibody (see Materials and

Methods chapter for details). Secondary antibodies used in this study were

conjugated with fluorochromes for green (Alexa 488), red (R-Phycoerythrin) and

far red (Allophycocyanine, Alexa 647) emission spectrums. In order to confirm

the expression of IDO protein in thymic cells I used the functional test with IFN-γ

treatment, shown to be the most potent IDO inducer in culture conditions (98).

The histograms for cell acquisitions are presented in Figure 28 for day 7, Figure

29 for day 11, Figure 30 for day 14 and Figure 31 for day 21 samples and display

the percentage of IDO positive events after subtraction of events with background

Day 7	Control	IFN-γ⁺
6 hours	1.98%	7.32%
12 hours	3.03%	18.86%
24 hours	1.75%	10%

Figure 28. Histograms of thymic cells acquisition for time course of IDO expression in control and IFN-γ+ groups after 6, 12 and 24 hours of treatment at day 7.
Cells, isolated from whole thymi in suspension, were cultured in presence of IFN-γ in media without addition of the substrate for the treatment groups. Control samples were incubated in the culture media. The samples were harvested after 6, 12 and 24 hours of treatment. Cells were fixed, permeabilized and labeled with anti-IDO antibodies, conjugated with R-PE fluorochrome. The fluorescence was detected using FACS-Calibur cytometer and analyzed by WinMDI software. Turquoise areas on the histograms show the binding of isotype control.

Day 11	Control	IFN-γ
6 hours	3.79% — IDO-Alexa 488	5.82% — IDO-Alexa 488
12 hours	9% — IDO-PE	26.14% — IDO-PE
24 hours	8.42% — IDO-PE	9.31% — IDO-PE
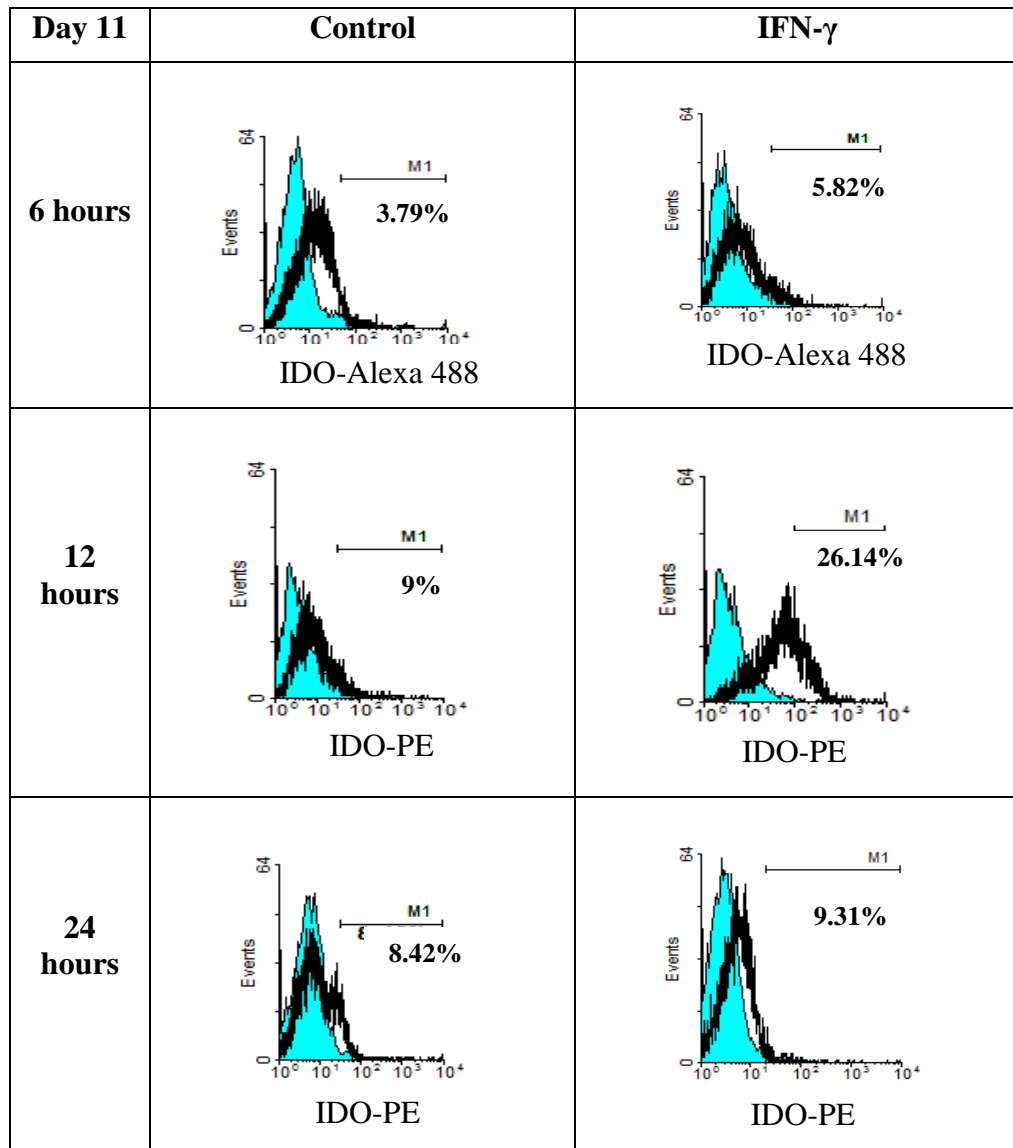
Figure 29. Histograms of acquisition for time course of IDO expression in cells of control and IFN-γ groups after 6, 12 and 24 hours of treatment at day 11.
The cells, isolated from whole thymi in suspension, were cultured in presence of IFN-γ in media without addition of the substrate (tryptophan) for the treatment groups. Control samples were incubated in media alone. The samples were harvested after 6, 12 and 24 hours of treatment and cells were fixed, permeabilized and labeled with anti-IDO antibodies. Secondary antibodies were conjugated with different fluorochromes. The fluorescence was detected using FACS-Calibur cytometer and analyzed by WinMDI software. Green areas on the histograms show the binding of isotype control. The percent of positive events on the histograms represent value after subtraction of the background fluorescence.
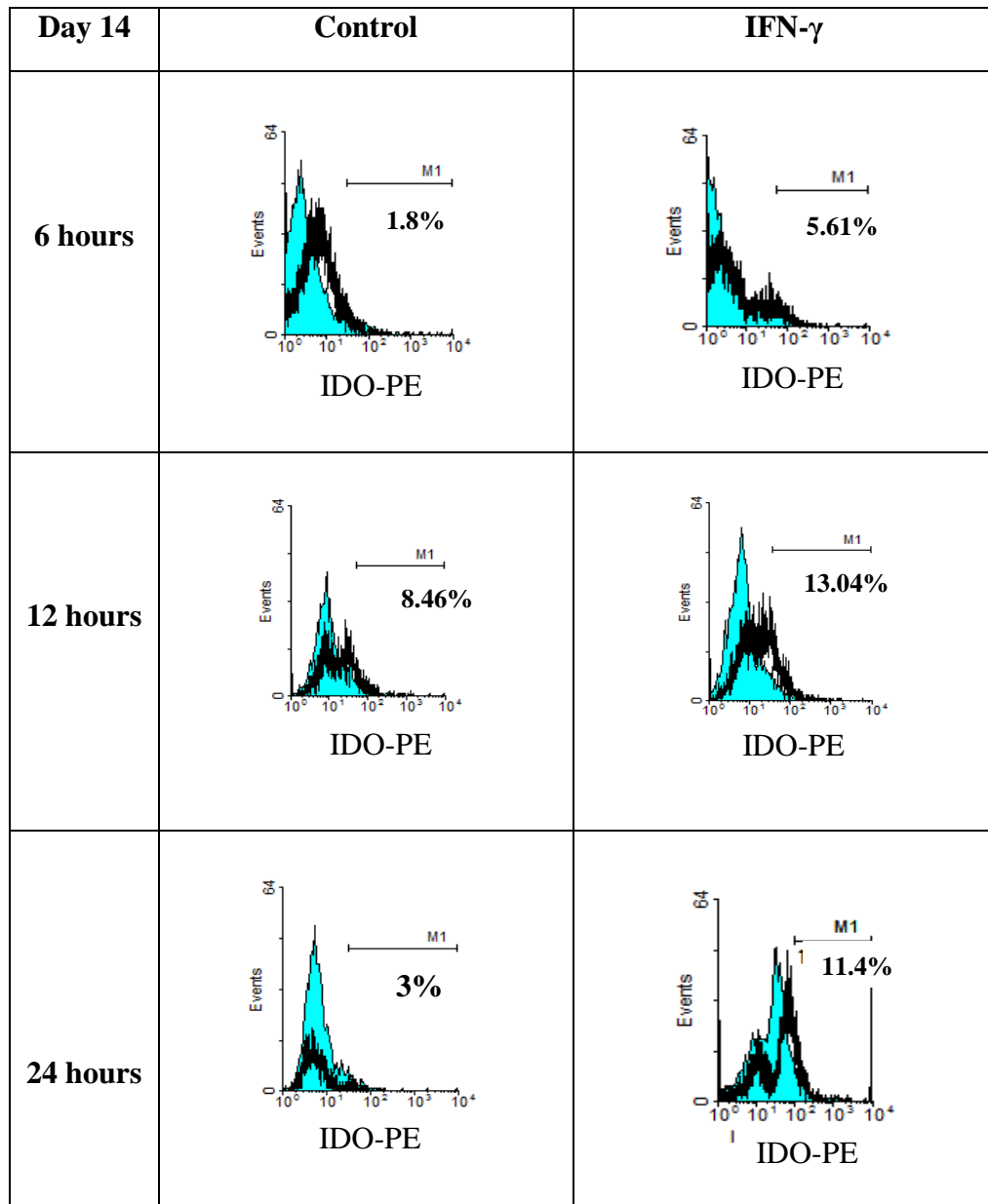
Figure 30. Histograms of acquisition for the time course of IDO expression in cells of control and IFN-γ groups after 6, 12 and 24 hours of treatment at day 14.
The cells, isolated from whole thymi in suspension, were cultured in presence of IFN-γ in media without addition of tryptophan   for the treatment groups. The control samples were incubated in the culture media. The samples were harvested after 6, 12 and 24 hours of treatment and cells were fixed, permeabilized and labeled with anti-IDO antibodies, conjugated with different fluorochromes. The fluorescence was detected using FACS-Calibur cytometer and analyzed by WinMDI software. Turquoise areas on the histograms show the binding of isotype control.
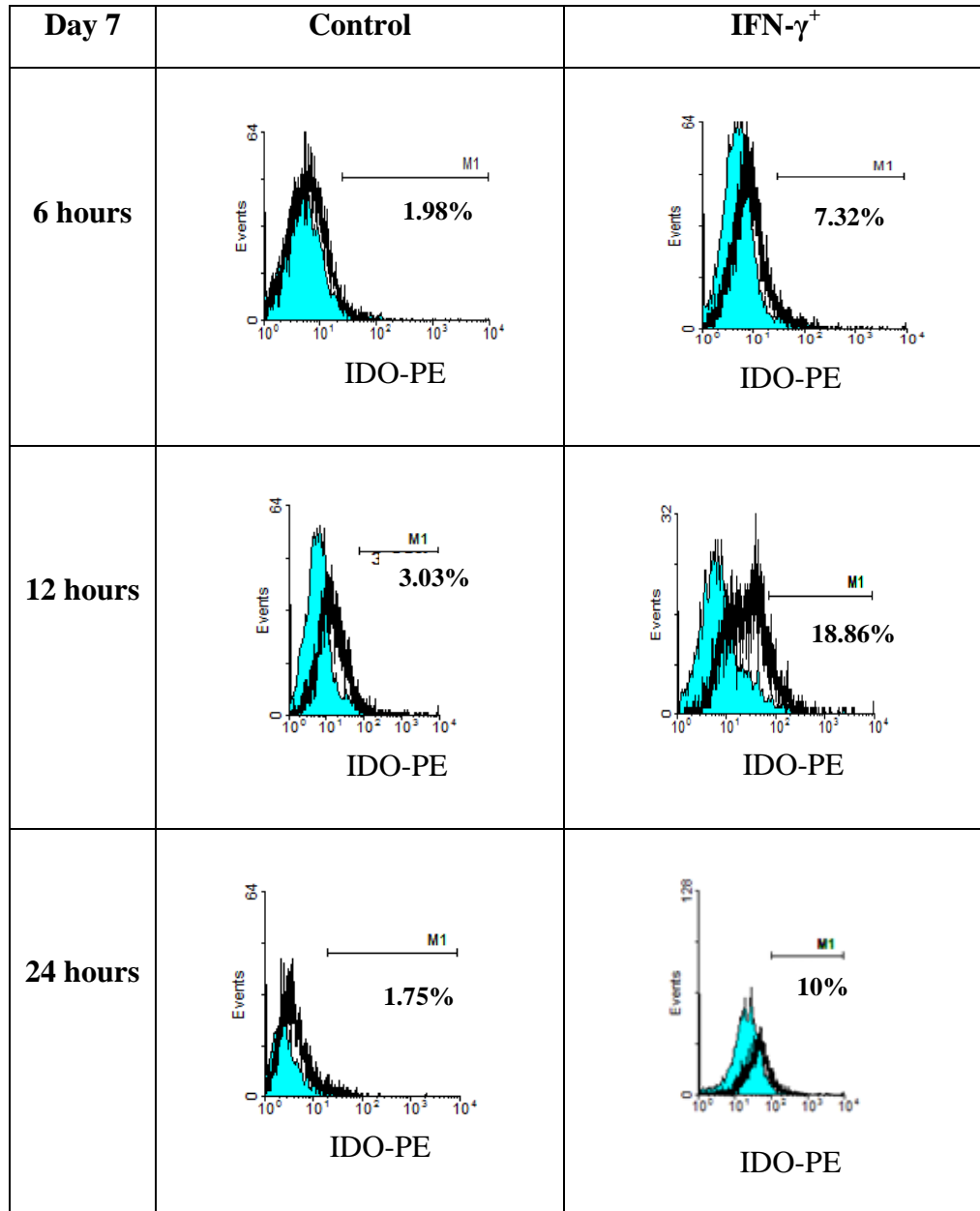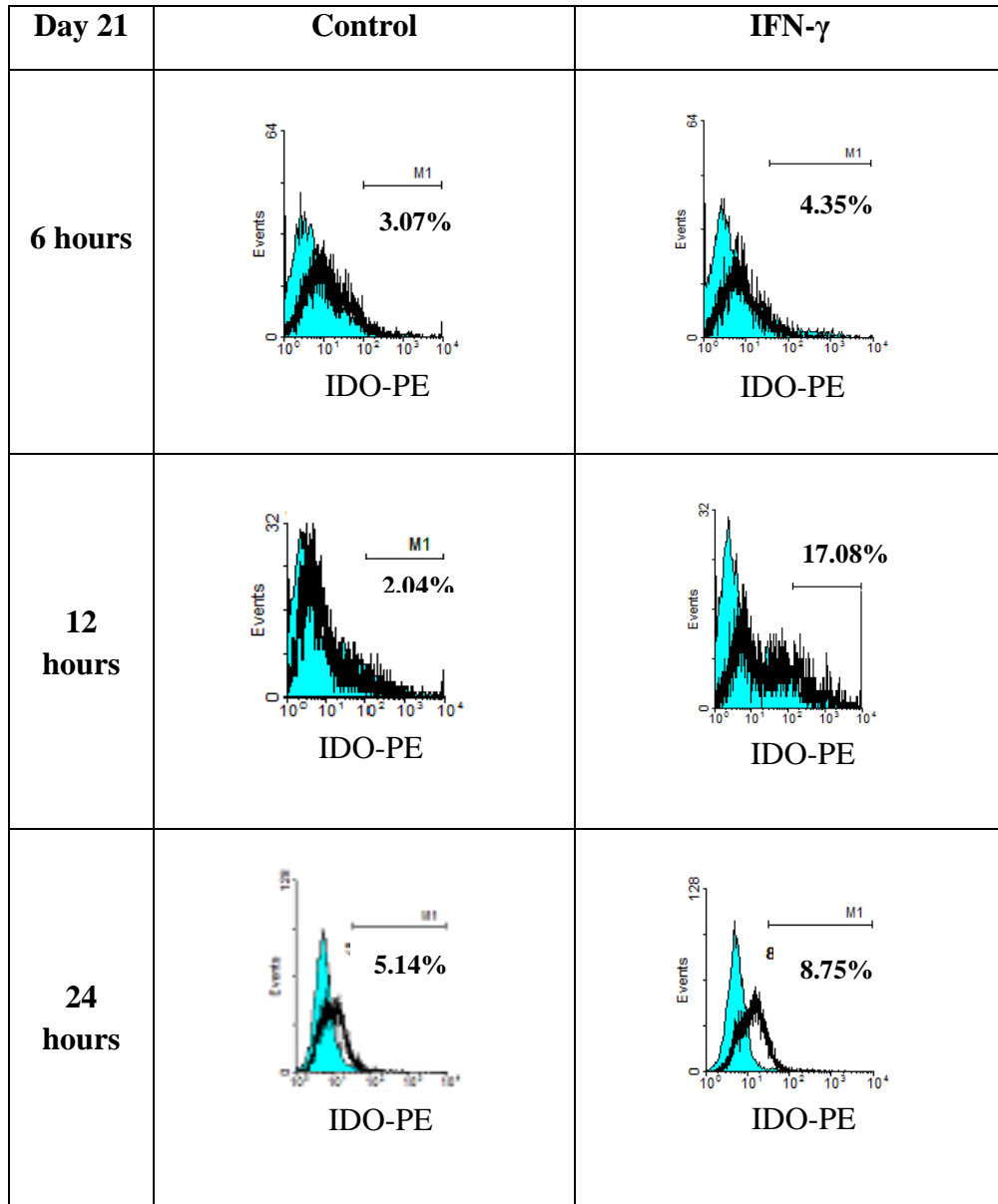
Figure 31. Histograms of acquisition for the time course of IDO expression in cells of control and IFN-γ groups after 6, 12 and 24 hours of treatment at day 21.

The cells, isolated from whole thymi in suspension, were cultured in presence of IFN-γ in media without addition of the substrate for the treatment groups. The control samples were incubated in the culture media. The samples were harvested after 6, 12 and 24 hours of treatment and cells were fixed, permeabilized and labeled with anti-IDO antibodies. The secondary antibodies were conjugated with different fluorochromes. The fluorescence was detected using FACS-Calibur cytometer and analyzed by WinMDI software. Turquoise areas on the histograms show the binding of isotype control.
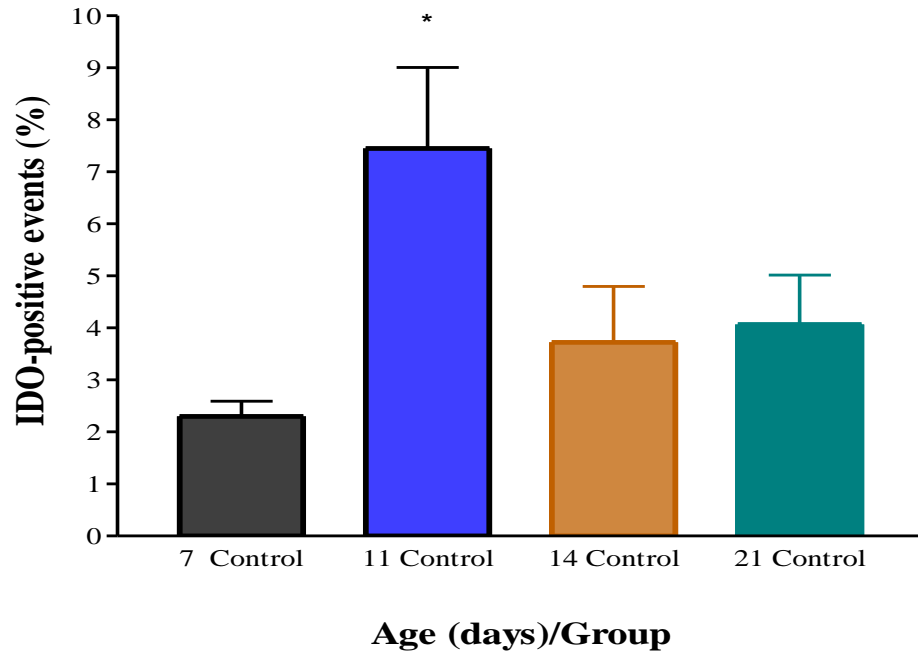
Figure 32. Summary of IDO expression by thymic cells in suspension at different ages for control group.
Thymic cells in suspension were harvested after 6, 12 and 24 hours of incubation without any treatment and substrate addition. Cells were 4% paraformaldehyde fixed, permeabilized and labeled with mouse anti-mouse IDO antibodies, conjugated with different fluorochromes. The fluorescence was detected using FACS-Calibur laser scatter and results were analyzed by WinMDI software. Totally five independent experiments were performed for the separate time point in the each age group.
Data presented as mean ±SEM.
*- p-value < 0.05, one-way ANOVA

fluorescence. A summary of the results is displayed in Figure 32 and represents the mean ± SEM.

In the absence of IFN-γ stimulation, IDO protein was expressed by 2.2 ± 0.3% of thymic cells at day 7 (Figure 32). In the next age group (11 days) a significant (ANOVA, p-value 0.016) increase in percentage of cells positive for IDO (7.2 ± 1.8%) in the control group was observed. At day 14, the percent of positive events were only 3.8 ± 1.1% of total cell counts and (4.2 ± 0.8%) at day 21 (Figure 32) with no significant difference in comparison with days 7 data (Figure 32). Our experiments confirmed that the stimulation with IFN-γ significantly upregulated the IDO expression in thymic cells at all age groups compared to the controls (paired t-tests, p-value < 0.001) and percent of positive events reached 10 ± 2.1% at day 7, 13.8 ± 3% at day 11, 10.2 ± 2% at day 14 and 12 ± 3.8% by the age of 21 days (Figure 32). The difference between age groups in IFN-γ stimulated IDO expression was not significant (ANOVA, p-value 0.764).

The time course showed no significant difference in IDO expression within 6, 12 and 24 hours of thymic cells culture under control conditions (ANOVA, p-value 0.742) (Figure 33, A.); the mean value of IDO$^+$ events was 3.7% after 6 hours, 4.0% by 12 and 5.1% by 24 hours of incubation. In contrast IFN-γ treated groups showed significant increase in IDO production between 6 and 12 hours after IFN-γ exposure (ANOVA, p-value 0.002, Figure 33, B). The mean percent value after 6 hours of stimulation was 7% and reached 17% by 12 hours time period. Culturing of cells in the presence of IFN-γ but in the absence of the substrate (tryptophan) caused a significant decrease in IDO expression. Percent of

A.

B.
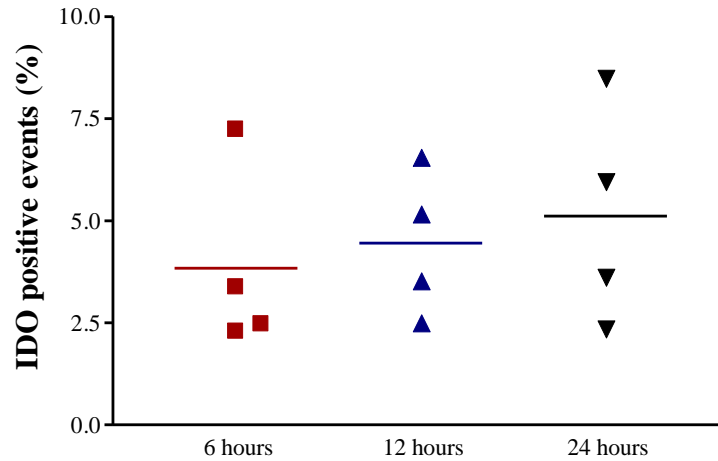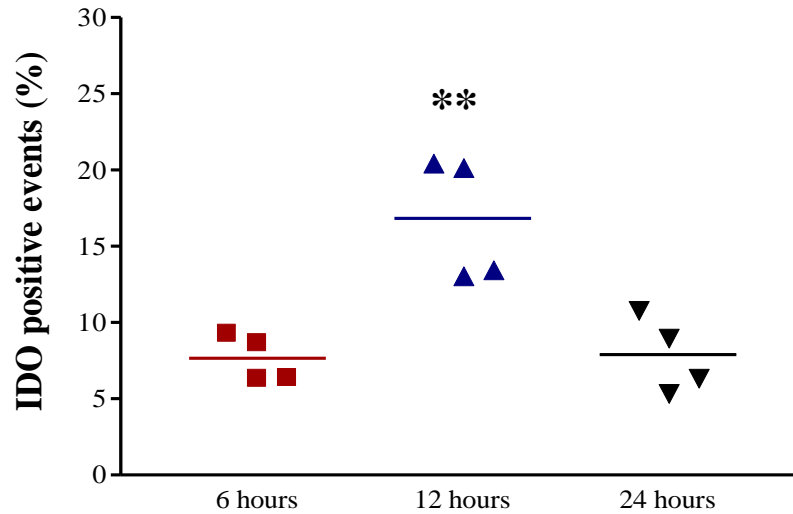
2**Figure 33. IDO expression after 6, 12 and 24 hours of culturing in control and IFN-γ treatment groups.**
Cells in control and treatment groups were harvested after 6, 12 and 24 hours time points of incubation without addition of tryptophan and analyzed for IDO expression by immunocytochemistry and flow cytometry. **A.** Change in IDO expression in control groups was not significant over the time periods analyzed. **B**. Time course of IDO protein expression following the IFN-γ stimulation. The number of IDO$^+$ cells was significantly higher after 12 hours of exposure compared with 6 and 24 hours samples.

**- p-value < 0.01, One-way ANOVA

IDO-positive events was only 7.5% after 24 hours of incubation (Figure 33 B.) and reached the level of 6 hours cultures. All experiments were carried out in duplicates with corresponding isotype controls.

RT-PCR analysis of thymic cells for detection of IDO mRNA

Total RNA was isolated from whole thymi at ages 7, 11, 14 and 21 days postnatally and subjected to reverse transcription following PCR amplification using specific primers (See Chapter 2 for details) for detection of IDO mRNA. RNA preparations from thymi, obtained from different mice revealed the presence of mRNA from IDO gene transcript in all the assessed age groups (Figures 34). The results were compared with reverse transcribed RNA isolated from normal mouse spleen, which served as a positive control. In all tested samples the amplified band was of the expected size (178 bp) and was detected in parallel with positive and negative controls. Sample of isolated RNA, treated without reverse transcriptase was routinely used in the PCR reactions to demonstrate the absence of genomic DNA contamination (Figure 34). Amplification of β-actin cDNA was routinely performed as the obligatory housekeeping gene control (Figure 34). A representative PCR product was extracted from the gel and sequenced using specific primers. The sequencing result demonstrated a 96% similarity with reported murine genome database for Indoleamine pyrrole dioxygenase.

A. Positive control

178 bp product

B.

β-actin

178 bp product

C.

No template control

178 bp product

E.

β-actin

178 bp product

D.

β-actin

178 bp
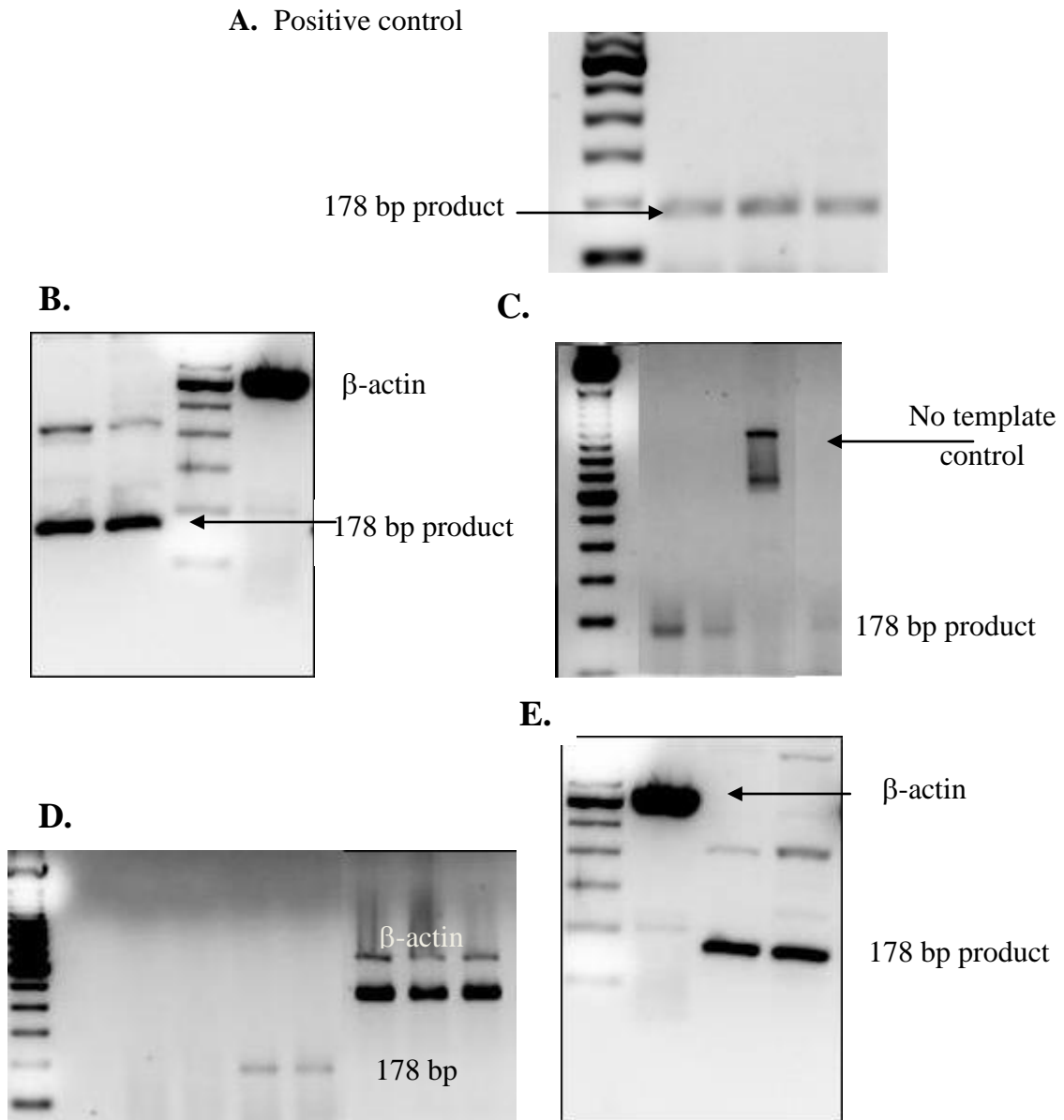
Figure 34. Detection of Indoleamine 2, 3-dioxygenase mRNA in total RNA isolated from spleen (A.) and whole thymi at days 7 (B), 11 (C), 14 (D) and 21 (E).
Using specific primers for IDO gene the PCR amplification of reverse transcribed mRNA was performed. The product was separated by electrophoresis on 1.4% Agarose gel, stained by Ethidium bromide and detected as band in transluminescence with the UV light. A housekeeping gene β-actin cDNA was amplified as a positive template control. The RNA, isolated from normal spleens was used as positive IDO control. The product of a known size (178 bp) was detected against 100 bp DNA control ladder.

Real Time semi-quantitative PCR analysis of thymic mRNA

The levels of IDO mRNA expression were detected by semi-quantitative real time PCR experiments and normalized against mRNA expression of a housekeeping gene, Elongation Factor 1α. A significant increase in IDO mRNA presence was observed in samples from day 11 thymi, compared to all other ages. IDO gene transcription activity was five folds lower at days 7 and 21 compared to day 11 samples (Figure 35, A.). The product was detected in five separate cDNA samples for each age group.

The same samples of cDNA were used to detect the activity of IFN-γ gene transcription. Identified levels of mRNA were normalized against housekeeping gene activity (Figure 36). The results revealed that maximum of IFN-γ gene transcription was detectable at day 7. A steady decrease in transcription of IFN-γ in thymi was observed to be at the minimum level at day 21. The activity of IDO gene expression was 20-28 folds higher (250-1250 U) than transcription of IFN-γ DNA (12-40 U), what was detected in comparison with levels of housekeeping gene mRNA (Figure 36). The expression of Elongation factor 1 α is characterized by relative stability compared to other housekeeping genes, which can be affected by cell proliferation in the tissue (204).

A.
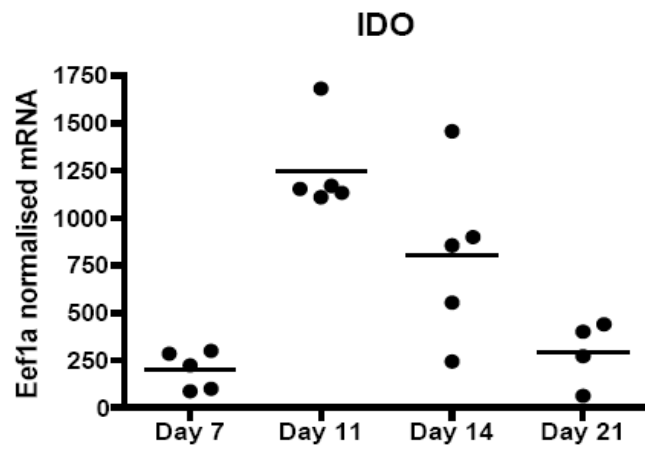
Figure 35. Detection of IDO mRNA by semi-quantitative real time PCR.

B.
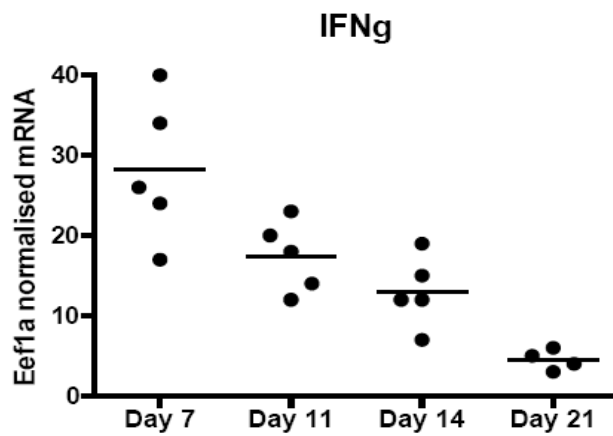
Figure 36. Detection of IFN-γ gene transcription activity by semi-quantitative real time PCR.

Expression of IDO protein by thymic eosinophils

In order to confirm our hypothesis that thymic eosinophils constitutively express the enzyme Indoleamine 2, 3-dioxygenase we analyzed the coexpression of this protein with the specific eosinophilic markers Siglec F and CCR3 on thymic cells. Whole thymic cell suspensions were incubated with combinations of antibody, developed against mouse IDO protein and anti-mouse Siglec F or CCR3 antibody following permeabilization for intracellular staining. The grouping of the fluorochrom-conjugated secondary antibody was matched to avoid the spectrum overlap (see Chapter 2 for details).

We observed the presence of IDO/CCR3 and IDO/Siglec F double positive cells in control groups for all selected ages. At day 7, IDO was expressed by $0.9 \pm 0.2\%$ of CCR3$^+$, and $0.7 \pm 0.2\%$ of Siglec F $^+$ cells (Figure 41). In contrast, day 11 cells showed an increase in numbers of double positive events to $2.6 \pm 0.9\%$ of IDO$^+$ CCR3$^+$ and $1.4 \pm 04\%$ of IDO$^+$ Siglec F$^+$ (Figure 41). For 14 days old thymi a decrease in numbers of double positive events to $1.7 \pm 0.3\%$ of IDO$^+$ CCR3$^+$ and $0.7 \pm 0.2\%$ of IDO$^+$ Siglec F$^+$ was detected, and this was similar to the decrease in absolute numbers of eosinophils (Figure 13, A.) as well as the percent of IDO$^+$ cells in thymus by day 14 (Figure32). At day 21 an identical pattern of IDO expression was observed. This protein was expressed by $2.0 \pm 0.5\%$ of CCR3$^+$ and $1.3 \pm 0.3\%$ of Siglec F$^+$ cells (Figure 41). These data correlated with an increase in absolute numbers of eosinophils identified by IHC on tissue sections (Figure 13, A).

	Isotype controls	Experiments
IFN-γ +		
IFN-γ +		
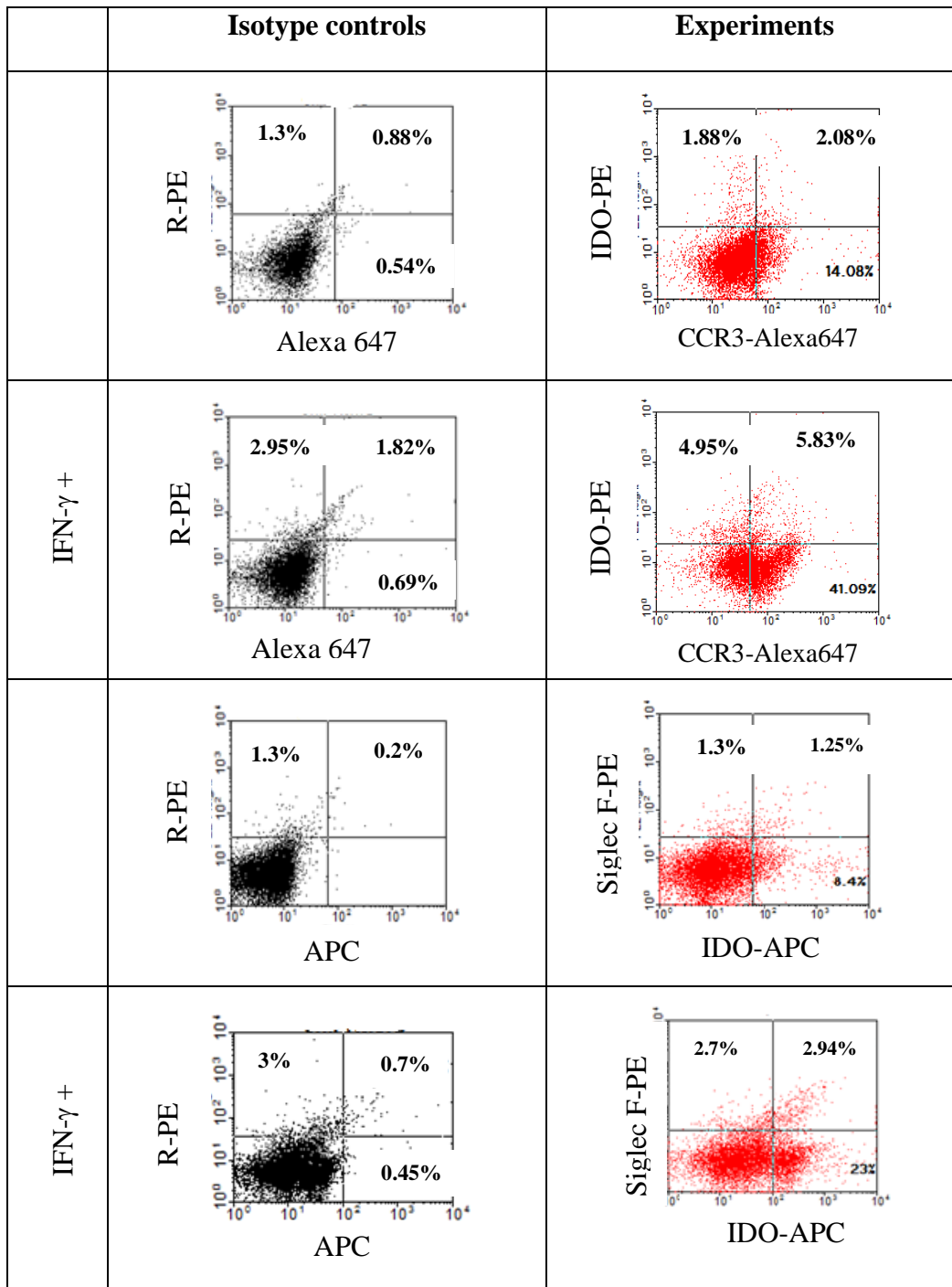
Figure 37. IDO expression by CCR3 and Siglec-F positive eosinophils at day 7.

Thymic cells in suspension were paraformaldehyde fixed, permeabilized and double labeled with IDO/Siglec F and IDO/CCR3 antibodies combinations. The fluorescence was assessed by FACS cytometry and analyzed using WinMDI software. The double-positive events were considered as IDO-expressing eosinophils.
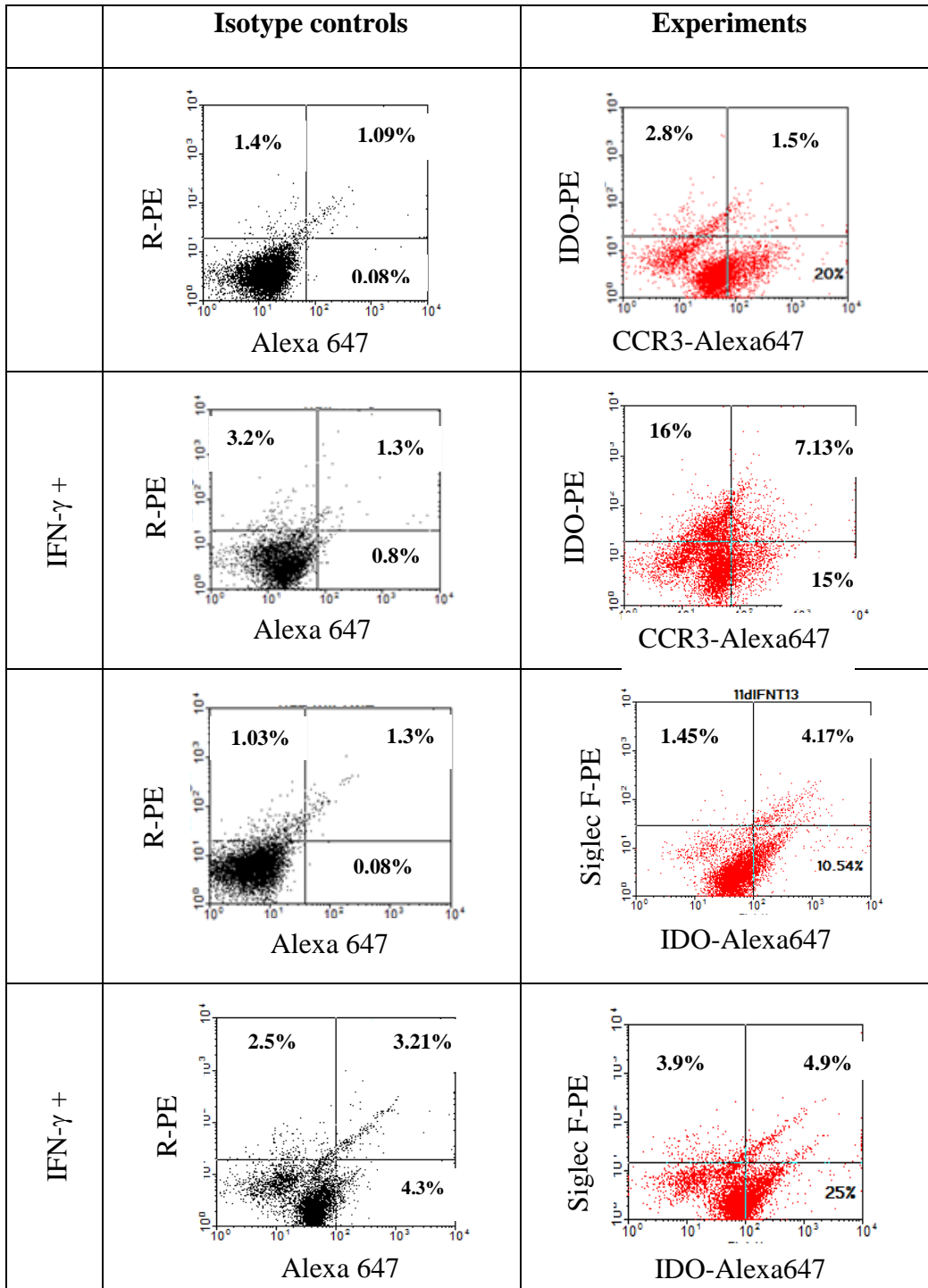
Figure 38. IDO expression by CCR3 and Siglec-F positive eosinophils at day11.
Thymic cells in suspension were paraformaldehyde fixed, permeabilized and double labeled with IDO/Siglec F and IDO/CCR3 antibodies combinations. The fluorescence was assessed by FACS cytometry and analyzed using WinMDI software. The double-positive events were considered as IDO-expressing eosinophils.
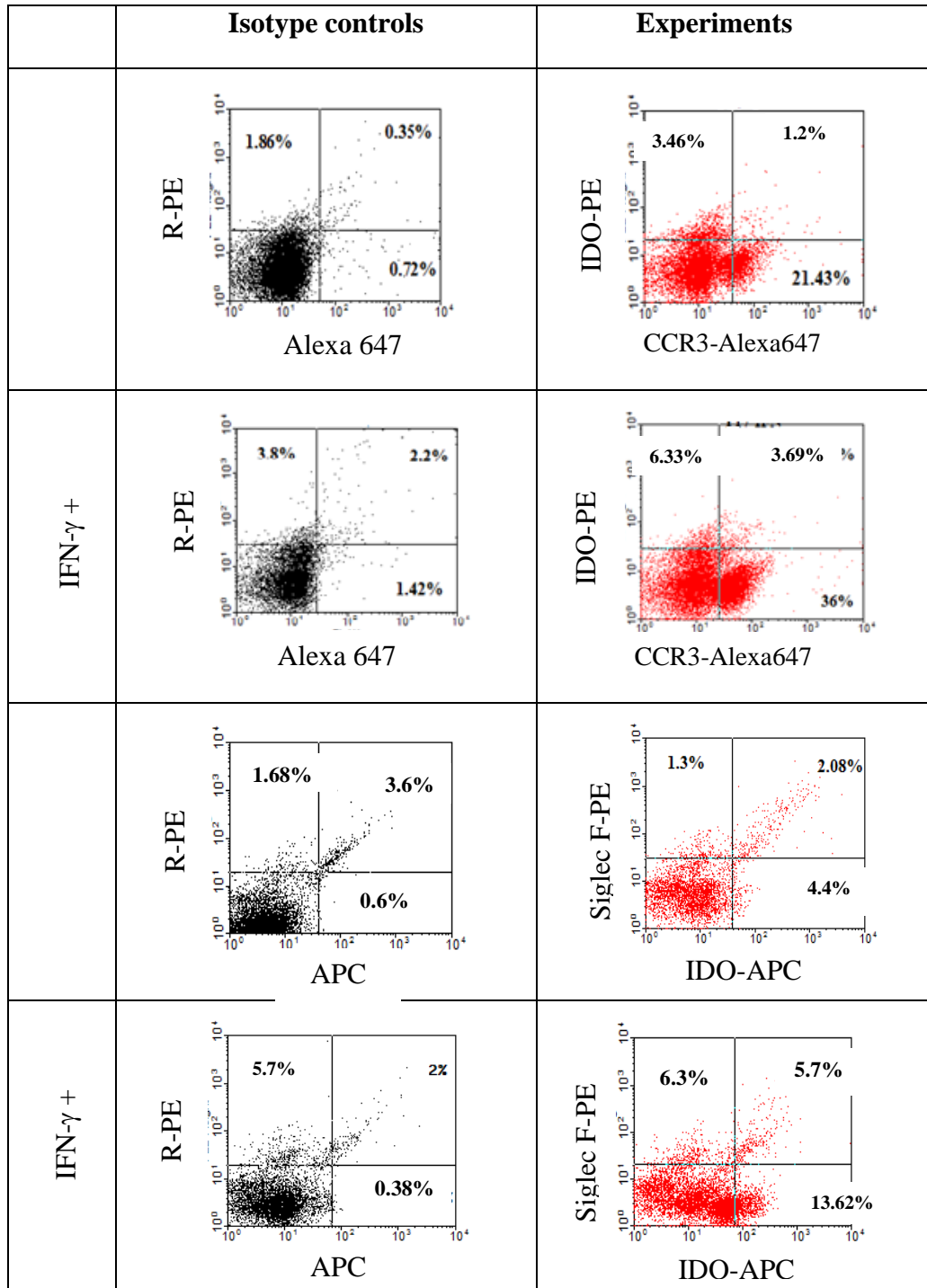
Figure 39. IDO expression by CCR3 and Siglec-F positive eosinophils at day 14.

Thymic cells in suspension were paraformaldehyde fixed, permeabilized and double labeled with IDO/Siglec F and IDO/CCR3 antibodies combinations. The double-positive events were considered as IDO-expressing eosinophils. The percentage value on experimental dot plots presented without subtraction of background fluorescence.

	Isotype controls	Experiments
	R-PE vs Alexa 647: 1.6%, 3.45%, 3.2%	IDO-PE vs CCR3-Alexa647: 4.67%, 3.79%, 15.08%
IFN-γ +	R-PE vs Alexa 647: 2.2%, 1.3%, 1.9%	IDO-PE vs CCR3-Alexa647: 11.5%, 10.87%, 10.23%
	R-PE vs APC: 0.97%, 1.3%, 1.1%	Siglec F-PE vs IDO-APC: 1.34%, 2.38%, 3.67%
IFN-γ +	R-PE vs APC: 4%, 2.85%, 1.7%	Siglec F-PE vs IDO-APC: 0%, 2.19%, 5.9%
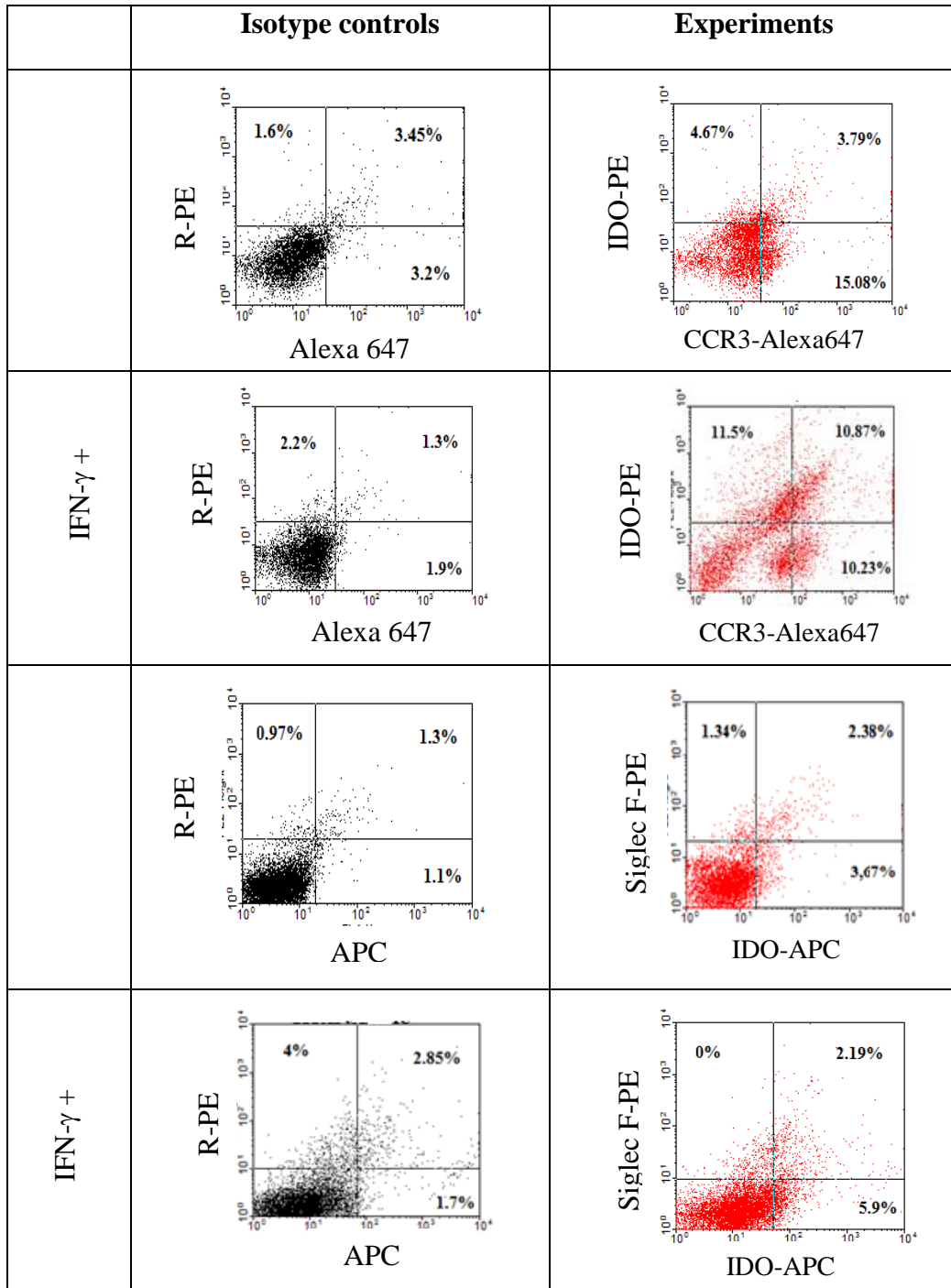
Figure 40. IDO expression by CCR3 and Siglec-F positive eosinophils at day 21.
Thymic cells in suspension were paraformaldehyde fixed, permeabilized and double labeled with IDO/Siglec F and IDO/CCR3 antibodies combinations. The fluorescence was assessed by FACS cytometry and analyzed using WinMDI software. The double-positive events were considered as IDO-expressing eosinophils. The percentage value on experimental dot plots presented with subtraction of background fluorescence.
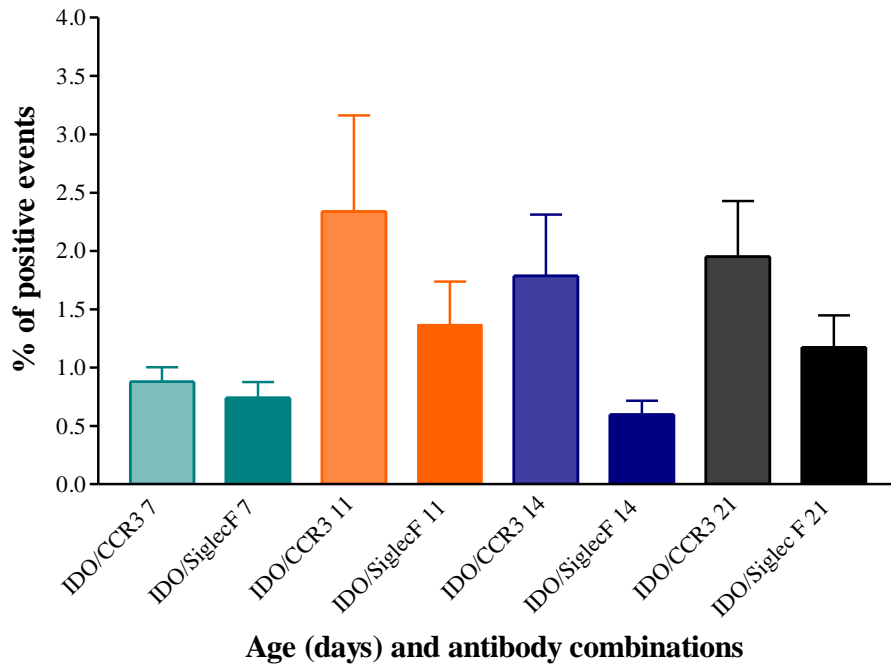
Figure 41. Summary of IDO expression by CCR3 and Siglec-F positive cells in whole thymic cells suspension in control groups.
The cells, harvested after 12 hours of culturing without any treatment and substrate addition, were permeabilized and double labeled sequentially with anti-IDO antibodies and either anti-CCR3 or anti-Siglec F antibodies. The detection of the fluorescence was performed using FACS-Calibur non-sorting dual laser instrument and analyzed by CellQuestPro software. The IDO/Siglec F and IDO/CCR3 double positive events were considered as eosinophils, expressing IDO protein. The percentage of IDO/Siglec F and IDO/CCR3 events was assessed separately and displayed on the bar graph as mean ± SEM.

A.

B.
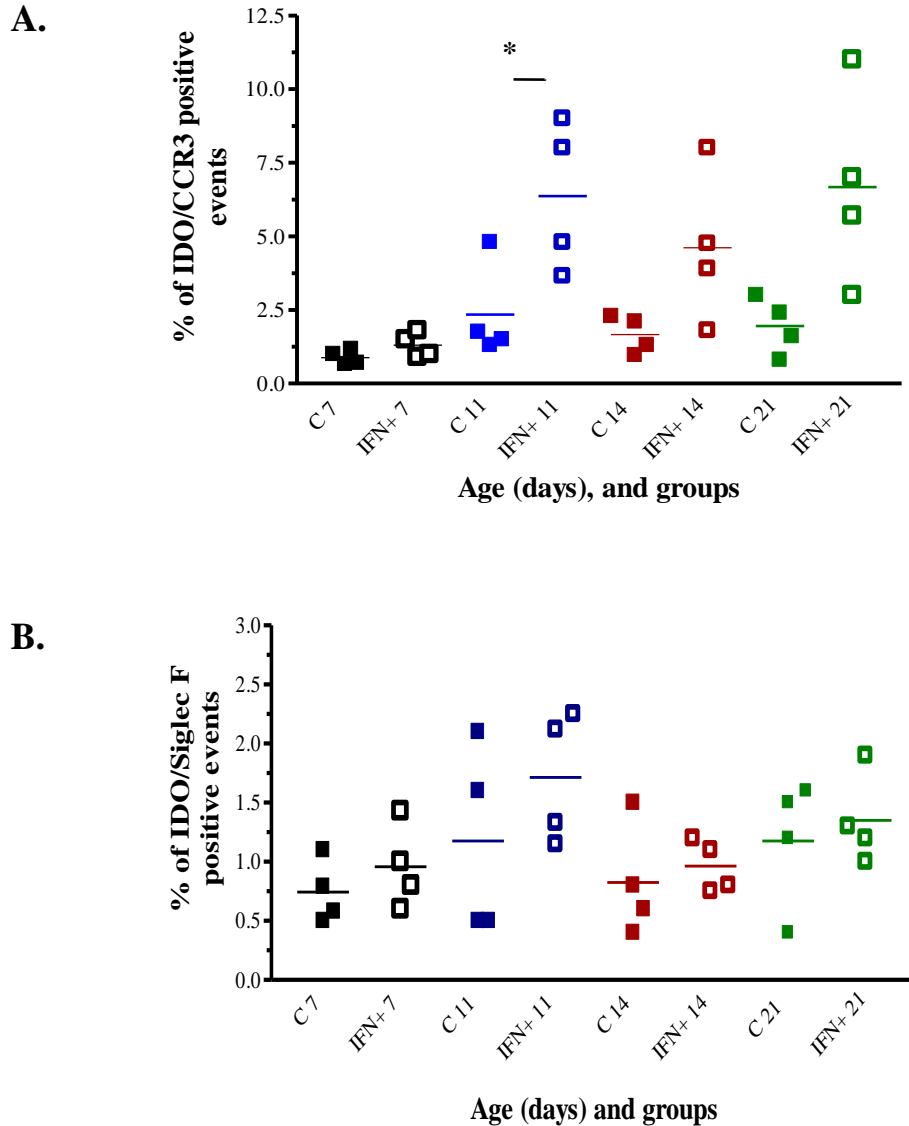
Figure 42. Impact of the IFN-γ stimulation on coexpression of IDO/CCR3 and IDO/Siglec-F molecules.

Cells, harvested after 12 hours of culturing in control and treatment conditions without tryptophan addition, were permeabilized and double labeled sequentially with anti-IDO antibodies and either anti-CCR3 or anti-Siglec F antibodies. Detection of the fluorescence was performed using FACS-Calibur non-sorting dual laser instrument and analyzed by CellQuestPro software. The data were separated into two groups: IDO[+]/Siglec F[+] and IDO[+]/CCR3^{+} events for control and treatment experiments to show the impact of IFN-γ exposure on coexpression of detected molecules. **A.** IDO[+]/CCR3^{+} events for all ages in control and treatment groups. **B.** IDO[+]/Siglec-F[+] events for all ages in control and treatment groups. Paired t-test was performed to demonstrate the difference between control and treatment groups, ***- p-**value < 0.05.

The observed differences in percentage of double positive IDO/CCR3 (ANOVA, p-value 0.268) and IDO/Siglec F (ANOVA, p-value 0.244) events between ages in the control group were not significant (Figure 41).

The percent of IDO/CCR3 double positive events was $1.4 \pm 0.1\%$ for day7, $6.2 \pm 1.3\%$ at day 11, $4.3 \pm 1.7\%$ at day 14 and $7 \pm 1.8\%$ at day 21. There was no significant variation in IDO expression by Siglec F^+ cells in the IFN-γ stimulated cells, and they accounted for $0.9 \pm 0.1\%$ at day 7, $1.8 \pm 0.2\%$ at day 11, $1.1 \pm 0.2\%$ at day 14 and $1.3 \pm 0.1\%$ at day 21 (Figure 42, B.). A significant difference in numbers of $IDO^+/CCR3^+$ cells between control and IFN-γ treated groups for age 11 (paired t-test, p-value 0.023) was observed. A similar difference for ages 7 (paired t-test, p-value 0.214), 14 days (p-value 0.713) and 21 days (p-value 0.351) was not significant. In parallel, it was interesting to observe that $IDO^+/Siglec\ F^+$ (double positive) events the difference was not significant in all age groups (Figures 42 B.). For day 7 results p-value was 0.371, for day11 – 0.313, for day 14 – 0.629, for day 21 – 0.598 (paired t-test).

Discussion

Although the existence and some aspects of eosinophilic infiltration in the mouse thymus have already been reported (70), this study has additional new observations that may further add to current understanding of the significance of this phenomenon.

Eosinophils were identified at early postnatal period using rat anti-mouse monoclonal antibodies raised against a highly specific eosinophilic marker, such as major basic protein -1 (MBP-1) homologue (210). This mAb ensured eosinophils were not misinterpreted as other cell types. The major basic protein (MBP) is abundant in eosinophils and immunohistochemical analyses revealed a very strong its message (211)

I have described the pattern of eosinophils compartmentalization in as much detail as possible using available techniques. My results revealed patterns and dynamics of eosinophilic infiltration within murine thymi starting at day 1 postnatally. The residence of eosinophils within thymic tissue was confirmed by immunohistochemical double staining method, for von Willebrandt factor expressing blood vessels and eosinophilic markers by M. Throsby in 2000 thus provided a background for my study (70). To attribute eosinophil residence to a specific compartment I used pathomorphological criteria such as a difference in hematoxylin staining intensity of thymic cortex and medulla (212). For studying

thymic morphology this decisive factor was considered as reliable and did not require specific staining.

Solitary MBP-positive eosinophils were identified within thymic tissue at days 1 and 4 postnatally. Beyond day 7, eosinophils were detected in cortex and cortico-medullary junction, significantly increased in numbers by day 11 (p-value < 0.05), dropped by day 14 and increased again at day 21. My results revealed that majority of eosinophils infiltrated the CMJ throughout all the time period described. The calculation of eosinophil density was performed using video camera-controlled morphological studies that enabled me to measure the areas of each thymic compartment separately. The results confirmed the predominance of eosinophils in CMJ compartment with a significant increase at day 21 (p-value < 0.01). Thus, it helped me to avoid misinterpretations of eosinophilic infiltration, linked to a depth of organ sectioning (193).

As an attempt to identify whether eosinophilic infiltration correlated with the specific changes in thymic morphology, I calculated cortico-medullary index. This parameter sensitively demonstrates the changes in thymic cellularity under physiological and pathological conditions (213).

The novel part of my study was investigating the expression of IDO by thymic cells and especially eosinophils. My attempt to reveal the IDO protein by immunohistochemistry showed solitary IDO-positive cells within whole tissue section, these results were not considered as convincing and are not presented. I exploited the preparation, combining whole thymic cell suspension, 4% PBS buffered Paraformaldehyde fixation and staining with fluorochrome conjugated

antibody for the acquisition by flow cytometry. The schematic representation of the protocol for this study is described in Chapter 2.

The flow cytometry experiments, performed in this study may be divided into three groups: the first included phenotyping of thymocytes in thymic cell suspension using CD4/CD8 markers to show the normal dynamics in stages of T-sell development. The second assembled the detection of eosinophils in cell suspension using double staining for the surface molecules CCR3/Siglec F and supporting of double staining results by single (CCR3 or Siglec F) marker expression. The third part of flow cytometry study helped me to identify IDO protein in thymic cells and reveal its' expression by thymic eosinophils.

In order to investigate the pattern of IDO expression by thymic cells I validated my results by performing a functional test upon IFN-γ stimulation, which has been shown to induce IDO expression (91). Due to accepted study design (see Chapter 2), phenotyping of eosinophils and detection of their markers in single staining was performed for control and treatments experiments. This added some additional observations to my study.

For IDO detection within thymic cells the samples were stained using the primary monoclonal anti-IDO antibodies and secondary antibodies, conjugated with two different fluorochromes for each sample (R-PE with APC and/or Alexa 488 with APC) to confirm the fluorescence signals. A significant increase was observed in the numbers of IDO expressing cells in control group in thymi of 11 days old mice (p-value < 0.05). IFN-γ stimulation upregulated IDO production with number of expressing cells increased in average to 17%. The maximum level

of IDO production under treatment conditions was detected between 6 and 12 hours of culturing, whereas in control group, the number of positive cells did not change significantly over the tested time course. Comparison of control and IFN-γ treated cell groups showed a baseline of IDO-positive cells in thymi. The control groups may represent the cells, synthesizing the IDO protein either constitutively (214), or induced by different agonists (215).

Eosinophils, expressing IDO protein were detected as IDO$^+$/CCR3$^+$ and IDO$^+$/Siglec F$^+$ events in control experiments for all age groups. The evaluation of IDO expression by thymic eosinophils showed that they were a majority of IDO-positive cells at ages 7 and 21 days (Figure 41).

An interesting observation was revealed in this study by comparison of pattern of eosinophilic infiltration with changes in thymocyte phenotype. The immunohistochemical analysis in this study showed that eosinophils predominantly infiltrated the medulla and CMJ by the time point of the first shift at the age 11 days. The expression of CD4/CD8 molecules, identified on thymocytes for each age group by flow cytometry, displayed the maximum of double-positive immature thymocytes (68 ± 2%) also at day 11, which correlated with the increase in eosinophil numbers. Our thymocyte phenotyping at all ages confirmed a typical pattern of thymocyte development, according to the literature (163). These results associated with an upregulation of IDO protein within thymic cells in control experiments, detected by flow cytometry (Figure 32). Thus, we revealed important correlations of thymocyte development time-points with eosinophils homing to the thymus and IDO expression.

The results of the eosinophil phenotyping revealed that in mice thymi there are two populations of eosinophilic cells: CCR3$^+$ Siglec F$^+$ and Siglec F$^+$ (209). The percent of double positive eosinophils did not vary significantly between control and treatment groups and correlated with eosinophils numbers within tissue sections. The maximum level of eosinophils was detected by flow cytometry at day 21 and comprised about 4.2% of total thymic cells.

The interesting observation was drawn from this study by phenotyping of cells in control and IFN-γ-exposed cell groups: the CCR3 expression was markedly upregulated by IFN-γ stimulation. The single CCR3 labeling revealed that percentage of positive cells in the treatment groups for all ages was significantly higher than in the control groups. The high percent of CCR3 $^+$ cells was detected also in permeabilized samples and it was twice as high compared to the unstimulated cells.

In regard to Siglec F acquisition our results showed that pattern of this molecule expression correlated with eosinophil numbers, quantitated within tissue sections. In cell suspensions this marker was expressed by about 4.2% of total cells at day 21, commensurate with when immunohistochemical analysis showing the maximal numbers of eosinophils in the thymi.

The total thymic RNA analysis by reverse transcription PCR helped to reveal the presence of mRNA for IDO protein. The specific amplification product was detected in reaction samples for all age groups and was confirmed by comparison with positive control templates, derived from normal mouse spleen. The results were further validated by sequencing of the extracted product using IDO-specific

primers with 96% homology to murine IDO pyrrole dioxygenase genomic sequence. To analyze the amounts of genetic material, corresponding IDO and IFN-γ genes transcripts, I used semi-quantitative real-time PCR. One of the most important prerequisite for these experiments was a very accurate RNA isolation and reverse transcription, minimizing the loss of genetic material. However, it is difficult to avoid variability in these initial steps. Therefore, quantification of a target and reference genes in the same sample was required for validation of the results. To be used as a housekeeping gene (HKG), the gene should have a stable expression rate in the sample (216). In my experiments a HKG elongation factor 1α has been used for results validation. The transcription rate of this specific gene was reported to be stable in the cells, undergoing extensive proliferation (204). Thymic tissue may be an example of a very fast changing cellular environment. The semi quantitative real time PCR analysis showed a significant increase in levels of mRNA for IDO protein in samples from 11 days old mice of compared with 7, 14 and 21 days old animals. These results correlated with significant increase in IDO expressing cells in day 11 control groups and the shift in eosinophil numbers as well as percentage of double positive thymocytes. We carried out the real time PCR analysis of cDNA samples that were reverse transcribed from total thymic RNA on the presence of IFN-γ transcript. The finding revealed that the levels of the IFN-γ mRNA, normalized against elongation factor 1α housekeeping gene expression, were significantly lower (5-40 U of Eef1α mRNA) than those of IDO mRNA (250-1250 U of Eef1α mRNA). The strongest IFN-γ message was detected at day 7 (Figures 35, 36).

In the finalizing remark to the "Results" section I could conclude that the experiments, performed in this study may be considered as an initial step for further exploration of eosinophil involvement in intrathymic T-cell development and their expression of IDO protein.

Chapter 4

Discussion

In this study I attempted to find a potential role for eosinophils infiltrating the mouse thymus in thymocyte development during early and late postnatal period. In humans, the presence of eosinophils in the thymus has been shown under homeostatic conditions (217) as well as accompanying thymic pathology (218). The existence of eosinophils has been explored in thymi of rats (219), swine (123), and horses (220). These and many other observations confirmed that in several mammalian species, the thymus is a site of eosinophils' homing. In mice eosinophils in the thymus have been routinely determined during analyzing of their trafficking pathways to various tissue sites (32).

As I have already described in the first chapter, in addition to the thymus, the eosinophils normally infiltrate the gastro-intestinal tract (GIT) and the female reproductive system (uterus and mammary glands). In these organs, infiltrating eosinophils have been shown to play a significant role in maintaining of homeostasis, development and functions (221). Compared to the amount of information available about the role of these cells in GIT and reproductive organs, our knowledge of thymic eosinophils still remains limited (211). Only in recent times there has been an increase in interest to investigate the role of thymus in immune function and an involvement of all thymic elements in T-cell development.

The experiments in mice involving myeloid leukemia induction and thymectomy performed by J. Miller in the 1950s pioneered our appreciation of the role of the thymus in immune response (222). Since then, our understanding of this enigmatic organ has expanded and mouse models have been extensively used for studying thymic development and function. Genetically modified animals, such as TCR transgenic mice, and athymic NUDE mice, are widely accepted as murine models for investigating intrathymic T-cell development (223). These and many other mouse models helped to dissect the properties of adaptive immunity and extrapolate the data to human studies. In humans, the function and nature of neonatal T-cells have been investigated mainly on cord blood samples, material from fetuses and postsurgical biopsies, because the access to human organs is very limited and requires special ethical approval (224). These facts may advocate for the limited observations of thymic eosinophils in human subjects. However, some progress in comparison of thymic cellular microenvironment and T-cell functions in humans and mice have been made (225). The processes of thymocyte maturation and selection in humans and mice start during gestation, although, at the time of birth mice thymi are immature relative to humans; the thymus of a newborn infant corresponds to a one-week old mouse thymus (226). This difference in maturity may help to evaluate some fetal stages of human thymic development using a mouse model. Moreover, genetically modified mouse models with deficiency in either Indoleamine 2, 3-dioxygenase (IDO) protein (227) or eosinophils (PHIL mouse) (188), which can contribute vastly to understanding of both of these elements in thymic function. Thus, murine models,

in spite of their limitations in relevance to human thymi, have an advantage to exploit in the study of T-cell maturation early in life; I therefore am justified in my choice to use mice for the study of thymic eosinophils.

The novel information about potential immune modulatory function of eosinophils (86) have prompted research towards exploring the interaction between eosinophils and various immune cell types during the inflammatory response as well as in homeostasis. Eosinophils act as part of adaptive and innate immunity as well as promoters of immune modulation within inflammatory sites including draining lymph nodes (228). But the main question posed in this study is the function of eosinophils in a primary lymphoid tissue, where antigen presentation and T-cell apoptosis have implications, different from those at the secondary sites (105). Eosinophils in the thymus are a part of the intrathymic microenvironment and may interconnect with other cell types in different ways. Even though the possible involvement of eosinophils in thymocytes development has been suggested (70), the potential pathways for interaction between them are yet to be elucidated. In my study I attempted to focus on the capacity of eosinophils in thymus to express IDO, which in turn is capable of cell function altering via breakdown of tryptophan.

All experiments, undertaken in this study could be divided into two groups: first part involving the pathomorphology of eosinophilic infiltration in thymus and its correlation with major events in thymocyte development; while the second part consisted from molecular biological and immunological techniques used to explore the presence of IDO message in the thymic tissue.

For the pathomorphological studies, I identified eosinophils using a highly specific eosinophilic marker, namely the major basic protein -1 (MBP-1) homologue (210), which has no interference with other cell types. This marker identified mature eosinophils, when the secondary granules were developed and accumulated this protein within them (211). Thus, immunohistochemistry, performed in my study (191) explored the mature MBP-positive eosinophils in mouse thymus. Previous studies on mouse thymic eosinophils (70) used different and non-specific markers.

Even though an age-related difference in eosinophilic infiltration of the thymus has been noticed previously (229), this study presents a very detailed assessment of the timing and compartmentalization of thymic eosinophils in mice. I investigated the thymi starting at day 1 postnatally with 2-3 days intervals. This helped to identify the onset age of thymic eosinophils as well as later changes in infiltration. My results revealed that unlike in humans (229), mouse mature eosinophils were found in the thymus only after birth (day 1 postnatally). Solitary cells were observed in the cortico-medullary junction (CMJ) and connective tissue compartments such as capsule, interlobular septae and trabecules. The appearance of MBP-positive eosinophils in these sites suggests their arrival from the blood circulation as well as infiltration through the connective tissue compartments. The CMJ is enriched with a well-developed capillary system (115) and is a site of influx of cellular elements migrating to the thymus (152). Trafficking and entry of the eosinophils into homing tissue is regulated by the actions of a specific system of chemokines, especially eotaxin and its' receptor CCR3 (53). Eotaxin has been

shown to be expressed by cells in the thymic medulla (230). This fact provides further support to the observation of residency of arriving mature eosinophils to the CMJ and medulla. In the cortex, eosinophils were found only at early ages (days 1-7). Later their location in this compartment became very limited and contributed less than 20% of all cells present. The presence of eosinophils in the thymic connective tissue suggested their penetration to the subcapsular and cortical areas through this compartment. My pathomorphology results showed that eosinophilic infiltration of the mouse thymus significantly increased by day 11 in comparison with earlier ages. At day 11 eosinophils were detected as scattered cells around CMJ as well as in the form of cellular aggregates. They were also observed in greater numbers in the medulla but less in the cortex. This first shift in the eosinophilic infiltration correlated with the predominance of semi-mature double positive thymocytes that would have progressed through a period of significant proliferation, positive selection and would have moved to the sites of negative selection (231). Eosinophils' numbers increase occurred while extensive negative selection was taken place and resided within compartments, associated with deletion of autoreactive pro-lymphocytes (232). Moreover, in the mouse thymus they express costimulatory molecules CD80/CD86 and present antigens (70) both of which have been shown to be essential elements for negative selection (233). All this observations suggest eosinophils' involvement in thymic function, but whether eosinophils have a role in selection process remains a subject of speculations.

Evaluation of eosinophilic infiltration in this study revealed fluctuations in these cells' density. After a significant increase in numbers at 11 days (p-value < 0.05), the incidence of eosinophils decreased by day 14 but underwent a second influx into the thymus by day 21. To investigate the morphological changes of the organ during postnatal period and their possible correlation with the eosinophilic infiltration, cortex-to-medulla ratio was measured and calculated. It is a sensitive indicator of acute, pathological and physiological alterations in thymic cellularity (213). Morphologically, thymic cortex is a compartment, tightly populated mainly by arriving lymphoid progenitors and proliferating immature thymocytes (113). The volume of cortex prevails this of medulla at young ages, when thymus is especially active. Cortical immature thymocytes are sensitive to any stress, such as infection, trauma, and ionizing radiation (234). These traumatic factors induce apoptosis of extensively proliferating cortical cells, thus, volume of cortex may become noticeably reduced. However, the lessening of thymic cortex cellularity is a physiological feature. Decline of thymic function after puberty is a normal process (109). With aging arrival of progenitors from bone marrow diminishes, cortical thymocytes decrease ability to rearrange TCRs and proliferate (112). Thymic involution and weight reduction starts in humans at the age of one year (224). The slight decrease in cellular density of the cortex, the drop in cortex- to-medulla ratio and the depletion of immature $CD4^+$ $CD8^+$ thymocytes have been observed at a rate of approximately 3% per year (224). In this study, I attempted to reveal the morphological changes in murine thymi during early postnatal development until weaning (21 days).

It is well-known that the dynamics of thymocyte development shows a specific pattern during ontogeny of mouse thymus. CD4/CD8 double negative immature thymocytes are the predominant cell population at day 1 after birth (161). My observations displayed that at this time point the volume of the cortex predominated comparing to the medulla with the cortex: medulla (C: M) coefficient being the highest at day1. The expansion of double positive cells proceeded during the first ten days of postnatal development (162). Previous data have been shown that after the extensive proliferation, double positive cells undergo positive selection and start trafficking towards thymic medulla (150). During this time period I observed gradual but non-significant decrease in C: M ratio. In the Balb/c mouse model, the reduction in thymic cellularity and the significant decrease in C: M ratio by day 21 reflected physiological changes that accompanied the movement of thymocytes through thymic compartments. This event correlated with significant increase in eosinophils' numbers and their density in the medulla and CMJ. Our data revealed that eosinophils infiltrated predominantly the CMJ throughout all the time period described. The 3D cell count showed a high proportion of eosinophils in this compartment with a significant increase at day 21. Eosinophils may therefore complete the specific cellular microenvironment of the CMJ and medulla of the mouse thymus and they could have served as identification marker of these compartments (235) In addition, our observations suggest that eosinophils may play a role during changes in thymic cellularity, but such a hypothesis requires further experimentation.

Beyond the detection on the tissue sections by immune binding with anti-MBP antibody, thymic eosinophils were also phenotyped following their isolation from whole thymi. The research experience from our laboratory and literature reports suggested the detection of eosinophils by labeling of eotaxin receptor (236). However, my results revealed that in murine thymi CCR3 molecule may be expressed in other cells beyond eosinophils. In control groups, the eotaxin receptor was detected on 6-9% of thymic cells, thus suggesting that CCR3 is widely expressed in thymus by cells of non-eosinophilic origin. Our findings were supported by other evidences that this chemokine receptor may be also expressed by mast cells (237), macrophages (238) and T helper type 2 lymphocytes (239). These facts indicated that eosinophils in thymic cell suspension should be phenotyped by the coexpression of two markers. In my study I have therefore used the antibodies raised against mouse sialic acid recognition immunoglobulin-like molecule Siglec F, which has been reported to be specifically expressed by cells of eosinophilic origin in mice (24) and suitable for detection of eosinophils by flow cytometry (207). The double labeling of CCR3 and Siglec F marker ensured the detection of eosinophils in cell suspensions (209).

As reviewed in the first chapter, mature eosinophils, delivered to the tissue via blood circulation express both molecules: CCR3 and Siglec F. The site of hematopoesis, such as bone marrow, contains cells at various stages of development, and thus bone marrow eosinophils could be divided by expression of CCR3 and Siglec F molecules into two populations. The first is a population of immature eosinophils that expresses only Siglec F marker and the second is a pool

of mature cells co-expresses Siglec F and CCR3 markers. I was able to examine these two populations of cells by analyzing the bone marrow of IL-5 transgenic mice (Chapter 3, Figure 15). The detection of the cells bearing CCR3 and Siglec F epitopes by flow cytometry in whole thymic cell suspension also confirmed the existence of two eosinophilic populations: immature Siglec F^+ and mature Siglec F^+/CCR3$^+$ eosinophils. These two populations of eosinophils slightly diverged from each other in side and forward scatter characteristics, displayed on FACS data analysis dot plots. The Siglec F^+ cells were distinct from double positive cells by being smaller size with and less developed granules (Chapter 3, Figures 22-25). These data suggest that eosinophilic precursors were recruited to the thymus and underwent further maturation as well as arrival of mature cells from blood circulation appeared to take place. Unfortunately, due to time limitation, in this project we did not attempt to explore other evidence of eosinophilopoiesis in the murine thymus. However, there are reports regarding myeloid hematopoiesis in human (240) and horse (220), which may advocate the notion of eosinophilopoiesis in this primary lymphoid organ. Flores *et.al.* (1999) reported findings of mitotic eosinophil precursors in thymi of children and supported this observation by detection of sufficient amounts of IL-5 mRNA in thymic cells to ensure eosinophil maturation. Murine thymic cells are also capable of synthesizing IL-5 in amounts adequate enough to promote eosinophil survival and differentiation (48). Based on the evidences from this project and other studies it is not possible to rule out that thymus may be a site of development for cells of eosinophilic lineage. The observation of immature eosinophils' occurrence in the

thymi suggests that in addition to the eotaxin/CCR3 pathway contribution to the thymic eosinophilia, other elements may play a role in attracting or generating eosinophil precursors for maturation in the thymus. This hypothesis requires further experimental work. Our data demonstrated the presence of mature and immature eosinophils in all age groups with a non-significant decrease in Siglec F^+ cells at day 14. The percent of Siglec F^+/$CCR3^+$ eosinophils did not vary significantly between control and IFN-γ treated cells. The maximum number of eosinophils was detected by flow cytometry at day 21 and composed about 4.2% of total thymic cells. In general, alterations in eosinophils' numbers, as detected by MBP staining correlated with my flow cytometry results (Figures 5, A. and 14, B).

Apart from morphological studies, I also attempted to explore the expression of the Indoleamine 2, 3-dioxygenase (IDO) by thymic cells, and ascertain any new information, which could fill the gap in knowledge of IDO function. The presence of IDO mRNA was detected in total RNA, isolated from whole thymi using reverse transcription PCR and semi-quantitative real-time PCR.

The expression of IDO protein was detected in thymic cell suspension by immunocytochemistry using fluorochrom-labeled antibody and laser scatter acquisition of the fluorescence. The results of the cDNA molecular cloning experiments showed that thymic cells transcribe the IDO DNA into messenger RNA in all age groups. The specific amplification product was detected in reaction samples for all ages and was confirmed by comparing with positive

control samples derived from normal mouse spleen. The results were validated by sequencing of the extracted product with specific primers. This determined a 96% homology with murine IDO pyrrole dioxygenase genomic sequence. Strikingly, real-time PCR analysis of total thymic RNA revealed a significant upregulation of IDO gene transcription in day 11 mice compared to day 7. This upregulation correlated with an increase in eosinophil count, detected on tissue sections. The amount of IDO mRNA, normalized against housekeeping gene expression, at day 14 was lower than at day 11, but this did not achieve statistical significance. There was also observed a slight but non-significant drop in eosinophilic infiltration. Interestingly, at day 21, a considerable decrease in level of IDO mRNA was detected, although this age was associated with a significant influx of eosinophils into the thymus. Also at day 21, a decline in number of cells expressing IDO protein was detected compared to day 11. Apparently, the IDO production may be associated with specific changes in thymic microenvironment. At day 21, when eosinophilic infiltration reached its maximum, Siglec F^+/CCR3$^+$ eosinophils expressed IDO protein, however, the percent of IDO$^+$ cells as well as IDO gene transcription appeared to be lower than at day 11. In contrast, day 11 revealed a correlating observation, which may suggest a link between increase in eosinophils' number, upregulation of IDO gene transcription and the highest percentage of double positive thymocytes. The dissociation between number of eosinophils and percent of IDO-expressing cells at day 21 may be explained by the mechanisms of IDO protein regulation that require further elucidation.

Transcription of IDO gene is regulated by gene-promoters, which have high responsiveness to type II Interferon (IFN-γ) and less avidity to type I Interferons (IFN-α/β) (91). In this study, in order to investigate the possible IFN-γ involvement in IDO regulation in the thymus, we performed real-time PCR analysis of IFN-γ gene transcription. The results revealed the presence of IFN-γ mRNA in thymic cells of all age groups. Literature reported that some immature thymocytes in cortical zone may produce IFN-γ constitutively (241). These $CD4^-$ $CD8^-$ cells reduce the amount of IFN-γ produced by the time of extensive proliferation and restore this production at the $CD4^+CD8^+CD3^{lo}$ stage (242). In our results the highest levels of IFN-γ mRNA were found in samples of day 7 thymi and the lowest were detected at day 21. These findings correlated with the expression of IDO mRNA in a special way. The highest IFN-γ gene transcription was detected at day 7 prior to upregulation of IDO expression at day 11. Transcription of both molecules (IFN-γ and IDO) was down modulated by day 21. There is a difference in the activity of transcription of IDO and IFN-γ genes throughout described period of time. The activity of IDO gene transcription was much higher than IFN-γ mRNA. IFN-γ might promote different states of immune activation depending on levels of its expression. Strong IFN-γ production induces high states of activation, whereas moderate expression is necessary to maintain tolerance (243). Our results may be characteristic of the thymic tolerogenic state.

In addition to IFN-γ there are other IDO induction pathways, employed by different cellular systems. Lipopolysaccharides (LPS) acting synergistically with TNF signaling are capable of inducing IDO gene in an IFN-γ independent fashion

(91). Ligation of costimulatory molecules CD80/CD86 on dendritic cells together with cytotoxic lymphocyte activation- 4 (CTLA-4)-immunoglobulin induces functional IDO production (185) thus representing another potent mechanism of IFN-γ-independent IDO stimulation. In this project we did not investigate the IDO induction pathways. However, there is the possibility that the mechanism of IDO stimulation through CD80/CD86 – CTLA-4 ligation may also be functional in the thymus (244). It would be of great interest to investigate the pathways of IDO induction in the thymus, using an IFN-γ deficient mouse model, or study the function of other mechanisms utilizing anti-CTLA-4 antibody in the fetal thymic organ culture (FTOC) (245).

In addition to the induced Indoleamine 2, 3-dioxygenase production there is an alternate pathway of constitutive expression of this protein by some cell types (246). It has been demonstrated that eosinophils (78) and specific subclasses of conventional $CD11c^+CD8\alpha^+$ together with plasmacytoid $CD11c^{interm}$ $B220^+$ dendritic cells (214) may produce this protein constitutively. Some observations suggest that constitutively expressed IDO might not be enzymatically active without additional stimulation by IFNs, TNF molecules, or CD80/CD86 ligation (247). However, in mice there is a population of DCs with $CD8\alpha^+/B220^-$ phenotype, which express constitutively enzymatically functional IDO (248). The same may be true for eosinophils in humans (78).

The novel concept of this study is showing the possibility for presence of a constitutive type of IDO production by thymic cells. In order to investigate the baseline levels of IDO^+ cells in the mouse thymus and show the potential to

upregulate this protein, I stimulated thymic cells in culture with purified IFN-γ as internal positive control. The results showed that IDO protein was detectable in about 2-7% of the cells, freshly isolated from whole thymi. The wide range between 2 and 7 in percentage of IDO$^+$ cells was linked to age-related variability. The percent of IDO-positive cells in control groups' suspensions at day 11 was significantly higher than at the earlier and later ages (p-value < 0.05). These results correlated with the increase in IDO mRNA levels as well as with the influx of eosinophils into the thymi at day 11 (Figures 13 and 35). IFN-γ stimulation caused a significant shift in IDO production and number of expressing cells increasing up to an average of 17%. Stimulation of thymic cells with IFN-γ resulted in typical pattern of induced IDO production with a maximum being observed between 6 and 12 hours of culturing (215). The percentage of IDO-producing cells decreased significantly by the 24 hours incubation time point. Decrease in percent of IDO$^+$ cells past 24 hour of treatment in the absence of tryptophan back to the baseline level suggested constitutive type of IDO expression in some thymic cells. In this study, there was no opportunity to phenotype thymic cells for detection of other potentially IDO-expressing cells beyond eosinophils. It would definitely be of a great interest and importance to perform such analysis in the future.

In general, the percent of IDO-positive events, detected in my experiments corresponded to the proportion of non-lymphoid cells in mouse thymi, described by other researchers (249). Our results showed the presence of IDO$^+$/CCR3$^+$ and IDO$^+$/Siglec F$^+$ cells in unstimulated and IFN-γ treated groups for all ages

selected for the study. This indicated that eosinophils expressed IDO under control and treatment conditions. They remained IDO-positive after prolonged stimulation with IFN-γ. This feature might indicate the constitutive type of IDO production by thymic eosinophils. The total percent of eosinophils, detected at day 7 was 1.6, as well as percent of IDO$^+$ cells was 2.2 ± 0.2, identifying eosinophils as a major source of this protein in this age group. At day 11 the number of eosinophils increased to 2.7%. This was accompanied by statistically significant increase in IDO$^+$ events to 7.3% (p-value < 0.05, Figure 32), what indicated IDO expression in non-eosinophilic cells and feature of IDO induction. However, my results showed that at day 11 eosinophils significantly contributed to IDO upregulation by influx to the thymi. At day 21 eosinophils were shown to be almost the only IDO-expressing cell population in the thymi (Figures 41 and 32). This was suggested by correlation between their percentage from total cells and expression of this protein predominantly by CCR3$^+$/Siglec F$^+$ eosinophils, signifying that they are a considerable source of constitutive IDO in the thymus.

Identification of IDO$^+$/CCR3$^+$ and IDO$^+$/Siglec F$^+$ cells revealed the existence of an IDO$^+$- cell population, which did not bear eosinophilic markers. More likely that thymic dendritic cells (185) and macrophages (250) may contribute to of IDO expression in the thymus. The non-lymphoid cellular population of thymus contains different subtypes of DCs. The conventional CD8α^+ cells, plasmacytoid and myeloid DCs could be found in thymic medulla as well as in CMJ (251). Macrophages in thymus were shown to play a role in process of apoptosis support in double positive thymocytes (252). These cells were

shown to be a potent source of IDO protein in many pathophysiological conditions (214).

Even though I did not aim to display patterns of eotaxin receptor CCR3 expression on mouse thymic cells, some interesting observations emerged from my experiments. The analysis of CCR3 expression on thymic cells exposed interesting feature: in control groups, the eotaxin receptor CCR3, was detected on 6-9% of thymic cells that was significantly higher than the percent of Siglec F$^+$ cells. This result revealed that CCR3 is widely expressed in murine thymi by cells of non-eosinophilic and non-stromal origin. Considering the current literature about the expression of CCR3 receptor by human thymocytes (230) and the data, received in this study, I could have proposed the novel opportunity for further research. In continuation of this project it would be interesting to investigate the possible role of eotaxin chemokine and its' receptor in cellular trafficking through thymic compartments.

One more interesting observation was drawn from this study: the CCR3 expression was markedly upregulated by IFN-γ stimulation. This feature was previously hinted in the literature data, which reported selective overexpression of some chemokine receptors in response to IFN-γ treatment (253). Our results showed significant increase in numbers of CCR3 expressing cells in IFN-γ treated cells. The IFN-γ stimulated the expression of this chemokine receptor on immature eosinophils, what was reflected in the difference in Siglec F$^+$/CCR3$^+$ events observed between control and treated groups. The high percent of CCR3$^+$

cells in permeabilized samples may also be the result of receptor internalization (60).

Regarding Siglec F detection, my results showed that expression of this molecule correlated with number of eosinophils, as quantitated within tissue sections. In cell suspensions this marker was expressed by about 4.2% of total cells at day 21, when maximal numbers of eosinophils were detected in the thymi by immunohistochemistry. The percent of IDO$^+$ Siglec F$^+$ eosinophils correlated with levels, detected for Siglec F$^+$ events in single staining. IFN-γ treatment did not influence the levels of Siglec F expression on thymic cells. The stimulation did not significantly alter the percentage of events with IDO$^+$/Siglec F$^+$ co-expression; however the trend was observed. This fact further supports the evidence from single stained samples. Percent of IDO$^+$ Siglec F$^+$ events did not exceed the total counts of cells expressing eosinophilic markers in our phenotyping experiments. Significant differences were observed in IDO/CCR3 co-expressing cells between control and treatment groups for ages 11 and 21 days. This result suggests that IFN-γ exposure upregulated IDO and CCR3 expression simultaneously on other cells of non-eosinophilic origin, such as macrophages (238).

In conclusion, the results, emerging from my study indicated the active involvement of eosinophils in maintaining of thymic cellular microenvironment and potential role in the negative selection of thymocytes. The detection of Indoleamine 2, 3-dioxygenase protein in murine thymi added a novel knowledge

in physiology of this organ and opened an exciting opportunity for further research.

Future directions

Even though some observations in this study are novel, they remain mainly descriptive, observational and hypothesis-generating. Their functional implications remain uncertain until further experiments have been performed. A primary future direction of this project would be an exploration of thymic function in the absence of eosinophils on the eosinophil-depleted mouse model (PHIL) that would directly indicate their role in thymic microenvironment. Another important issue, which needs to be addressed, is the function of IDO in the thymus.

1. **Isolation of dendritic cells and eosinophils populations from whole thymi and demonstration of IDO expression by these cell populations.**

2. **Accumulation of kynurenines in thymic cells culture media and thymic cells isolation buffer**

3. **Demonstration of IDO production and enzymatic activity on the mice model of the acute negative selection by eosinophils and dendritic cells.**

4. **Demonstration of the role of eosinophils in thymocytes selection on the eosinophil-deficient mouse model (PHIL mouse).**

References:

1. Wardlaw, A.J., Moqbel, R., Kay, A.B. 1995. Eosinophils: biology and role in disease. Advances in immunology. FJ Dixon (Ed), Academic Press, 60: 151-266.

2. Kroegel, C., Virchow, J-C, and Warner, J.A. 1994. Pulmonary immune cells in health and disease: the eosinophil leukocyte. *Eur. Respir. J;* 7, 519-543.

3. Dvorak, A.M., Ackerman, S.J., Weller, P.F. 1990. Subcellular morphology and biochemistry of eosinophils. *In*: *Harris JR, ed. Blood Cell Biochemistry*. Vol. 2. Megakaryocytes, platelets, macrophages and eosinophils. London, Plenum Publishing; 237–344.

4. Gotlib, J., Cross, N.C.P., Gilliland, D. G. 2006. Eosinophilic disorders: Molecular pathogenesis, new classification, and modern therapy. *Best Practice & Research Clinical Haematology;* 19, (3): 535–569.

5. Cormier, A., Taranova, A., Bedient, C., Nguyen, T., Protheroe, C.,Pero, R., Dimina, D., Ochkur, S. I., O'Neill, K., Colbert, D., Lombari, T. R., Constant, S., McGarry, M. P., Lee, J. J., and Lee, N. A. 2006. Pivotal Advance: Eosinophil infiltration of solid tumors is an early and persistent inflammatory host response *J. Leukoc. Biol.* 79: 1131–1139.

6. Gleich, G. J., Adolphson, C. R., and Leiferman, K. M. 1993.The biology of the Eosinophilic leukocyte. *Annu. Rev. Med.* 44:85-10.

7. Dvorak, A.M., Letourneau, L., Login, G.R., Weller, P.F., Ackerman, S.J. 1988. Ultrastructural localization of the Charcot-Leyden crystal protein (lysophosphatase) to distinct crystalloid-free granule population in mature human eosinophils. *Blood*; 72: 150–158.

8. Mahmudi-Azer, S., Velazquez, J.R., Lacy, P., Denburg, J.A., Moqbel, R. 2000. Immunofluorescence analysis of cytokine and granule protein expression during eosinophil maturation from cord blood-derived CD34 progenitors. *J Allergy Clin Immunol*; 105 (6): 1178-84.

9. Bainton, D.F., Farquhar, M. 1970. Segregation and packing of granule enzymes in eosinophil leukocytes. *J Cell Biol*; 45: 54–73.

10. Wasmoen, T.L., Bell, M.P., Loegering, D.A., Gleich, G.J., Prendergast, F.G., McKean, D.J. 1988. Biochemical and amino acid sequence analysis of human eosinophil granule major basic protein. *J Biol Chem*; 263: 12559–12563.

11. Temkin, V., Aingorn, H., Puxeddu, I., Goldshmidt, O., Zcharia, E., Gleich, G.J., Vlodavsky, I., Levi-Schaffer, F. 2004. Eosinophil major basic protein: first identified natural heparanase-inhibiting protein. *J Allergy Clin Immunol*; 113(4):703-9.

12. White, S.R., Ohno, S., Munoz, N.M., Gleich, G.J., Abrahams, C., Solway, J. 1990. Epithelium-dependent contraction of airway smooth muscle caused by eosinophil MBP. *Am J Physiol*; 259: L294-303.

13. Piliponsky, A.M., Pickholtz, D., Gleich, G.J., Levi-Schaffer, F. 2001.Human eosinophils induce histamine release from antigen-activated rat peritoneal mast cells: a possible role for mast cells in late-phase allergic reactions. *J. Allergy Clin. Immunol.* 107:993–1000.

14. Carreras, E., Boix, E., Navarro, S., Rosenberg, H.F., Cuchillo, C.M., Nogués, M.V. 2005. Surface-exposed amino acids of eosinophil cationic protein play a critical role in the inhibition of mammalian cell proliferation. *Mol Cell Biochem* ; 272(1-2):1-7.

15. Yang, D., Chen, Q,. Su, S.B., Zhang, P., Kurosaka, K., Caspi, R.R., Michalek, S.M., Rosenberg, H.F., Zhang, N., Oppenheim, J.J. 2008. Eosinophil-derived neurotoxin acts as an alarmin to activate the TLR2-MyD88 signal pathway in dendritic cells and enhances Th2 immune responses. *J Exp Med;* 205: 79-90.

16. Olson, R.L., and Little, C. 1983. Purification and some properties of myeloperoxidase and eosinophil peroxidase from human blood. *Biochem J*; 209: 781–787.

17. Dechatelet, L.R., Shirley, M.R., McPhail, L.C., Huntley, C.C., Muss, H.B., Bass, D.A. 1977. Oxidative metabolism of human eosinophils. *Blood*; 50: 525–535.

18. Foegh, M.L., Maddox, Y.T., Ramwell, P.W. 1986. Human peritoneal eosinophils and formation of arachidonate cyclo-oxygenase products. *Scand J Immunol*; 23: 599–603.

19. Hartnell, A., Kay, A.B., Wardlaw, A.J. 1992. INF-γ induces expression of FcγRIII (CD16) on human eosinophils. *J Immunol*; 148: 1471–1478.

20. Nechansky, A., Robertson, M.W., Albrecht, B.A., Apgar, J.R., Kricek, F. 2001. Inhibition of antigen-induced mediator release from IgE-sensitized cells by a monoclonal anti-Fc epsilon RI alpha-chain receptor antibody: implications for the involvement of the membrane-proximal alpha-chain region in Fc epsilon RI-mediated cell activation. *J Immunol*.15; 166(10):5979-90.

21. Anwar, A.R., Kay, A.B. 1977. Membrane receptors for IgG and complement (C4, C3b and C3d) on human eosinophils and neutrophils and their relation to eosinophilia. *J Immunol*; 119: 976–985.

22. DiScipio, R.G., Schraufstatter, I.U. 2007. The role of the complement anaphylatoxins in the recruitment of eosinophils. *Int Immunopharmacol*.; 7(14):1909-23.

23. Kelm, S. et al. 1994.Sialoadhesin, myelin-associated glycoprotein and CD22 define a new family of sialic acid-dependent adhesion molecules of the immunoglobulin superfamily. *Curr. Biol.* 4, 965–972.

24. Zhang, M., Angata, T., Cho, J.Y., Miller, M., Broide, D.H., Varki, A. 2007. Defining the in vivo function of Siglec-F, a CD33-related Siglec expressed on mouse eosinophils. *Blood.* 15; 109(10):4280-7.

25. Angata, T. 2006. Molecular diversity and evolution of the Siglec family of cell-surface lectins. *Mol. Divers.* 10, 555–566.

26. Tateno, H., Li, H., Schur, M.J., Bovin, N., Crocker, P.R., Wakarchuk, W.W., Paulson, J.C. 2007. Distinct endocytic mechanisms of CD22 (Siglec-2) and Siglec-F reflect roles in cell signaling and innate immunity. *Mol Cell Biol*.; 27(16):5699-710.

27. Zhang, J.Q., Biedermann, B., Nitschke, L., Crocker, P.R. 2004. The murine inhibitory receptor mSiglec-E is expressed broadly on cells of the immune system whereas mSiglec-F is restricted to eosinophils. *Eur J Immunol;* 34(4): 1175-84.

28. Voehringer, D., van Rooijen, N., Locksley, R.M. 2007. Eosinophils develop in distinct stages and are recruited to peripheral sites by alternatively activated macrophages. *J Leukoc Biol*; 81(6):1434-44.

29. Yamaguchi, Y., Hayashi, Y., Sugama, Y. 1988. Highly purified murine interleukin-5 stimulates eosinophil function and prolongs survival. IL-5 as an eosinophil chemotactic factor. *J Exp Med*; 167: 1737–1742.

30. Palframan, R.T., Collins, P.D., Severs, N.J., Rothery, S., Williams, T.J., Rankin, S.M. 1998**.** Mechanisms of acute eosinophil mobilization from the bone marrow stimulated by interleukin 5: the role of specific adhesion molecules and phosphatidylinositol 3-kinase. *J Exp Med*; 188(9):1621-32.

31. Rothenberg, M.E., Luster, A.D., Lilly, C.M., Drazen, J.M., Leder, P. 1995. Constitutive and allergen-induced expression of eotaxin mRNA in the guinea pig lung. *J Exp Med*; 181(3):1211-6.

32. Matthews, A.N., Friend, D.S., Zimmermann, N., Sarafi, M.N., Luster, A.D., Pearlman, E., Wert, S.E., Rothenberg, M.E. 1998. Eotaxin is required for the baseline level of tissue eosinophils. *Proc Natl Acad Sci U S A.* 26; 95(11):6273-8.

33. Dulkys, Y., Kluthe, C., Buschermöhle, T., Barg, I., Knöss, S., Kapp, A., Proudfoot, A.E., Elsner, J. 2001. IL-3 induces down-regulation of CCR3 protein and mRNA in human eosinophils. *J Immunol.* 15; 167(6):3443-53.

34. Fukuda, T., Dunnette, S.L., Reed, C.E., Ackerman, S.J., Peters, M.S., Gleich, G.J. 1985. Increased numbers of hypodense eosinophils in the blood of patients with bronchial asthma. *J Allergy Clin Immunol*; 132: 981–985.

35. Nerlov, C., Graf, T. 1998. PU.1 induces myeloid lineage commitment in multipotent hematopoietic progenitors. *Genes Dev*. 12:2403–12.

36. Walsh, J.C., DeKoter, R.P., Lee, H.J., Smith, E.D., Lancki, D.W. 2002. Cooperative and antagonistic interplay between PU.1 andGATA-2 in the specification of myeloid cell fates. *Immunity* 17:665–76.

37. McNagny, K., Graf, T. 2002. Making eosinophils through subtle shifts in transcription factor expression. *J. Exp. Med.* 195, F43–F47.

38. Nerlov, C., McNagny, K.M., Doderlein, G., Kowenz-Leutz, E., Graf, T. 1998. Distinct C/EBP functions are required for eosinophil lineage commitment and maturation. *Genes Dev*.12:2413–2.

39. Yu, C., Cantor, A.B., Yang, H., Browne, C., Wells, R.A. 2002. Targeted deletion of a high-affinity GATA-binding site in the GATA-1 promoter leads to selective loss of the eosinophil lineage in vivo. *J. Exp. Med.* 195:1387–95.

40. Zhu, J., and Emerson S. G. 2002. Hematopoietic cytokines, transcription factors and lineage commitment. *Oncogene;* 21, 3295 – 3313.

41. Iwasaki, H., Mizuno, S., Mayfield, R., Shigematsu, H., Arinobu, Y., Seed, B., Gurish, M. F., Takatsu, K., Akashi, K. 2005. Identification of eosinophil lineage–committed progenitors in the murine bone marrow *J Exp Med*. 12: 1891–1897

42. Anderson, K.L., Smith, K.A., Perkin, H., Hermanson, G., Anderson, C.G., Jolly, D.J., Maki, R.A., Torbett, B.E. 1999. PU.1 and the granulocyte- and macrophage colony-stimulating factor receptors play distinct roles in late-stage myeloid cell differentiation. *Blood*; 94(7):2310-18.

43. Sehmi, R., Wood, L.J., Watson, R., Foley R, Hamid Q, O'Byrne PM. 1997. Allergen-induced increases in IL-5 receptor alpha-subunit expression on bone marrow-derived CD34⁺ cells from asthmatic subjects: a novel marker of progenitor cell commitment towards eosinophilic differentiation. *J Clin Invest*; 100:2466-75.

44. Shalit, M., Sekhsaria, S., Malech, H.L. 1995. Modulation of growth and differentiation of eosinophils from human peripheral blood CD34+ cells by IL5 and other growth factors. *Cell Immunol*; 160(1):50-7.

45. Dent, L.A., Strath, M., Mellor, A.L., Sanderson, C.J. 1990. Eosinophilia in transgenic mice expressing interleukin 5. *J Exp Med*; 172: 1425–1431.

46. Kopf, M., Brombacher, F., Hodgkin, P. D., Ramsay, A. J., Milbourne, E. A., Dai, W. J., Ovington, K. S., Behm, C. A., Kohler, G., Young, I. G., Matthaei, K. I. 1996. IL-5-deficient mice have a developmental defect in CD5_ B-1 cells and lack eosinophilia but have normal antibody and cytotoxic T cell responses. *Immunity;* 4, 15–24.

47. Garlisi, C.G., Falcone, A., Kung, T.T., Stelts, D., Pennline, K.J., Beavis, A.J., Smith, S.R., Egan, R.W., Umland, S.P. 1995. T cells are necessary for Th₂ cytokine production and eosinophil accumulation in airways of antigen-challenged allergic mice. *Clin Immunol Immunopathol*; 75: 75– 83.

48. Ryan, P.J., Willson, T., Alexander, W.S., Rago, L. D., Mifsud, S., Metcalf, D. 2001.The multi-organ origin of interleukin-5 in the mouse. *Leukemia;* 15, 1248–1255.

49. Salvi, S., Semper A, Blomberg A, Holloway J, Jaffar Z, Papi A, Teran L, Polosa R, Kelly F, Sandstrom T, Holgate S, Frew A. 1999. Interleukin-5 production by human airway epithelial cells. *Am J Respir CellMol Biol*; 20: 984–991.

50. Du, J., Stankiewicz, M.J., Liu, Y., Xi, Q., Schmitz, J.E. 2002. Novel combinatorial interactions of GATA-1, PU.1, and C/EBP isoforms regulate transcription of the gene encoding eosinophil granule major basic protein. *J. Biol. Chem*. 277: 43481–94.

51. Garcia-Zepeda, E.A., Rothenberg, M.E., Ownbey, R.T., Celestin, J., Leder, P., Luster, A.D. 1996. Human eotaxin is a specific chemoattractant for eosinophil cells and provides a new mechanism to explain tissue eosinophilia. *Nat Med;* 2:449-56.

52. Abdelilah, S.G., Hamid, Q., Mansour, N., Delespesse, G., Renzi, P.M. 2003. The CCR3 receptor is involved in eosinophil differentiation and is up-regulated by Th2 cytokines in CD34+ progenitor cells. *J Immunol;* 170(1):537-47.

53. Elsner, J., and Kapp, A**.** 2000. Activation of human eosinophils by chemokines. *Chem. Immunol*. 76: 177–207.

54. Palframan, R.T., Collins, P.D., Williams, T.J., Rankin, S.M. 1997. Eotaxin induces a rapid release of eosinophils and their progenitors from the bone marrow. *Blood*; 91:2240-8.

55. Ulfman, L.H., Kuijper, P.H., van der Linden, J.A., Lammers, J.W., Zwaginga, J.J., Koenderman, L. 1999. Characterization of eosinophil adhesion to TNF-alpha-activated endothelium under flow conditions: alpha 4 integrins mediate initial attachment, and E-selectin mediates rolling. *J Immunol*; 163(1):343-50.

56. Tachimoto, H., and Ebisawa, M. 2007. Effect of interleukin-13 or tumor necrosis factor-alpha on eosinophil adhesion to endothelial cells under physiological flow conditions. *Int Arch Allergy Immunol.;* 143 Suppl 1:33-7

57. Mould, A.W., Matthaei, K.I., Young, I.G., Foster, P.S. 1997. Relationship between interleukin-5 and eotaxin in regulating blood and tissue eosinophilia in mice. *J Clin Invest.* 1;99(5):1064-71

58. Okigami, H., Takeshita, K., Tajimi, M., Komura, H., Albers, M., Lehmann, T.E., Rölle, T., Bacon, K.B. 2007. Inhibition of eosinophilia in vivo by a small molecule inhibitor of very late antigen (VLA)-4. *Eur J Pharmacol*; 559(2-3):202-9.

59. Barthel, S.R., Johansson, M.W., McNamee, D.M., Mosher, D.F. 2008. Roles of integrin activation in eosinophil function and the eosinophilic inflammation of asthma. *J Leukoc Biol;* 83(1):1-12.

60. Rothenberg, M.E., Ownbey, R., Mehlhop, P.D., Loiselle, P.M., van de Rijn, M., Bonventre, J.V., Oettgen, H.C., Leder, P., Luster, A.D. 1996. Eotaxin triggers eosinophil-selective chemotaxis and calcium flux via a distinct receptor and induces pulmonary eosinophilia in the presence of interleukin 5 in mice. *Mol Med;* 2(3):334-48.

61. Kato, M.,Kephart, G.M., Talley, N.J., Wagner, J.M., Sarr, M.G., Bonno, M., McGovern, T., Gleich, G.J. 1998. Eosinophil infiltration and degranulation in normal human tissue. *Anat Rec;* 252:418–425.

62. Mishra, A., Hogan, S.P., Lee, J.J., Foster, P.S., Rothenberg, M.E. 1999. Fundamental signals that regulate eosinophil homing to the gastrointestinal tract. *J Clin Invest*; 103(12):1719-27.

63. Mishra, A., Brandt, E. B., Hogan, S. P., Rothenberg, M. E. 2001.Gastrointestinal eosinophils. *Immunological Reviews*; 179: 139–155.

64. Kato, M., Kephart, G.M., Morikawa, A., Gleich, G.J. 2001. Eosinophil infiltration and degranulation in normal human tissues: evidence for eosinophil degranulation in normal gastrointestinal tract. *Int Arch Allergy Immunol*; 125 Suppl 1:55-8.

65. Gouon-Evans, V., Rothenberg, M.E., Pollard, J.W. 2000. Postnatal mammary gland development requires macrophages and eosinophils. *Development* 127:2269–82.

66. Sferruzzi-Perri, A.N., Robertson, S.A., Dent, L.A. 2003. Interleukin-5 transgene expression and eosinophilia are associated with retarded mammary gland development in mice. *Biol. Reprod.* 69:224–33.

67. Robertson, S.A., Mau, V.J., Young, I.G., Matthaei, K.I. 2000. Uterine eosinophils and reproductive performance in interleukin 5-deficient mice. *J Reprod Fertil*; 120(2):423-32.

68. McMaster, M.T., Newton, R.C., Dey, S.K., Andrews, G.K. 1992. Activation and distribution of inflammatory cells in the mouse uterus during the preimplantation period. *J. Immunol*. 148:1699–705

69. Lee, I., Yu, E., Good, R.A., Ikehara S. 1995. Presence of eosinophilic precursors in the human thymus evidence for intra-thymic differentiation of cells in eosinophils. *Pathology international;* 45(9): 655-662.

70. Throsby,M., Herbelin, A., Ple´au, J.-M., and Dardenne, M. 2000. CD11c [+] eosinophils in the murine thymus: developmental regulation and recruitment upon MHC class I-restricted thymocyte deletion. *J Immunol*; 165: 1965–1975.

71. Lucey, D. R., Nicholson-Weller, A., Weller, P. F.1989. Mature human eosinophils have the capacity to express HLA-DR. *Proc. Natl. Acad. Sci.USA;* 86, 1348–1351.

72. Padigel, U.M., Lee, J.J., Nolan, T.J., Schad, G.A., Abraham, D. 2006. Eosinophils can function as antigen-presenting cells to induce primary and secondary immune responses to Strongyloides stercoralis. *Infect Immun*; 74(6):3232-8.

73. Gajewska, B.U., Swirski, F.K., Alvarez, D., Ritz, S.A., Goncharova, S., Cundall, M., Snider, D.P., Coyle, A.J., Gutierrez-Ramos, J.C., Stämpfli, M.R., Jordana, M. 2001.Temporal-spatial analysis of the immune response in a murine model of ovalbumin-induced airways inflammation. *Am J Respir Cell Mol Biol*; 25(3):326-34.

74. Sabin, E.A., Kopf, M.A., Pearce, E.J. 1996. Schistosoma mansoni egg-induced early IL-4 production is dependent upon IL-5 and eosinophils. *J Exp Med;* 184:1871-8.

75. Kasaian, M.T., Miller, D.K. 2008. IL-13 as a therapeutic target for respiratory disease. *Biochem Pharmacol;* 76(2):147-55.

76. Humbles, A.A., Lloyd, C.M., McMillan, S.J., Friend, D.S., Xanthou, G., McKenna, E.E., Ghiran, S., Gerard, N.P., Yu, C., Orkin, S.H., Gerard, C. 2004. A critical role for eosinophils in allergic airways remodeling. *Science;* 305(5691):1776-9.

77. MacKenzie, J.R., Mattes, J., Dent, L.A., Foster, P.S. 2001. Eosinophils promote allergic disease of the lung by regulating CD4 (+) Th2 lymphocyte function *J Immunol;* 167(6):3146-55.

78. Odemuyiwa, S.O., Ghahary, A., Li, Y., Puttagunta, L., Lee, J.E., Musat-Marcu, S., Ghahary, A., Moqbel, R. 2004. Cutting edge: human eosinophils regulate T cell subset selection through indoleamine 2, 3-dioxygenase. *J Immunol;* 173:5909-13.

79. Tamura, N., Ishii, N., Nakazawa, M., Nagoya, M., Yoshinari, M., Amano, T., Nakazima, H., Minami, M. 1996. Requirement of CD80 and CD86 molecules for antigen presentation by eosinophils. *Scand J Immunol;* 44(3):229-38.

80. Lu, P., Urban, J.F., Zhou, X.D., Chen, S.J., Madden, K., Moorman, M., Nguyen, H., Morris, S.C., Finkelman, F.D., Gause, W.C. 1996. CD40-mediated stimulation contributes to lymphocyte proliferation, antibody production, eosinophilia, and mastocytosis during an in vivo type 2 response, but is not required for T cell IL-4 production. *J Immunol*; 156(9): 3327-33.

81. Przewoski E. 1896. Über die lokale Eosinophilie beim Krebs nebst Bemerkungen über die Bedeutung der eosinophilen Zellen im Allgemeinen. *Zentral allg Path u path Anat;* 7: 177.

82. Wedemeyer, J., Vosskuhl, K. 2008. Role of gastrointestinal eosinophils in inflammatory bowel disease and intestinal tumors. *Best Pract Res Clin Gastroenterol*; 22(3):537-49.

83. Stenfeldt, A.L., and Wenneras, C. 2004. Danger signals derived from stressed and necrotic epithelial cells activate human eosinophils. *Immunology;* 112:605–614.

84. Lotfi, R., Lee, J.J. and Lotze. M. 2007. Eosinophilic granulocytes and damage-associated molecular pattern molecules (DAMPs): role in the inflammatory response within tumors. *J Immunother;* 30:16–28.

85. Fidler, I. J., Gersten, D. M., Budmen, M. B. 1976. Characterization in vivo and in vitro of tumor cells selected for resistance to syngeneic lymphocyte-mediated cytotoxicity. *Cancer Res.* 36**,** 3160–3165.

86. Astigiano, S., Morandi, B., Costa, R., Mastracci, L., D'Agostino, A., Ratto, G.B., Melioli, G., Frumento, G. 2005.Eosinophil granulocytes account for indoleamine 2,3-dioxygenase-mediated immune escape in human non-small cell lung cancer. *Neoplasia.* (4):390-6.

87. Jacobsen, E., Taranova, A.G., Lee, N. A. and Lee, J. J. 2007. Eosinophils: Singularly destructive effector cells or purveyors of immunoregulation? *J Allergy Clin Immunol;* 119, (6): 1313-1320.

88. Gershon, R. K., Maurer, P.H., and Merryman, C.F.1973. A cellular basis for genetically controlled immunologic unresponsiveness in mice: Tolerance Induction in T-Cells. *ProcNatl Acad Sci U S A.*; 70(1): 250–254.

89. Moffett, J., and Namboodiri, M. 2003.Tryptophan and immune response. *Immunol Cell Biol*; 81: 247-265.

90. Satyanarayana, U., and Rao, B.S. 1977. Effect of dietary protein level on some key enzymes of the tryptophan-NAD pathway. *Br. J. Nutr.*; 38: 39–45.

91. Taylor, M. W., and Feng, G. 1991. Relationship between interferon-γ, Indoleamine 2, 3-dioxygenase, and tryptophan catabolism. *FASEB J.* 5: 2516.

92. Fujigaki, S., Saito, K., Sekikawa, K., Tone, S., Takikawa, O., Fujii, H., Wada, H., Noma, A., Seishima, M. 2001. Lipopolysaccharide induction of indoleamine 2,3-dioxygenase is mediated dominantly by an IFN-gamma-independent mechanism. *Eur J Immunol;* 31(8):2313-8.

93. Munn, D.H., Sharma, M.D., Mellor, A.L. 2004. Ligation of B7-1/B7-2 by human CD4+ T cells triggers indoleamine 2,3-dioxygenase activity in dendritic cells. *J Immunol.*; 172(7): 4100-10.

94. Alberati-Giani, D., Ricciardi-Castagnoli, P., Köhler, C., Cesura, A.M. 1996. Regulation of the kynurenine metabolic pathway by interferon-

gamma in murine cloned macrophages and microglial cells. *J Neurochem.;* 66(3):996-1004.

95. Britan, A., Maffre, V., Tone, S., Drevet, J.R. 2006 .Quantitative and spatial differences in the expression of tryptophan-metabolizing enzymes in mouse epididymis. *Cell Tissue Res.;* 324(2):301-10.

96. Munn, D. H., M. Zhou, J. Attwood, I. Bondarev, S. Conway, B. Marshall,C. Brown, and A. Mellor. 1998. Prevention of allogeneic fetal rejection by tryptophan catabolism. *Science;* 281:1191.

97. Mahnke, K., Schmitt, E., Bonifaz, L., Enk, A.H., Jonuleit, H. 2002. Immature, but not inactive: the tolerogenic function of immature dendritic cells. *Immunol. Cell Biol.*; 80: 477–83.

98. Munn, D. H., Sharma, M. D., Lee, J.R., Jhaver, K. G., Johnson, T. S., Keskin, D. B., Marshall, B. Chandler, P. , Antonia, S. J., Burgess, R., Craig, L. S. Jr. Mellor, A. L. 2002. Potential Regulatory Function of Human Dendritic Cells Expressing Indoleamine 2,3-Dioxygenase. *Science* 297, 1867-74.

99. Munn, D.H., Sharma, M.D., Hou, D., Baban, B., Lee, J.R., Antonia, S.J., Messina, J.L., Chandler, P., Koni, P.A., Mellor, A.L. 2004. Expression of Indoleamine 2, 3-dioxygenase by plasmacytoid dendritic cells in tumor draining lymph nodes. *J. Clin. Invest.* 114, 280–290.

100. Murray, H.W., Szuro-Sudol, A., Wellner, D., *et al.* 1989. Role of tryptophan degradation in respiratory burst-independent antimicrobial activity of gamma interferon-stimulated human macrophages. *Infect. Immun.*; 57: 845–9.

101. Pfefferkorn, E.R., Eckel, M., Rebhun, S. 1986. Interferon-gamma suppresses the growth of *Toxoplasma gondii* in human fibroblasts through starvation for tryptophan. *Mol. Biochem. Parasitol.*; 20: 215–24.

102. Saito, K., Heyes, M.P. 1996. Kynurenine pathway enzymes in brain. Properties of enzymes and regulation of quinolinic acid synthesis *Adv Exp Med Biol.;* 398:485-92.

103. Heyliger, S.O., Mazzio, E.A., Soliman, K.F. 1999. The anti-inflammatory effects of quinolinic acid in the rat. *Life Sci.*; 64: 1177–87.

104. Fallarino, F., Grohmann, U., Vacca, C., *et al.* 2002. T cell apoptosis by tryptophan catabolism. *Cell Death Differ*; 9: 1069–77.

105. Pabst, R. 2007. Plasticity and heterogeneity of lymphoid organs. What are the criteria to call a lymphoid organ primary, secondary or tertiary? *Immunology Letters;* 112: 1–8.

106. Lambolez, F., Arcangeli, M-L., Joret, A-M., Pasqualetto,V., Cordier, C., Di Santo, J.P., et al. 2006. The thymus exports long-lived fully committed T cell precursors that can colonize primary lymphoid organs. *Nat Immunol;* 7:76–82.

107. Miller, J.F. 2002.The discovery of thymus function and of thymus-derived lymphocytes. *Immunol Rev;* 185: 7-14.

108. Ribatti, D., Crivellato, E., Vacca, A. 2006. Miller's seminal studies on the role of thymus in immunity *Clin Exp Immunol;* 144(3): 371-5.

109. Kendall, M.D., Johnson, H.R., Singh, J. 1980. The weight of the human thymus gland at necropsy. *J Anat;* 131(Pt 3):483-97.

110. Hirokawa, K., Utsuyama, M., Kobayashi, S. 2001. Hypothalamic control of thymic function. *Cell Mol Biol (Noisy-legrand)*; 47:97–102.

111. Hirokawa, K., Utsuyama, M., Kasai, M., Kurashima, C., Ishijima, S., Zeng, X. Y. 1994. Understanding the mechanism of the age-change of thymic function to promote T cell differentiation. *Immunol. Lett.* 40:269.-277.

112. Aspinall, R. 1997. Age-associated thymic atrophy in the mouse is due to a deficiency affecting rearrangement of the TCR during intrathymic T cell development. *J. Immunol.* 158:3037.-3045.

113. von Gaudecker, B.1978. Ultrastructure of the age-involuted adult human thymus. *Cell Tissue Res;* 186:507-525.

114. von Gaudecker, B. 1991. Functional histology of the human thymus. *Anat Embryol;* 183:1-15.

115. Kendall, M.D. 1989.The morphology of perivascular spaces in the thymus. *Thymus*; 13(3-4):157-64.

116. Hammar, J. A. 1926. Die Menschenthymus in Gesundheit und Krankheit: I. Das normal Organ. *Z. Zellforsch*., Suppl. 6.

117. Castleman, B., and Norris, E. H.1949. The pathology of the thymus in myasthenia gravis. *Medicine (Baltimore),* 28, 27-58.

118. Hugo, P., and Boyd, R. 2002. Thymus. *Encyclopedia of Life Sciences* © 1-11.

119. von Gaudecker, B., Miiller-Hermelink, H.K. 1980. Ontogeny and organization of the stationary non-lymphoid cells in the human thymus. *Cell Tissue Res;* 207:287-306.

120. van de Wijngaert, F.P., Kendall, M.D., Schuurman, H.J., Rademakers, L.H., Kater, L. 1984. Heterogeneity of epithelial cells in the human thymus. An ultrastructural study. *Cell Tissue Res.*; 237(2):227-37.

121. Ortiz-Hidalgo, C. 1992. Early clinical pathologists 5: the man behind Hassall's corpuscles. *J Clin Pathol.*; 45(2):99-101.

122. Bodey, B., Kaiser, H.E.1997.Development of Hassall's bodies of the thymus in humans and other vertebrates (especially mammals) under physiological and pathological conditions: immunocytochemical, electronmicroscopic and in vitro observations. *In Vivo*; 11(1):61-85.

123. Gaudecker, B., and Schmale, E.-M. 1974. Similarities between Hassall's corpuscles of the human thymus and the epidermis, *Cell Tissue Res* 151: 347–368.

124. Rosario, P., Loris, Z., Giuseppe, S., Claudia, E., Stefano, M.P.1995. Quantitative determination of thymic eosinophilia in swine *Ital J Anat Embryol.*; 100(3):171-8.

125. Wekerle, H., and Ketelsen, U.-P. 1980. Thymic nurse cells. Ia-bearing epithelium involved in T-lymphocyte differentiation. *Nature (Lond.)* 283:402.

126. Smith, D. C. 1979. From extracellular to intracellular: the establishment of a symbiosis. *Proc. R. Soc. Lond. B Biol. Sci.* 204:115.

127. van de Wijngaert, F.P., Rademakers, L.H.P.M., Schuurman, H-J, DeWeger, R.A., Kater, L. 1983. Identification and in situ localization of the thymic nurse cell in man. *J Immunol* 130: 2348-2351.

128. Surh, C.D., Ernst, B., Sprent, J. 1992.Growth of epithelial cells in the thymic medulla is under the control of mature T cells.*J Exp Med;* 176(2):611-6.

129. Penit, C., Lucas, B., Vasseur, F., Rieker, T., Boyd, R.L. 1996. Thymic medulla epithelial cells acquire specific markers by post-mitotic maturation. *Dev Immunol;* 5(1):25-36.

130. Millet, V., Naquet, P., Guinamard, R.R. 2008. Intercellular MHC transfer between thymic epithelial and dendritic cells. *Eur J Immunol;* 38(5):1257-63.

131. Moore, M.A.S., and Owen, J.J.T. 1967. Experimental studies on the development of the thymus. *J. Exp. Med.* 126:715–26.

132. Auerbach, R. 1960. Morphogenetic interactions in the development of the mouse thymus gland. *Dev. Biol.* 2:271–85.

133. Bockman, D.E., and Kirby, M.L. 1984. Dependence of thymic development on derivatives of the neural crest. *Science;* 223: 498–500.

134. Bockman, D. E., and Kirby, M. L. 1989. Neural crest functions in thymus development. *Immunol. Ser;* 45, 451–467.

135. Shinohara, T., and Honjo, T. 1997. Studies *in vitro* on the mechanism of epithelial/mesenhymal interaction in the early fetal thymus. *Eur J Immunol;* 27:522-527.

136. Anderson, M., Anderson, S.K., Farr, A.G. 2000 .Thymic vasculature: organizer of the medullary epithelial compartment? *Int Immunol*; 12(7): 1105-10.

137. Gordon, J., Wilson, V.A., Blair, N.F., Sheridan, J., Farley, A. 2004. Functional evidence for a single endodermal origin for the thymic epithelium. *Nat. Immunol.* 5:546–53.

138. Bennett, A.R., Farley, A., Blair, N.F., Gordon, J., Sharp, L., Blackburn, C.C. 2002. Identification and characterization of thymic epithelial progenitor cells. *Immunity* 16:803–14.

139. Su, D., Ellis, S., Napier, A., Lee, K. & Manley, N. R. 2001. Hoxa3 and Pax1 regulate epithelial cell death and proliferation during thymus and parathyroid organogenesis. *Dev. Biol.* 236,316–329.

140. Hetzer-Egger, C., Schorpp, M., Haas-Assenbaum, A., Balling, R., Peters, H., Boehm, T. 2002. Thymopoiesis requires Pax9 function in thymic epithelial cells. *Eur J Immunol*; 32(4):1175-81.

141. Gordon, J., Bennett, A. R., Blackburn, C. C., Manley, N. R. 2001. Gcm2 and Foxn1 mark early parathyroid- and thymus-specific domains in the developing third pharyngeal pouch. *Mech. Dev.* 103, 141–143.

142. Klug, D.B., Carter, C., Gimenez-Conti, I.B., Richie, E.R. 2002. Cutting edge: thymocytes-independent and thymocytes-dependent phases of epithelial patterning in the fetal thymus. *J Immunol;* 169(6): 2842-5.

143. Miller, J.F.A.P. 1960. Analysis of the thymus influence in leukaemogenesis. *Nature;* 191:248–9.

144. Miller, J.F.A.P. 1961. Immunological function of the thymus. *Lancet*; 2: 748-749.

145. DeKoter, R.P., Lee, H.J., Singh, H. 2002. PU.1 regulates expression of the interleukin-7 receptor in lymphoid progenitors. *Immunity*; 16(2):297-309.

146. Ford, C.E., Micklem, H.S., Evans, E.P., Gray, J.S, Ogden, D.A. 1966. The inflow of bone marrowcells to the thymus. *Ann.NYAcad. Sci.* 129:283–96.

147. Mori, S., Ken Shortman and Li Wu. 2001. Characterization of thymus-seeding precursor cells from mouse bone marrow. *Blood*; 98: 696-704.

148. Jenkinson, E.J, Jenkinson, W.E., Rossi, S.W., Anderson, G. 2006. The thymus and T-cell commitment: the right niche for Notch? *Nat. Rev. Immunol*. 6:551–55.

149. Allman, D., Karnell, F.G., Punt, J.A., Bakkour, S., Xu, L., Myung, P., Koretzky, G.A., Pui, J.C., Aster, J.C., Pear, W.S. 2001. Separation of Notch1 promoted lineage commitment and expansion/transformation in developing T cells. *J Exp Med;* 194(1):99-106.

150. Anderson, G., Lane, P. J. L., and Jenkinson, E. J. 2007. Generating intrathymic microenvironments to establish T‑cell tolerance. *Nature* 7(12):954-63.

151. Savino, W., Areˆ as Mendes-da-Cruz, D., Smaniotto, S., Silva-Monteiro, E., Villa-Verde, D.M. S. 2004. Molecular mechanisms governing thymocyte migration: combined role of chemokines and extracellular matrix *J.Leukoc. Biol.* 75: 951–961.

152. Lind, E. F., Prockop, S. E., Porritt, H. E. & Petrie, H. T. 2001. Mapping precursor movement through the postnatal thymus reveals specific microenvironments supporting defined stages of early lymphoid development. *J. Exp. Med.* 194, 127–134.

153. Haynes, B.F., and Heinly, C.S. 1995. Early human T cell development: analysis of the human thymus at the time of initial entry of hematopoietic stem cells into the fetal thymic microenvironment. *J Exp Med;* 181(4):1445-58.

154. Godfrey, D. I., J. Kennedy, T. Suda, A. Zlotnik. 1993. A developmental pathway involving four phenotypically and functionally distinct subsets of CD3⁻CD4⁻CD8⁻ triple-negative adult mouse thymocytes defined by CD44 and CD25 expression. *J. Immunol.* 150:4244.-4252.

155. Kawakami, N., Nishizawa, F., Sakane, N., Iwao, M., Tsujikawa, K., Ikawa, M., Okabe, M., Yamamoto, H .1999. Roles of integrins and CD44 on the adhesion and migration of fetal liver cells to the fetal thymus. *J Immunol;* 163(6):3211-6

156. Godfrey, D. I., J. Kennedy, P. Mombaerts, S. Tonegawa, A. Zlotnik. 1994. Onset of TCR-β gene rearrangement and role of TCR- βexpression during CD3–CD4–CD8– thymocytes differentiation. *J. Immunol.* 152:4783.-4792.

157. Turka, L.A., Schatz, D.G., Oettinger, M.A., Chun, J.J., Gorka, C., Lee, K., McCormack, W.T., Thompson, C.B .1991. Thymocyte expression of RAG-1 and RAG-2: termination by T cell receptor cross-linking. *Science;* 253(5021):778-81.

158. Gill, J., Malin, M., Sutherland, J., Gray, D., Hollander, G., Boyd, R. 2003. Thymic generation and regeneration. *Immunological Reviews.* 195: 28–50.

159. Bluestone, J.A., Pardoll, D., Sharrow, S.O., Fowlkes, B.J.1987. Characterization of murine thymocytes with CD3-associated T-cell receptor structures. *Nature*; 326(6108):82-4.

160. Carleton, M., Haks, M.C., Smeele, S.A., Jones, A., Belkowski, S.M., Berger, M.A., Linsley, P., Kruisbeek, A.M., Wiest, D.L. 2002. Early growth response transcription factors are required for development of CD4(-)CD8(-) thymocytes to the CD4(+)CD8(+) stage. *J Immunol;* 168(4):1649-58.

161. Egerton, M., Shortman, K., Scollay, R. 1990.The kinetics of immature murine thymocyte development in vivo. *Int Immunol;* 2(6):501-7.

162. Li, Y., Pezzano, M., Philp, D., Reid, V., Guyden, J. 1992 .Thymic nurse cells exclusively bind and internalize CD4+CD8+ thymocytes *Cell Immunol*; 140(2):495-506.

163. Shortman, K., Vremec, D., Egerton, M. 1991.The kinetics of T cell antigen receptor expression by subgroups of CD4+8+ thymocytes:

delineation of CD4+8+3(2+) thymocytes as post-selection intermediates leading to mature T cells. *J Exp Med*; 173(2):323-32.

164. Xiao, S-Y., Li, Y., Chen, W. 2003. Kinetics of thymocyte developmental process in fetal and neonatal mice *Cell Research;* 13(4):265-273.

165. Tanaka, Y., Williams, O., Tarazona, R., Wack, A., Norton, T., Kioussis, D. 1997. In vitro positive selection of alpha beta TCR transgenic thymocytes by a conditionally immortalized cortical epithelial clone. *Int Immunol*. 9(3): 381-93.

166. Anderson, G., Owen, J.J., Moore, N.C., Jenkinson, E.J. 1994. Thymic epithelial cells provide unique signals for positive selection of CD4+CD8+ thymocytes in vitro. *J Exp Med;* 179(6):2027-31.

167. Murphy, K. M., Heimberger, A. B., Loh, D. H. 1990. Induction by antigen of intrathymic apoptosis of CD4+ CD8+ TCR$_{Lo}$ thymocytes in vivo. *Science* 250, 1720–1723.

168. Barton, G.M, and Rudensky AY. 1999. Requirement for diverse, low-abundance peptides in positive selection of T cells. *Science;* 283:67–70.

169. Hogquist, K.A., and Bevan, M.J. 1996. The nature of the peptide/MHC ligand involved in positive selection. *Semin Immunol;* 8:63–68.

170. Miller, J.F., and Flavell, R.A. 1994. T-cell tolerance and autoimmunity in transgenic models of central and peripheral tolerance. *Curr Opin Immunol*; 6(6):892-9.

171. Surh, C.D., and Sprent J. 1994. T-cell apoptosis detected in situ during positive and negative selection in the thymus. *Nature;* 372:100–3

172. Kishimoto, H., and Sprent, J., 1997. Negative selection in the thymus includes semimature T cells. *J. Exp. Med.* 185, 263–271.

173. Ueno, T., Saito, F., Gray, D.H., Kuse, S., Hieshima, K., Nakano, H., Kakiuchi, T., Lipp, M., Boyd, R.L., Takahama, Y. 2004. CCR7 signals are essential for cortex-medulla migration of developing thymocytes. *J Exp Med;* 200(4):493-505.

174. Hoffmann, M.W., Heath, W.R., Ruschmeyer, D., Miller, J.F. 1995. Deletion of high-avidity T cells by thymic epithelium. *Proc Natl Acad Sci U SA*; 92(21): 9851-5.

175. Smith, K.M., Olson, D.C., Hirose, R., Hanahan, D. 1997. Pancreatic gene expression in rare cells of thymic medulla: evidence for functional contribution to T cell tolerance. *Int Immunol;* 9(9):1355-65.

176. Klein, L., Klugmann, M., Nave, K.A., Tuohy, V.K., Kyewski, B. 2000. Shaping of the autoreactive T-cell repertoire by a splice variant of self protein expressed in thymic epithelial cells. *Nat Med;* 6(1):56-61.

177. Bonasio, R., Scimone, M. L., Schaerli, P., Grabie, N., Lichtman, A., and von Andrian, U. 2006.Clonal deletion of thymocytes by circulating dendritic cells homing to the thymus. *Nat Immunol*; 2-10.

178. Schönrich, G., Momburg, F., Hämmerling, G.J., Arnold, B. 1992. Anergy induced by thymic medullary epithelium. *Eur J Immunol;* 22(7):1687-91.

179. Allison, J., Stephens, L.A., Kay, T.W., Kurts, C., Heath, W.R., Miller, J.F., Krummel, M.F. 1998. The threshold for autoimmune T cell killing is influenced by B7-1.*Eur J Immunol;* 28(3):949-60.

180. Williams, J,A., Sharrow, S.O., Adams, A.J., Hodes, R.J. 2002. CD40 ligand functions non-cell autonomously to promote deletion of self-reactive thymocytes. *J Immunol;* 168(6):2759-65.

181. Trop, S., Charron, J., Arguin, C., Lesage, S., Hugo, P. 2000. Thymic selection generates T cells expressing self-reactive TCRs in the absence of CD45. *J Immunol;* 165(6):3073-9.

182. Wack, A. Ladyman, H. M. Williams, O. Roderick, K., Ritter M.A., and Kioussis, D. 1996. Direct visualization of thymocytes apoptosis in neglect, acute and steady-state negative selection. *Intern Immunology;* 8 (10): 1537-1548.

183. Weih, F., Ryseck, R-P., Chen, L., Bravo, R. 1996. Apoptosis of nur77/N10- transgenic thymocytes involves the Fas/Fas ligand pathway. *Proc Natl Acad Sci U S A* 93:5533-5538.

184. Palmer, E. 2003. Negative selection – clearing out the bad apples from the T-cell repertoire. *Nature Immunol.* (3): 383-391.

185. Mellor, A.L., Chandler, P., Baban, B., Hansen, A.M., Marshall, B., Pihkala, J., Waldmann, H., Cobbold, S., Adams, E., Munn, D.H. 2004. Specific subsets of murine dendritic cells acquire potent T cell regulatory functions following CTLA4-mediated induction of indoleamine 2, 3 dioxygenase. *Int Immunol*; 16(10):1391-401.

186. Hogan S.P., Matthaei, K.I., Young, J.M., Koskinen, A., Young, I.G., Foster, P.S. 1998. A novel T-cell-regulated mechanism modulating allergen-induced airways hyperreactivity in BALB/c mice independently of IL-4 and IL-5. *J Immunology.* 161:1501-1509.

187. Health Sciences laboratory Animal Services, University of Alberta. 2004. Mouse handling. Training Lab manual.

188. Ebeling, C., Forsythe, P., Ng, J., Gordon, J.R., Hollenberg, M., Vliagoftis, H. 2005. Proteinase-activated receptor 2 activation in the airways enhances antigen-mediated airway inflammation and airway

hyperresponsiveness through different pathways. *J Allergy Clin Immunol.;* 115(3):623-30.

189. Luna, L. G. 1968. Manual of histologic staining methods of the Armed Forces Institute of Pathology, edited by Lee G. Luna. 3d ed. New York, Blakiston Division, McGraw-Hill.

190. Werner, M., Chott, A., Fabiano, A., Battifora, H. 2000. Effect of formalin tissue fixation and processing on immunohistochemistry. *Am J Surg Pathol.* 24(7):1016-9.

191. Lee, J. J., Dimina, D., Macias, M.P., Ochkur, S.I., McGarry, M.P., O'Neill, K.R., Protheroe, C., Pero, R., Nguyen, T., Cormier, S.A., Lenkiewicz, E., Colbert, D., Rinaldi, L., Ackerman, S.J., Irvin, C.G., Lee, N.A. 2004. Defining a link with asthma in mice congenitally deficient in eosinophils. *Science*; 305(5691):1773-6.

192. Boenisch, T. 2006. Heat-induced antigen retrieval: what are we retrieving? *J Histochem Cytochem.* 54(9):961-4.

193. Goto, T., Befus, D., Low, R., Bienenstock, J. 1984. Mast cell heterogeneity and hyperplasia in bleomycin-induced pulmonary fibrosis of rats. *Am Rev Respir Dis*. 130(5):797-802.

194. Williams, N., Kraft, N., Shortman, K. 1972. The separation of different cell classes from lymphoid organs. VI. The effect of osmolarity of gradient media on the density distribution of cells. *Immunology.* 22(5):885-99.

195. Fowlkes, B., Waxdal, M., Sharrow, S., Thomas, C., Asofsky, R, Mathieson, B.1980. Differential binding of fluorescein-labeled lectins to mouse thymocytes: subsets revealed by flow microfluorometry. *J Immunol.* 125(2):623-30.

196. Shortman, K, Williams, N, Adams, P. 1972. The separation of different cell classes from lymphoid organs. V. Simple procedures for the removal of cell debris. Damaged cells and erythroid cells from lymphoid cell suspensions. *J Immunol Methods*. 1(3):273-87.

197. Coté RJ. 2001. Aseptic technique for cell culture. *Curr Protoc Cell Bio*; Chapter 1: Unit 1.3. Review.

198. Compensation principles. Salk Institute http://flowcyt.salk.edu/howto/compensation/compensation-howto.html

199. Davidson, W. and Parish, C.1975. A procedure for removing red cells and dead cells from lymphoid cell suspensions. *J Immunol Methods.* 7:291-300.

200. Palmer, M., and Prediger, E. 2007. Assessing RNA quality. *Ambion TechNotes 11(1); http://www.ambion.com/techlib/tn/111/8.html*

201. Manchester, K.L. 1995 Value of A_{260}/A_{280} ratios for measurement of purity of nucleic acids. *Biotechniques;* 18, 62-63.

202. Skrypina, N.A., Timofeeva, A.V., Khaspekov, G.L., Savochkina, L.P., and Beabealashvilli, R. 2003. Total RNA suitable for molecular biology analysis. *J.Biotechnol;* 105: 1-9.

203. Sambrook, J., Fritsch, E.F., and Manniatis, T. 1989. Molecular Cloning: A laboratory manual, 2nd edn. *Cold Spring harbor Laboratory Press, NY.*

204. Hamalainen, H.K., Tubman, J.C., Vikman, S., Kyrölä, S.T., Ylikoski, E. Warrington, J.A., and Lahesmaa, R. 2001. Identification and validation of endogenous reference genes for expression profiling of T helper cell differentiation by quantitative real-time RT-PCR. *Analytical Biochemistry* 299, 63–70.

205. Moore, D.S. 2007. The basic practice of statistics. 5th edition. *W.H. Freeman and Company, NY.*

206. Shortman, K., Egerton, M., Spangrude, G.J., Scollay, R. 1990. The generation and fate of thymocytes. *Semin Immunol;* 2(1):3-12.

207. Stevens, W. W., Kim, T. S., Pujanauski, L. M., Hao, X., Braciale, T. J. 2007. Detection and quantitation of eosinophils in the murine respiratory tract by flow cytometry. *J Immunol Methods*; 327: 63–74.

208. Dorman SC, Babirad I, Post J, Watson RM, Foley R, Jones GL, O'Byrne PM, Sehmi R. 2005. Progenitor egress from the bone marrow after allergen challenge: role of stromal cell-derived factor 1alpha and eotaxin. *J Allergy Clin Immunol.* 115(3):501-7.

209. Aizawa, H., Zimmermann, N., Carrigan, P.E., Lee, J.J., Rothenberg, M.E., Bochner, B.S. 2003. Molecular analysis of human Siglec-8 orthologs relevant to mouse eosinophils: identification of mouse orthologs of Siglec-5 (mSiglec-F) and Siglec-10 (mSiglec-G). *Genomics*; 82(5):521-30.

210. Plager, D.A., Loegering, D.A., Checkel, J.L., Tang, J., Kephart, G.M., Caffes, P.L., Adolphson, C.R., Ohnuki, L.E., Gleich, G.J. 2006. Major basic protein homolog (MBP2): a specific human eosinophil marker. *J Immunol;* 177(10):7340-5.

211. Hogan, S P., Rosenberg, H. F. Moqbel, R. Phipps, S. Foster, P. S. Lacy, P. Kay, A. B., and Rothenberg, M. E. 2008. Eosinophils: biological properties and role in health and disease. *Clin Exp Allergy*, 1–42.

212. Kampinga, J., Berges, S., Boyd, R.L., Brekelmans, P., Colic, M., et al. 1989. Thymic epithelial antibodies: immunohistological analysis and introduction of nomenclature. *Thymus* 13:165–73.

213. Zhukova EM. 2005. Role of capsaicin-sensitive neurons in the regulation of structural organization of the thymus. *Bull Exp Biol Med;* 140(2):249-52

214. Popov, A., and Schultze, J. L. 2008. IDO-expressing regulatory dendritic cells in cancer and chronic infection. *J Mol Med*; 86:145–160.

215. Mellor, A.L., Baban, B., Chandler, P., Marshall, B., Jhaver, K., Hansen, A., Koni, P.A., Iwashima, M., Munn, D.H. 2003. Cutting edge: induced Indoleamine 2, 3- dioxygenase expression in dendritic cell subsets suppresses T cell clonal expansion. *J Immunol.;* 171(4):1652-5.

216. Huggett, J., Dheda, K., Bustin, S., Zumla, A. 2005. Real-time RT-PCR normalization; strategies and considerations. *Genes Immun.* 6(4):279-84

217. Müller E. 1977. Localization of eosinophils in the thymus by the peroxidase reaction *Histochemistry;* 52(3):273-9.

218. Bhathal, P. S., and Campbell, P. E. 1965. Eosinophil leucocytes in the child's thymus. *Aust. Ann. Med.,* 14, 210-213.

219. Sin, Y.M., Saintemarie, G. 1965. Granulocytopoiesis in the rat thymus. I. Description of the cells of the neutrophilic and eosinophilic series. *Br J Haematol*; 11(6):613-23.

220. Contreirasa, E.C., Lenzic, H. L. Meirellesd, M. N. L., Caputoc, L. F. G., Caladoe, T. J. C. Villa-Verdea, D. M. S., and Savino, W. 2004. The equine thymus microenvironment: a morphological and immunohistochemical analysis. *Developmental & Comparative Immunol;* 28 (3): 251-264.

221. Lawler DF, Hopkins J, Watson ED. 1999. Immune cell populations in the equine corpus luteum throughout the oestrous cycle and early pregnancy: an immunohistochemical and flow cytometric study. *J Reprod Fertil;* 117(2):281-90.

222. Miller, J.F.A.P. 1994. The thymus: maestro of the immune system. *BioEssays;* 16(7): 509-513.

223. Durkin, H. G., and Waksman, B. H. 2001. Thymus and tolerance. Is regulation the major function of the thymus? *Immunological Reviews* 182: 33–57.

224. Schönland, S.O., Zimmer, J.K., Lopez-Benitez, C.M., Widmann, T., Ramin, K.D., Goronzy, J.J., Weyand, C.M. 2003. Homeostatic control of T-cell generation in neonates. *Blood;* 102(4):1428-34.

225. Adkins, B. Neonatal T cell function. 2005. *J Pediatr Gastroenterol Nutr*; 40 Suppl 1:S5-7.

226. Adkins, B. T-cell function in newborn mice and humans. 1999. *Immunol Today;* 20(7): 330-335.

227. Baban, B., Chandler, P., McCool, D., Marshall, B., Munn, D.H., Mellor, A.L. 2004. Indoleamine 2,3-dioxygenase expression is restricted to fetal trophoblast giant cells during murine gestation and is maternal genome specific. *J Reprod Immunol;* 61(2):67-77.

228. Adamko, D.J., Odemuyiwa, S.O., Vethanayagam, D., Moqbel, R. 2005.The rise of the phoenix: the expanding role of the eosinophil in health and disease. *Allergy;* 60(1):13-22.

229. Flores, K.G., Li, J., Sempowski, G.D., Haynes, B.F., Hale, L.P. 1999. Analysis of the human thymic perivascular space during aging. *J Clin Invest.*; 104(8):1031-9.

230. Franz-Bacon, K., Dairaghi, D.J., Boehme, S.A., Sullivan, S.K., Schall, T.J., Conlon, P.J., Taylor, N., Bacon, K.B. 1999. Human thymocytes express CCR-3 and are activated by eotaxin. *Blood*; 93:3233-3240.

231. de Visser, K.E., Cordaro, T.A., Kioussis, D., Haanen, J.B., Schumacher, T.N., Kruisbeek, A.M. 2000. Tracing and characterization of the low-avidity self-specific T cell repertoire. *Eur J Immunol*; 30(5):1458-68.

232. Green, DR. The suicide in the thymus, a twisted trail. 2003. *Nat Immunol.*; 4(3):207-8.

233. Buhlmann, J. E., Krevsky-Elkin, S. and Sharpe, A. H. 2003. A role for the B7-1/B7-2:CD28/CTLA-4 pathway during negative selection *J Immunology,* 170: 5421–5428.

234. Hobson KG, Cho K, Adamson LK, Greenhalgh DG. 2002. Burn-induced thymic apoptosis corresponds with altered TGF-beta(1) and Smad 2/3. *J Surg Res;* 105(1): 4-9.

235. Milićević, N.M., Nohroudi, K., Labudović-Borović, M., Milićević, Z., Pfeffer, K., Westermann, J. 2006. Metallophilic macrophages are lacking in the thymus of lymphotoxin-beta receptor-deficient mice. *Histochem Cell Biol;* 126(6):687-93.

236. Grimaldi, J.C., Yu, N.X., Grunig, G., Seymour, B.W., Cottrez, F., Robinson, D.S., Hosken, N., Ferlin, W.G., Wu, X., Soto, H., O'Garra, A., Howard, M.C., Coffman, R.L. 1999. Depletion of eosinophils in mice through the use of antibodies specific for C-C chemokine receptor 3 (CCR3). *J Leukoc Biol;* 65(6):846-53.

237. Nakamura, T., Ohbayashi, M., Toda, M., Hall, D.A., Horgan, C.M., Ono, S.J. 2005. A specific CCR3 chemokine receptor antagonist inhibits both early and late phase allergic inflammation in the conjunctiva. *Immunol Res*; 33(3):213-21.

238. Moon, K.A., Kim, S.Y., Kim, T.B., Yun, E.S., Park, C.S., Cho, Y.S., Moon, H.B., Lee, K.Y. 2007. Allergen-induced CD11b+ CD11c (int) CCR3+ macrophages in the lung promote eosinophilic airway inflammation in a mouse asthma model. *Int Immunol.*; 19(12):1371-81.

239. Sallusto, F., Mackay, C.R., Lanzavecchia, A. 1997. Selective expression of the eotaxin receptor CCR3 by human T helper 2 cells. *Science*. 277:2005-2007.

240. Bodey, B., Bodey, B. Jr, Siegel, S.E., Kaiser, H.E. 1998. Intrathymic non-lymphatic hematopoiesis during mammalian ontogenesis. *In Vivo;* 12(6):599-618.

241. Wakkach, A., Chastre, E., Bruand C, Cohen-Kaminsky S, Emami S, Gespach C, Berrih-Aknin S. 2001. Phenotypic and functional characterization of human thymic stromal cell lines. *Cell Mol Biol (Noisy-le-grand).*; 47(1):167-78.

242. Zlotnik, A., Moore, T.A. 1995. Cytokine production and requirements during T-cell development. *Curr Opin Immunol*; 7(2):206-13.

243. Konieczny, B. T., Dai, Z., Elwood, E. T., Saleem, S., Linsley, P. S., Baddoura, F. K., Larsen, C. P., Pearson, T. C., and Lakkis, F. G. 1998. IFN-gamma is critical for long-term allograft survival induced by blocking the CD28 and CD40 ligand T Cell costimulation pathways. *J Immunol;* 160: 2059–2064.

244. Kwon, H., Jun, H.S., Khil, L.Y., Yoon, J.W. 2004. Role of CTLA-4 in the activation of single- and double-positive thymocytes. *J Immunol;* 173(11):6645-53.

245. Lamhamedi-Cherradi, S-E., Zheng, S-J., Maguschak, K.A., Peschon, J., Chen, J.Y. 2003. Defective thymocyte apoptosis and accelerated autoimmune diseases in TRAIL–/– mice. *Nature Immunol;* 4(3): 255-260.

246. Orabona, C., Tomasello, E., Fallarino, F., Bianchi, R., Volpi, C., Bellocchio, S., Romani, L., Fioretti, M. C., Vivier, E., Puccetti, P., and Grohmann, U. 2005. Enhanced tryptophan catabolism in the absence of the molecular adapter DAP12. *Eur. J. Immunol.*. 35: 3111–3118.

247. Fallarino, F., Orabona, C., Vacca, C., Bianchi, R., Gizzi, S., Asselin-Paturel, C., Fioretti, M.C., Trinchieri, G., Grohmann, U., Puccetti, P. 2005. Ligand and cytokine dependence of the immunosuppressive pathway of tryptophan catabolism in plasmacytoid dendritic cells. *Int Immunol*; 17:1429–1438.

248. Fallarino, F., Vacca, C., Orabona, C., Belladonna, M.L., Bianchi, R., Marshall, B., Keskin, D.B., Mellor, A.L., Fioretti, M.C., Grohmann, U., Puccetti, P. 2002. Functional expression of indoleamine 2,3-dioxygenase by murine CD8 alpha(+) dendritic cells. *Int Immunol 14*:65–68.

249. Thomas, S.R., Salahifar, H., Mashima, R., Hunt, N.H., Richardson, D.R., Stocker, R. 2001. Antioxidants inhibit indoleamine 2,3-dioxygenase in IFN-γ-activated human macrophages: Posttranslational regulation by pyrrolidine dithiocarbamate. *J Immunol.*; 166(10):6332-40.

250. Wu, L., Vremec, D., Ardavin, C., Winkel, K., Süss, G., Georgiou, H *et al*. 1995. Mouse thymus dendritic cells: kinetics of development and changes in surface markers during maturation. *Eur J Immunol;* 25: 418–425.

251. Sommandas, V., Rutledge, E. A., Van Yserloo, B., Fuller, J., Lernmark, Å., and Drexhage, H. A. 2007. Low-density cells isolated from the rat thymus resemble branched cortical macrophages and have a reduced capability of rescuing double-positive thymocytes from apoptosis in the BB-DP rat. *J. Leukoc. Biol.* 82: 869–876.

252. Zella, D, Barabitskaja O, Burns JM, Romerio F, Dunn DE, Revello MG, Gerna G, Reitz MS Jr, Gallo RC, Weichold FF. 1998. Interferon-gamma increases expression of chemokine receptors CCR1, CCR3, and CCR5, but not CXCR4 in monocytoid U937 cells. *Blood*; 91(12):4444-50.

Appendix A

Histochemical Reagents

Weigert's Iron Hematoxylin solutions kit (Sigma-Aldrich, Saint Louise, USA) includes**:** Solution A (1%Hematoxylin w/v in Ethanol), and solution B (1.2% Ferric chloride w/v, 1% Hydrochloric acid v/v). Weigert's hematoxylin contains equal parts of these solutions and is stable for 10 days at room temperature.

1% Biebrich Scarlet (Ponceau BS, Fluka, Fair Lawn, NJ, USA) w/v solution in distilled water

Working solution contains 1% Biebrich Scarlet solution and Weigert's hematoxylin in 1:10 v/v ratio.

Concentrated hydrochloric acid (Fisher Scientific, UN 1789) was diluted in 70% ethanol to prepare 1% acid alcohol solution. Alkaline solution for hematoxylin development is 0.5% Lithium Carbonate (Sigma-Aldrich, Saint Louise, USA) w/v in water.

Reagents for Immunohistochemistry

Balanced Salt Solutions

Balanced salt solutions are composed of inorganic salts and may be supplemented with glucose. BSSs maintain cells in viable state for short period of time and are not intended to promote growth. It is the primary solution used in enzymatic treatments of cells and tissue and the final rinse of cells prior to transfer in a growth medium.

Tris Balanced Salt Solution with Tween20

100 mM Tris-HCl Buffer (pH 7,6), 150mM NaCl, 0,05% Tween 20 (TNT, Fisher

Scientific, Fair Lawn, NJ, USA)

Reagents for Flow Cytometry

Hank's Balanced Salt Solution

COMPONENTS	Molecular weight	Mg/L	Molarity mM
KCl	75	400	5.33
KH_2PO_4 (monobasic)	136	60	0.441
$NaHCO_3$	84	350	4.17
NaCl	58	8000	137.93
Na_2HPO_4 (dibasic, anhydrous)	142	48	0.338

Working buffer:

Use 1x HBSS (Sigma-Aldrich, Saint Louise, USA) to 300 ml final volume.

6.0 ml of FBS or FCS (2% final)

3.0 g of D-Glucose (1% final) (Sigma-Aldrich, Saint Louise, USA)

Adjust the osmolarity to mouse plasma, controlling by microosmometry using μ

OSMETTE micro osmometer (osmolarity of mouse plasma is 308-312 mOSM)

using 10% NaCl.

Lysis buffer:

Tris base (Trizma®base, Sigma-Aldrich, Saint Louise, USA)

Ammonium chloride 99.99% (Sigma-Aldrich, Saint Louise, USA)

Double distilled water

EDTA 0.5M (EMD,)

Preparation:

Prepare 0.02 M Tris base and 0.155M NH$_4$Cl.

Mix 9 volumes of 0.155M NH$_4$Cl and 1 volume of 0.02M Tris base solutions.

Add 1.8 ml of 0.5M EDTA.

Adjust the pH to 7.2-7.4, filter and store @ 4˚C.

Cell Culture Media

RPMI 1640 HEPES modification – 500 ml (Sigma-Aldrich, Saint Louise, USA)

Compone nt	β- mercaptoetha nol	Penicillin	Streptomycin	L- glutamin e	Sodium Pyruvat e	FBS
Concentr ation	50 µM	100U/ml	100mg/ml	4mM	1mM	10%

Buffer for Flow Cytometry

1x Hank's BSS, supplemented with 1% Bovine Serum Albumin (Sigma-Aldrich, Saint Louise, USA), 0.09% Sodium Azide (NaN$_3$, Sigma-Aldrich, Saint Louise, USA) and adjusted to mouse osmolarity by D-Glucose (0.7-1% final).

Permeabilising Buffer

0.1% Saponin (Sigma-Aldrich, Saint Louise, USA) in the Flow buffer (see above).

Paraformaldehyde 4% w/v in PBS

4g of paraformaldehyde (Fisher Scientific, Fair Lawn, NJ, USA) added to 85 ml H$_2$O at 80˚C

Adjusted with NaOH (10-4 M) to increase the pH until a cloudy suspension dissolves.

Add 10 ml of PBS10X and cool down on ice, pH to 7.2-7.3

Complete with H2O to 100 ml, add sucrose 0.54g

 Keep in freezer -20˚C up to one year.

PCR Reagents

Reverse Transcription Master Mix

Component	Volume	Final Concentration
RNaseOUT™, Recombinant RNase Inhibitor – 40 U/µL (Invitrogen, Burlington, ON, Canada)	1µL	2 U/µL
5x First Strand Buffer (250mM Tris-HCL, pH 8.3, 375 mM KCl, 15 mM MgCl$_2$)	4µL	1x
0.1 M DTT	2µL	0.01M
10 mM dNTPs mixture	1µL	0.5 mM each
M-MLV Reverse Transcriptase (Invitrogen, Burlington, ON, Canada)	1µL	10 Units/µL

Amplification PCR Master Mix

Component	Volume	Final Concentration
10xPCR buffer without MgCl$_2$, 200mM Tris-HCl (pH 8.4), 500mM KCl	2.5 µL	1x
50 mM MgCl$_2$	0.75 µL	1.5 mM
5 pM/µL Primers	1.25 µL each	0.2pM/µL
10mM dNTP mixture	1µL	0.4 mM each
5 U/µL Platinum® Taq DNA polymerase (Invitrogen, Burlington, ON, Canada)	0.4µL	2.0 units/reaction
DNase, RNase-free water	To 25µL	N/A